

CHARACTERIZING THE CERVICAL RESPONSE TO INFLAMMATION DURING
INFECTION-MEDIATED PRETERM BIRTH

APPROVED BY SUPERVISORY COMMITTEE

Mala Mahendroo, Ph.D.

W. Lee Kraus, Ph.D.

Carole Mendelson, Ph.D.

Vishal Patel, M.D.

DEDICATION

I wish to dedicate my dissertation to my parents and sister, Bob, Lisa, and Briana Willcockson, without whose constant support, this work would not have been completed.

CHARACTERIZING THE CERVICAL RESPONSE TO INFLAMMATION DURING
INFECTION-MEDIATED PRETERM BIRTH

by

ALEXANDRA RAE WILLCOCKSON

DISSERTATION

Presented to the Faculty of the Graduate School of Biomedical Sciences

The University of Texas Southwestern Medical Center at Dallas

In Partial Fulfillment of the Requirements

For the Degree of

DOCTOR OF PHILOSOPHY

The University of Texas Southwestern Medical Center at Dallas

Dallas, Texas

December 2017

Copyright

by

ALEXANDRA RAE WILLCOCKSON, 2017

All Rights Reserved

ACKNOWLEDGEMENTS

First and foremost, I would like to thank my mentor, Mala Mahendroo, for taking me on as her second graduate student. I appreciate her guidance, support, and patience these past five years. I could not have persisted without her. I also owe a big “thank you” to my committee, Lee Kraus, Carole Mendelson, and Vishal Patel, for pushing me to focus and really dig deep into one specific biological question. Thank you to Tulip Nandu, the computational biologist and bioinformatics guru who completed RNA-seq analyses on this project.

I could not have completed my thesis work without the guidance of the past and present Mahendroo Lab members who laid the ground work for my project to take place. To my fellow grad student friends and classmates, I owe many thank yous for great conversations over wonderful food. Lastly, thank you to my love, John W. Brende, for always reminding me I’m a strong, independent, (scientific) woman!

CHARACTERIZING THE CERVICAL RESPONSE TO INFLAMMATION DURING
INFECTION-MEDIATED PRETERM BIRTH

ALEXANDRA RAE WILLCOCKSON, Ph.D.

The University of Texas Southwestern Medical Center at Dallas, 2017

MALA MAHENDROO, Ph.D.

Preterm birth, a delivery that occurs prior to 37 weeks of a 40 week gestation in women, is a leading cause of infant morbidity and mortality. Additionally, children born preterm who make it through their first year of life are at increased risk of medical complications throughout their lives. Costs associated with prematurity exceed \$26 million each year in the United States alone, where nearly 1 in 10 babies is born preterm. The fact that preterm birth rates have only slightly declined overall in the past 20 years can be attributed to the multiple, and most yet-to-be-identified, etiologies of the syndrome. More than 65% of all preterm births have no clinically identifiable cause. Of the premature deliveries with an identifiable cause, infection contributes to 40%. Regardless of the cause or timing of

delivery, changes in the cervix precede the onset of labor. A better understanding of the pathological processes involved in premature cervical remodeling will allow for development of detection technologies and therapeutic approaches to preventing preterm birth. The goal of this study was to identify cervical pathways, distinctly regulated in response to inflammation, that lead to premature changes in extracellular matrix components, decreasing tissue biomechanical integrity and leading to preterm birth. Cervical elastic fiber ultrastructure becomes acutely disrupted in response to inflammation but not at term. RNA-seq studies identified enrichment of inflammasome activation and protease pathways in the cervix, both also exclusive to inflammation. Inflammasome-induced protease upregulation and subsequently increased activity targeting elastic fibers are potential mechanisms of premature cervical remodeling in response to inflammation, leading to preterm birth. These findings add to the understanding of how the tissue responds to inflammation and how this response can induce extracellular matrix changes that impact the biomechanical integrity of the cervix. Future investigations will focus on potential therapeutic approaches that target mechanisms upstream of protease activation to prevent disrupted extracellular matrix architecture. The effects of these studies have the potential to extend beyond first pregnancies impacted by infection; risk of preterm birth in subsequent pregnancies, which increases exponentially as the number of preterm deliveries a woman experiences increases, may also be lessened.

TABLE OF CONTENTS

TITLE PAGE.....	i
DEDICATION.....	ii
ACKNOWLEDGEMENTS.....	v
ABSTRACT.....	vi
TABLE OF CONTENTS.....	viii
PUBLICATIONS.....	xi
LIST OF FIGURES.....	xii
LIST OF TABLES.....	xv
LIST OF DEFINITIONS.....	xvi
CHAPTER 1: INTRODUCTION & LITERATURE REVIEW.....	1
1.1 PHYSIOLOGY.....	1
1.1.1 Parturition as Coordination.....	1
1.1.2 Steroid Hormones in Pregnancy & Parturition.....	2
1.1.3 MicroRNAs in Pregnancy & Parturition.....	4
1.2 PRETERM BIRTH.....	5
1.2.1 Introduction.....	5
1.2.2 Risk Factors.....	5
1.2.3 Etiology.....	7
1.2.3 Therapies.....	9
1.3 THE CERVIX.....	13
1.3.1 Introduction.....	13
1.3.2 Epithelium.....	13
1.3.3 Stroma.....	14
1.3.4 The Extracellular Matrix.....	14
Collagen.....	14
Elastin.....	16
1.3.5 Physiologic Cervical Softening.....	17
1.3.6 Physiologic Cervical Ripening.....	17
1.3.7 Postpartum Tissue Repair.....	18
1.3.8 LPS-Mediated Preterm Birth.....	19
1.4 GOAL OF RESEARCH.....	21
CHAPTER 2: CERVICAL TRANSCRIPTOME SIGNATURES IN TERM & LPS-MEDIATED PRETERM BIRTH.....	27

2.1 INTRODUCTION	27
2.2 RESULTS.....	30
2.2.1 RNA-seq identifies unique transcriptomes in LPS-mediated preterm and term cervical ripening.....	30
2.2.2 Gene ontology analyses identify exclusive pathways in LPS-mediated preterm birth.....	31
2.2.3 Components of the inflammasome are upregulated in LPS-mediated preterm birth.....	32
2.2.5 Inflammasome Activation in Epithelial Cells.....	34
2.2.6 Cervical Small RNAs Induced in LPS-Mediated Preterm & Term Birth.....	36
2.2.7 miR-210 and The Hifs.....	37
2.2.8 Other miRs in Term and LPS-mediated Preterm Birth	37
2.2.9 mechanomiRs & ECM-targeting miRs.....	38
2.3 DISCUSSION.....	39
2.4 MATERIALS & METHODS.....	46
2.4.1 Mice.....	46
2.4.2 Inflammation Preterm Labor Model.....	46
2.4.3 RNA Sequencing.....	47
2.4.4 Transcriptome Data Analysis.....	47
2.4.5 RNA isolation and quantitative PCR.....	48
2.4.6 Caspase Activity Assays.....	48
2.4.7 IL1B ELISA.....	49
2.4.8 Cell Culture Inflammasome Induction.....	49
2.4.9 Small RNA-seq.....	50
2.4.10 Microarray.....	50
2.4.11 Initial Validation of Small RNA-seq & Microarray: qPCR Studies.....	50
2.4.12 MechanomiR & ECM Targeting miR qPCR Studies.....	51
CHAPTER 3: TRANSCRIPTIONAL SIGNATURES OF INFLAMMATION	
INFLUENCING CERVICAL ECM.....	83
3.1 INTRODUCTION.....	83
3.2 RESULTS.....	85
3.2.1 Expression of proteases in the cervix is upregulated in LPS-mediated preterm birth.....	85
3.2.2 Cervical elastic fiber ultrastructure is disrupted in LPS-mediated preterm birth.....	86
3.2.3 Cervical tissue resilience decreased at 75% yield force in LPS-mediated preterm birth but not at term.....	88
3.2.4 Neither solubility nor extractability of cervical elastin is altered in LPS-mediated preterm birth	89
3.2.5 No increase in TGF β signaling with disrupted matrix	90
3.2.6 Investigations of cervical protease activity in LPS-mediated preterm birth....	90
3.2.7 Regulation of cervical protease expression in LPS-mediated preterm birth....	92
3.3 DISCUSSION	94
3.4 MATERIALS & METHODS.....	99

3.4.1 Mice.....	99
3.4.2 Inflammation Preterm Labor Model.....	99
3.4.3 RNA Sequencing.....	100
3.4.4 Transcriptome Data Analysis.....	100
3.4.5 RNA isolation and quantitative PCR.....	101
3.4.6 Elastin staining.....	101
3.4.7 Biomechanical Testing	102
3.4.8 Elastin solubility testing.....	103
3.4.9 Elastin extractability testing.....	103
3.4.10 TGF β Signaling	104
3.4.11 In Situ zymography.....	105
3.4.12 Collagenase and Elastase Activity Assays.....	105
3.4.13 Neutrophil Elastase Assay.....	106
3.4.14 Intrauterine IL1B Administration.....	107
3.4.15 Anakinra	107
CHAPTER 4: POSTPARTUM STUDIES & A LOOK AHEAD.....	138
4.1 INTRODUCTION.....	138
4.2 RESULTS.....	140
4.2.1 Experimental setup.....	140
4.2.2 Changes in 24-hour postpartum collagen fiber parameters following an LPS-mediated preterm birth.....	141
4.2.3 Lactation affects 21-day postpartum collagen fiber parameters.....	141
4.2.4 Elastic fiber ultrastructure following term and infection preterm birth.....	142
4.2.5 Biomechanical changes following LPS-mediated preterm birth.....	143
4.3 DISCUSSION.....	143
4.4 MATERIALS & METHODS.....	150
4.4.1 Mice.....	150
4.4.2 Second harmonic generation imaging and analyses.....	150
4.4.3 Transmission electron microscopy.....	151
4.4.5 Biomechanical testing.....	151
BIBLIOGRAPHY.....	160

PRIOR PUBLICATIONS

Willcockson AR, Nandu T, Nallasamy S, Kraus WL, Mahendroo MS. 2017 Cervical transcriptome signature identifies pathways that drive LPS-mediated preterm birth. *Biology of Reproduction* (under review)

Jimenez PT, Frolova AI, Chi MM, Grindler NM, **Willcockson AR**, Reynolds KA, Zhao Q, Moley KH. 2013. DHEA-mediated inhibition of the pentose phosphate pathway alters oocyte lipid metabolism in mice. *Endocrinology* 154(12): 4835-44.

Purcell SH, Aerni-Flessner LB, **Willcockson AR**, Diggs-Andrews KA, Fisher SJ, Moley KH. 2011. Improved insulin sensitivity by GLUT12 overexpression in mice. *Diabetes* 60(5): 1478-82.

LIST OF FIGURES

Figure 1.1 Regions of the Cervix	23
Figure 1.2 Inflammasome Activation	24
Figure 1.3 Comparisons of LPS-Mediated Preterm & Term Birth.....	26
Figure 2.1 RNA-Seq Analyses of the Pregnant Mouse Cervix Demonstrate Unique Transcriptome Profiles In Term and LPS-Mediated Preterm Cervical Remodeling.....	52
Figure 2.2 Gene Ontology and KEGG Pathway Analyses of Term and LPS-Mediated Preterm Cervical Remodeling.....	55
Figure 2.3 Components of the Inflammasome Are Upregulated in LPS-Mediated Preterm Birth Exclusively.....	57
Figure 2.4 Cervical Caspase 1 and 4 Activities Are Unchanged In LPS-Mediated Preterm Birth.....	59
Figure 2.5 End1 Cell Proinflammatory Responses to LPS and PamCSK	61
Figure 2.6 Ect1 Cell Response to PamCSK and ATP or Flagellin Treatment.....	62
Figure 2.7 Low And Unchanging Caspase Activity Ect1 And End1 Cells In Response To PamCSK And ATP Or Flagellin Treatment.....	64
Figure 2.8 Intracellular Il1b In Ect1 And End1 Lysate.....	66
Figure 2.9 Cervical MicroRNAs in Term and LPS-Mediated Preterm Birth	67
Figure 2.10 Cervical MicroRNAs in Term and LPS-Mediated Preterm Birth	74
Figure 2.11 Housekeeping Gene Candidates for MicroRNAs qPCR.....	76
Figure 2.12 Expression of MechanoMiRs throughout Pregnancy & In Response to LPS.....	77

Figure 2.13 Expression of ECM-Targeting MicroRNAs throughout Pregnancy & in Response to LPS	79
Figure 2.14 Ect1 Cell Response to PamCSK and ATP or Flagellin Treatment	81
Figure 3.1 Protease Genes and Pathways are Upregulated in the Cervix during LPS-mediated Preterm Birth Exclusively.....	108
Figure 3.2 Elastin Staining in the Cervix Demonstrates Similar Morphology in LPS-Mediated Preterm and Term Birth.....	110
Figure 3.3 Immunofluorescence Staining for Tropoelastin Suggests Altered Cervical Elastin Morphology upon LPS Treatment on Day 15.....	111
Figure 3.4 Elastic Fiber Ultrastructure is Disrupted in the Cervix of LPS-Treated Mice before Onset of Preterm Birth.....	113
Figure 3.5 Cervical Biomechanical Studies Indicated Reduced Resilience in LPS-Mediated Preterm Birth but not at Term	114
Figure 3.6 Cervical Elastin Solubility and Extractability in LPS-Mediated and Term Birth.....	116
Figure 3.7 Latent TGF β Binding Proteins and Phosphorylation of SMAD2/3 in LPS-Mediated Preterm Birth.....	118
Figure 3.8 Assays Measuring Protease Activity in LPS-Mediated Preterm Birth	120
Figure 3.9 Elastase Activity Assays	122
Figure 3.10 Neutrophil Elastase Activity Assay.....	124
Figure 3.11 Time course of Ilb, Adamts4, Ctsl, and Mmp13 Gene Upregulation in Response to Intrauterine LPS.....	125

Figure 3.12 Intrauterine IL1B Alone does not Upregulate Proinflammatory and Protease Genes In Uterus.....	127
Figure 3.13 Intrauterine IL1B Influences Proinflammatory and Protease Gene Expression in the Cervix.....	129
Figure 3.14 IP Administration of Anakinra does not Abrogate Upregulation of Proteases in Response to IP LPS.....	131
Figure 3.15 IP Administration of Anakinra does not Abrogate Upregulation of Proteases in Response to IU LPS.....	133
Figure 3.16 IU Administration of Anakinra Fails to Prevent Uterine Upregulation of Proinflammatory and Protease Expression in Response to LPS.....	134
Figure 3.17 IU Administration of Anakinra Fails to Prevent Cervical Upregulation of Proinflammatory and Protease Expression in Response to LPS.....	136
Figure 4.1 Postpartum Tissue Repair Experimental Scheme and Cervical Collagen Fiber Differences 24hours after a Term or LPS-Mediate Preterm Birth.....	152
Figure 4.2 Cervical Collagen Fiber Diameter and Anisotropy Differences 21 Days after a Term or LPS-Mediated Preterm Birth.....	154
Figure 4.3 Transmission Electron Microscopy Images in 24-Hour Postpartum Term and LPS-Mediated Preterm Mouse Cervices.....	156
Figure 4.4 Load-to-Break Tissue Biomechanical Parameters Measured in Postpartum Samples Following a Birth at Term or a Preterm Birth Mediated by LPS.....	158

LIST OF TABLES

TABLE 2-1 Fold Change of Canonical Parturition Genes Measured By RNA-Seq.....	54
TABLE 2-2 Fold Change of Proinflammatory Genes, Measured by RNA-Seq.....	54
TABLE 2-3 Downregulated MicroRNAs in Day 15 LPS vs Day 15 Cervices.....	69
TABLE 2-4 Upregulated MicroRNAs in Day 15 LPS vs Day 15 Cervices.....	70
TABLE 2-5 Downregulated MicroRNAs in Day 18 vs Day 15 Cervices.....	71
TABLE 2-6 Upregulated MicroRNAs in Day 18 vs Day 15 Cervices.....	72
TABLE 2-7 Differentially Expressed Cervical MicroRNAs & mRNA Targets in Term and LPS-Mediated Preterm Birth.....	73
TABLE 2-8 Mechanically Regulated & ECM-Targeting MicroRNAs.....	78

LIST OF DEFINITIONS

17-OHPC- 17-alpha hydroxyprogesterone caproate

DAMPs-Damage Associated Molecular Patterns

ECM – Extracellular Matrix

ELISA- Enzyme Linked Immunosorbent Assay

GO- Gene Ontology

HA- Hyaluronic Acid

IP – Intraperitoneal

IU – Intrauterine

LPS –Lipopolysaccharide

miR- MicroRNA

mRNA- Messenger RNA

PCR- Polymerase Chain Reaction

polyA- Poly Adenylated

PRR- Pattern Recognition Receptor

PTB – Preterm Birth

qPCR- Quantitative Polymerase Chain Reaction

RNA- ribonucleic acid

RNA-seq- RNA Sequencing

SHG –Second Harmonic Generation

SLRPs- Small Leucine Rich Proteoglycans

TEM –Transmission Electron Microscopy

CHAPTER ONE

Introduction & Literature Review

PARTURITION

1.1 Physiology

At its most basic level, the survival of a species depends on successful reproduction. While not all details of the physiological processes of reproduction—from its developmental origins to the maturation and ultimate shutdown of reproductive capacity—have been elucidated, its study has provided insights into the great hurdles over which a species must leap to ensure the propagation of genes and ultimate survival of lineages. The process of parturition, or preparation of the female body for the expulsion of the fetus (es) from the uterus, involves a complex set of physiological processes that must be appropriately timed to ensure delivery of a baby who is fit to live outside of the womb yet not overly developed so as to induce a strain on the maternal milieu, which ultimately may be used again for subsequent pregnancies.

1.1.1 Parturition as Coordination

Multiple fetal and maternally derived signals must coordinate for effective and timely parturition. Fetal lung maturation ensures that once expelled from the uterus and detached from its umbilical cord, the baby can utilize oxygen. Work done in the mouse demonstrates surfactant proteins produced in the developing fetal lung act as signals to the maternal tissues

to initiate labor (Gao et al., 2015). Fetal membranes begin to detach from the uterine lining for fetal transportation out of the cavity. Maternal uterine quiescence must be overcome and uterine contractions must begin. The cervix completes its transition from a closed and rigid structure to one that is open and flexible to allow for the delivery of the fetus from the uterus. These individual processes must be coordinated for successful and appropriately timed delivery.

1.1.2 Steroid Hormones in Pregnancy & Parturition

Much of reproduction occurs under the direction of the steroid hormones progesterone and estrogen. In the context of pregnancy, “pro-gestational” hormone progesterone is needed to maintain pregnancy. Compared to a non-pregnant state, serum estrogen levels during pregnancy are elevated (“Implantation, Embryogenesis, and Placental Development,” 2010). Concentration of estrogen in the serum also increases throughout pregnancy.

Progesterone maintains uterine quiescence through suppression of inflammatory responses in the uterus, specifically through its modulation of immune cell properties (Tibbetts, Conneely, & O'Malley, 1999). In the human myometrium, progesterone blocks the NF- κ B -mediated upregulation of prostaglandin synthase-2 (*PTGS2*) that is induced by Interleukin 1 beta (IL1B) and upregulates the negative regulator I κ B α to keep NF- κ B inactivated (Hardy, Janowski, Corey, & Mendelson, 2006).

In humans, the idea of a functional withdrawal of progesterone activity, to overcome the elevated circulating levels of the hormone and to allow for parturition to occur, has been widely studied, starting with a proposal by Csapo and Pinto-Dantas in 1965 (Csapo & Pinto-

Dantas, 1965; Mesiano, 2013). Evidence of this ‘progesterone block’ includes the resulting increase in myometrial sensitivity to prostaglandins and oxytocin—contraction-promoting molecules measured in the tissue near the end of pregnancy and prematurely with use of progesterone receptor antagonist RU486 in a variety of species (Chwalisz, 1994). The action of progesterone occurs via liganded receptor signaling initiated by two nuclear isoforms Progesterone Receptor A and Progesterone Receptor B, the latter of which have been shown to repress expression of key contractile gene connexin 43 in the myometrium (Nadeem et al., 2016). With increased localized metabolism of progesterone at the end of pregnancy, via 20alpha-hydroxysteroid dehydrogenase, the progesterone receptor is more likely to be unliganded and the repression of gene transcription decreased, leading to the initiation of myometrial contractions.

The role of microRNAs (miRs) in modulating progesterone action in the myometrium represents an additional layer of regulation of steroid action at the end of pregnancy. microRNA-200 family members and their targets *ZEB1/2* transcription factors function in the human myometrium to modulate expression of oxytocin receptor and connexin-43, downstream of progesterone and its receptor (Renthal et al., 2010). miR-200a specifically has been shown to increase myometrial progesterone metabolism, providing another example of decreased localized action of the hormone (Williams, Renthal, Condon, Gerard, & Mendelson, 2012).

In the mouse, serum progesterone concentrations decrease and estrogen levels increase at the end of pregnancy (B. C. Timmons et al., 2014). Studies demonstrate that targeted mutations in the gene encoding the progesterone metabolizing enzyme 5α reductase

type 1 result in maintained high levels of progesterone in the cervix shortly before labor, with subsequent failure of parturition (Mahendroo, Porter, Russell, & Word, 1999). Circulating estrogen levels increase throughout pregnancy and peak at the end of pregnancy as well (Mesiano, 2013). In this environment, proteins involved in uterine contractions including connexin 43 and oxytocin receptor are upregulated in both human and mouse myometrium (Chow & Lye, 1994; Fuchs, Fuchs, Husslein, & Soloff, 1984; Renthal et al., 2010).

1.1.3 MicroRNAs in Pregnancy & Parturition

In addition to the myometrial microRNAs mentioned previously, miRs in the context of parturition play a variety of roles. In the placenta, an organ important for exchange of gases, nutrients, and also infection, a primate-specific group of microRNA known as chromosome 19 miRNA cluster (C19MC) assist in communication among the placental, fetal, and maternal compartments (Chang et al., 2017). In the context of hypoxia, a potential consequence of placental injury, microRNAs are differentially expressed and targeting a variety of placental development gene networks, indicating their potential use for therapeutic modulation during placental pathology (Donker, Mouillet, Nelson, & Sadovsky, 2007; Mouillet, Chu, Nelson, Mishima, & Sadovsky, 2010).

MicroRNAs have also been studied for their potential use as circulating biomarkers. Maternal plasma miR-141 and miR-29a are increased in women with preeclampsia compared to normotensive controls (H. Li, Ge, Guo, & Lu, 2013). A number of microRNAs, including those in the miR-548 family, are present in higher concentrations in the plasma of women at 20 weeks gestation and destined for preterm delivery than in the plasma women who later deliver at term (Gray, McCowan, Patel, Taylor, & Vickers, 2017). Functional analyses of

why these circulating miRs are differentially expressed and the transcripts they target are lacking.

1.2 Preterm Birth

1.2.1 Introduction

Preterm birth is defined as a delivery that occurs prior to 37 weeks of a 40 week gestation in humans. Premature delivery is a primary cause of infant morbidity and mortality worldwide. Children who are born preterm and survive infancy are at increased risk of medical complications throughout their lives, and the financial burden of medical care associated with preterm deliveries exceeds \$26 million annually in the United States (2007). The 2015 preterm birth rate in the US was 9.6% (Martin, Hamilton, Osterman, Driscoll, & Mathews, 2017) . Although much research is underway to understand why preterm births occur, the rate peaked at 12.8% (2006) and has only very slowly decreased to its current level over the past ten years (Martin, Hamilton, Osterman, Curtin, & Matthews, 2015). The sustained high rates of preterm birth can be attributed to the variety of etiologies, some not yet discovered, of the syndrome (Romero et al., 2006). In more than two thirds of cases, an exact cause of preterm birth cannot be pinpointed (Ferrero et al., 2016).

1.2.2 Risk Factors

Throughout the years, much focus has been placed on risk factors associated with preterm birth. Identification of pregnant women with risk factors could someday lead to

personalized therapies for preterm birth prevention, although clinical modalities are currently lacking.

With respect to maternal age, there appears to be a goldilocks effect; both young and advanced maternal age are risk factors for preterm delivery (da Silva et al., 2003; Hediger, Scholl, Schall, & Krueger, 1997; Newburn-Cook & Onyskiw, 2005). Additionally, under or overweight women, as measured by pre-pregnancy body mass index (BMI) are at increased risk of delivering preterm (Kosa et al., 2011).

Maternal race is also a significant risk factor— specifically, minority women including African-Americans and American Indian/Alaska Natives, are at increased risk of delivering prematurely. According to the March of Dimes via data calculated from the National Vital Statistics Reports, “in the United States, the preterm birth rate among black women is 48% higher than the rate among all other women” (Martin et al., 2017). Genetic (polymorphisms in key inflammatory genes) and socioeconomic factors (maternal stress, environmental exposures) are likely contributors to preterm birth. While the exact reasons that black and Native American mothers are at increased risk for premature delivery remain elusive, access to prenatal healthcare can reduce preterm birth rates (Anum, Springel, Shriver, & Strauss, 2009; Burris, Collins, & Wright, 2011; Wadhwa, Entringer, Buss, & Lu, 2011).

Preterm birth rates among minority women, specifically Hispanic and African-American pregnant mothers, who delivered at Parkland Hospital, Dallas, Texas, between 1988 and 2006 were significantly lower than preterm birth rates for minority women across the United States as a whole (Leveno, McIntire, Bloom, Sibley, & Anderson, 2009).

Parkland Hospital System employs community clinics that provide frontline prenatal care for pregnant women. These clinics identify high-risk pregnancy complications and provide referral services to a centralized, specialized clinic at Parkland Hospital for proper care. The authors suggest this model of clinical care may be responsible for decreased preterm birth rates among minority populations.

Short interpregnancy interval, or a short time interval between delivery and conception of a subsequent pregnancy, is another risk for preterm birth (Khoshnood, Lee, Wall, Hsieh, & Mittendorf, 1998; Klerman, Cliver, & Goldenberg, 1998). In fact, the shorter the interval (<6 months compared to >12 months), the higher the risk of adverse maternal and neonatal outcomes. These outcomes, including preterm deliveries, low birth weight infants, intrauterine growth restriction, and neonatal mortality occur more frequently with short (<12 months) intervals (Conde-Agudelo, Rosas-Bermudez, & Kafury-Goeta, 2006). A number of hypotheses, including maternal nutritional depletion with lactation demands, incomplete uterine and/or cervical healing, and poor endometrial blood vessel remodeling, have been proposed to explain the detrimental effects of short interpregnancy intervals (Conde-Agudelo, Rosas-Bermudez, Castano, & Norton, 2012).

The best predictor of premature delivery is the presence of an obstetric history of preterm birth (Ferrero et al., 2016). The percentage of recurrent preterm birth increases with the number of previous preterm deliveries—16% after 1 previous, 41% after 2 previous, and 67% after 3 previous preterm births (Bloom, Yost, McIntire, & Leveno, 2001). This pattern is highlighted by data demonstrating that the majority of recurrent preterm deliveries occur within a 2 week window before or after the gestational age at the previous preterm delivery.

1.2.3 Etiology

Preterm deliveries exist in the realm of three distinct circumstances—provider-initiated delivery based on maternal or fetal complications, preterm labor arising spontaneously with fetal membranes intact, and premature rupture of membranes leading to eventual delivery (Goldenberg, Culhane, Iams, & Romero, 2008). Of these classifications, spontaneous preterm births include non-provider initiated premature deliveries with and without intact membranes and account for 40-45% and 25-30% of preterm births respectively. Various causes for spontaneous preterm deliveries have been identified. Among these are tissue biomechanical disruptions including uterine overdistention and cervical insufficiency, uteroplacental ischemia, and infection/inflammation (Romero et al., 2006). In nearly 2/3 of preterm cases, an exact cause of preterm delivery cannot be pinpointed (Ferrero et al., 2016).

Of the approximately 33% of cases with known cause, infection and inflammation are thought to contribute to 25-40% of cases, although that may be a low estimate owing to the fact that a subclinical infection or otherwise un-culturable agent may be present (Goldenberg et al., 2008). A number of infectious agents, including both viruses and bacteria, have been measured in the reproductive tract of women, specifically in the amniotic cavity (Hillier et al., 1988; Reddick, Jhaveri, Gandhi, James, & Swamy, 2011). Although systemic infections such as periodontal disease have been linked to preterm deliveries, the majority of detected (via PCR) or cultured organisms are thought to be vaginal in origin (Jeffcoat et al., 2001; Offenbacher et al., 1996).

A multitude of studies have focused on the role of dysbiosis of the vaginal microbiome and preterm deliveries. In nonpregnant women, the vaginal microbiome is diverse. In pregnancy, the diversity and abundance of bacteria are decreased and the predominant bacterial species is *Lactobacillus* (Aagaard et al., 2012; White, Creedon, Nelson, & Wilson, 2011). Pregnant women without *Lactobacilli*, a condition termed abnormal vaginal flora (AVF), are at increased risk of preterm delivery, compared to women with normal vaginal flora (Donders et al., 2009). Patients with bacterial vaginosis, a more specific form of AVF occurring most commonly as an asymptomatic accumulation of *Gardnerella vaginalis*, *Prevotella sp.*, *Bacteroides sp.*, *Mobiluncus sp.* and *M hominis*, are also at increased risk of preterm delivery. Vaginal dysbiosis has been associated with increased cytokine production and collagenase secretion, correlating with premature cervical remodeling in a study conducted in the UK to understand the impact of cervical sutures on the vaginal microbiome and preterm birth (Kindinger et al., 2016).

Regardless of the cause or origin of the infection, antibiotics are not preventative of preterm deliveries, and may in fact destroy healthy, bacterial colonies (Kenyon, Taylor, Tarnow-Mordi, & Group, 2001). A potential reason for the lack of therapeutic effect of antibiotic agents may be ineffective timing of administration, with prescribing of the pharmaceuticals occurring after a diagnosis has been made and pathological changes to the reproductive system already underway. When given prophylactically, however, antibiotics are similarly found to be ineffective in the prevention of preterm birth (Simcox, Sin, Seed, Briley, & Shennan, 2007). Other potential confounders in studies previously published

include a lack of targeted approach for the specific type of antibiotic given to a specific sub-population of women at a certain interval (Joergensen, Kjaer Weile, & Lamont, 2014).

1.2.4 Therapies

The efficacy of clinical therapies for prevention of preterm birth is limited, at best. Clinical modalities for prevention of preterm birth include tocolytics, cerclage, vaginal progesterone, and intramuscular 17-alpha hydroxyprogesterone caproate (17OHP-c).

Tocolytics include a variety of medications whose goal is to extend pregnancy for women in preterm labor (Obstetricians & Gynecologist, 2003). They act as anti-contractile agents on a number of myometrial targets (Haas, Benjamin, Sawyer, & Quinney, 2014). Although tocolytics have not been shown to directly improve the outcomes of neonates born to mothers utilizing this therapy, their main clinical use has been to provide enough time (48 hours most commonly) for administration of antenatal corticosteroids to mature the fetal lung (American College of, Gynecologists, & Committee on Practice, 2012; Haas et al., 2009).

Cervical cerclage, also called a cervical stitch, is used in women with cervical insufficiency, a diagnosis based on previous cervical dilatation without clear pathology in the second trimester (American College of & Gynecologists, 2014). Two assumptions underlie the clinical therapy of cervical cerclage—first that the cervical tissue is somehow structurally inept to maintain the fetus in the uterus and second that placement of the sutures will provide structural support to the tissue (House & Socrate, 2006). Limited success of cervical cerclage, likely based on existence of flaws within the outlined assumptions, has been demonstrated (Berghella, Odibo, To, Rust, & Althuisius, 2005). In women with a singleton pregnancy, existence of obstetrical history of preterm birth, and a measured short cervix on

ultrasound, there may be a benefit of cerclage (Alfirevic, Stampalija, Roberts, & Jorgensen, 2012).

Previous premature delivery is the most robust risk factor for preterm births in subsequent pregnancies (Ferrero et al., 2016). It is in this obstetrical population where there is most need for clinical strategies for therapeutic preterm birth prevention. Given the role of “pro-gestational” hormone progesterone in maintaining pregnancy, as outlined previously in this chapter, two progesterone-related treatments have been investigated for their effectiveness in reducing recurrent preterm birth rates—vaginal progesterone and intramuscular 17-OHPC.

From a study in Sao Paulo, Brazil, preterm birth rates in women treated with 100mg vaginal progesterone daily were 13.8% versus 28.5% in those administered placebo (da Fonseca, Bittar, Carvalho, & Zugaib, 2003). Drawbacks to this study include a higher-than-average preterm birth rate in the control group and a difference in risk factors—specifically previous preterm births—between treatment and control groups. A second study conducted in hospitals in the London-area, Chile, Brazil, and Greece demonstrated that vaginal progesterone decreased preterm birth incidence in women with a short cervix (<15mm) but otherwise asymptomatic (Fonseca et al., 2007). A more recently published study completed in hospitals in the UK and Sweden showed no reduction in preterm birth with the treatment of vaginal progesterone in women with a short (<25mm) cervix (Norman et al., 2016). Inconsistency in the labeling of cervixes as ‘short’ (<15mm vs <25mm) may account for differences in study outcomes.

Another widely studied modality is intramuscular 17-alpha hydroxyprogesterone caproate (17-OHPC), a synthetic progestogen. 17-OHPC was first studied in the mid-twentieth century in the context of spontaneous abortions/miscarriages (Bevis, 1951; Davis & Wied, 1957; Shearman & Garrett, 1963). There appeared to be no evidence to support its clinical use in these circumstances, but a later study showed promise for its use in preventing premature labor (Johnson, Austin, Jones, Davis, & King, 1975). 17-OHPC (originally marketed as Delalutin) was thought to be superior to progesterone for 4 main reasons: “(1) the high potency of the compound; (2) the prolonged action (approximately 2 weeks in the non-pregnant woman) ; (3) the marked solubility in oil (125 mg./ml.), which permits high dosage ; and (4) the minimal local irritation following injection even of large quantities” (Reifenstein, 1958). Much confusion has occurred surrounding the naming of natural progestogens (17P) and synthetic progestogens (17-OHPC), even influencing the interpretations of meta-analyses based on the origins of the agents being used (Goldstein, Berrier, Rosen, Sacks, & Chalmers, 1989; Keirse, 1990; Romero & Stanczyk, 2013). In more recent clinical trials beginning with the Meis trial, the standard of care for women with a history of spontaneous preterm birth became 250mg intramuscular 17-OHPC weekly from 16-20 weeks gestation until 36 completed weeks of gestation (Meis et al., 2003). Other researchers have commented on the unusually high preterm birth rate in the placebo group (nearly 55% compared to 12.3% nationwide in 2003) as reason to question the generalizability of results from this study (Martin et al., 2005). Recent work has demonstrated that in women with a history of preterm birth, there was no change in gestational age at delivery in pregnancies with 17-OHPC administration compared to

previous, non-17-OHPC delivery in the same women (Nelson et al., 2017). Where administration of 17-OHPC fits into the clinical modalities of care for women at risk of preterm birth has yet to be determined definitively.

1.3 The Cervix

1.3.1 Introduction

The cervix, a structure located at the base of the uterus, remains closed and rigid during pregnancy and transitions to an open and compliant structure during parturition for the delivery of the fetus at the end of gestation. These biomechanical changes dictating the structure and therefore function of the tissue are mediated through changes to the composition and organization of the extracellular matrix (ECM), the connective tissue-rich group of proteins and other matrix molecules synthesized by cells in the stroma. A second important group of extracellular molecules form a pericellular matrix that surround the cervical epithelial cells that line both the internal lumen (os) and the ectocervix and provide immune surveillance plus a protective barrier for the cervix and the upper female reproductive tract.

1.3.2 Epithelium

The epithelial cells that line both the central canal/lumen (os) and the ectocervix are mucus secreting, and increasingly so as pregnancy progresses (Akgul, 2014) (figure 1.1).

The mouse ectocervix and endocervix are composed of squamous mucosal cells that transition to columnar epithelial cells at the cervical and uterine boundary. The epithelium is

a dynamic cervical layer during pregnancy, with increased cell number and cell size observed. Aside from the physical barrier presented by the mucosal epithelial cells of the cervix, a pericellular matrix is crucial for maintaining barrier function in the tissue. Hyaluronic acid (HA), a glycosaminoglycan, is an important pericellular matrix component in the cervical epithelium. Without epithelial HA, the cervical epithelial barrier function is compromised and preterm birth rates of mice treated with live, vaginal *E. coli* are higher than in wildtype mice (Akgul, 2014).

1.3.3 Stroma

The stromal compartment of the cervix is comprised of a number of cell types and a variety of molecules synthesized by those cells. The cervix is a well-vascularized tissue that receives its blood supply via the uterine artery (Pilarczyk, Kozik, & Czerwinski, 2002). A recent study identified four distinct zones of vascularization of the cervix, with each zone consisting of different kinds of vasculature (capillaries, arterioles, venules, etc.) suggesting unique functions of the architecture (Bereza et al., 2012). Fibroblasts are the predominant cell type in the stroma, although work done in the mid-1990s demonstrated that smooth muscle cells make up 10-15% of the cervical cell population, with highest concentrations at the internal os and lower concentrations near the external os (Leppert, 1995). Recent studies estimate smooth muscle cells account for 50-60% of cervical cells in the internal os with smooth muscle cells making up about 10% of cells at the external os (Vink et al., 2016).

1.3.4 The Extracellular Matrix

Collagen

The predominant extracellular matrix protein in the cervix is collagen, specifically fibrillar types I and III; relative amounts of these molecules remain constant throughout pregnancy. (Akins, Luby-Phelps, Bank, & Mahendroo, 2011). Collagen's synthesis, processing, and assembly occur in a highly coordinated fashion with the help of a number of matricellular and glycoproteins. Factors known to modulate collagen structure, including matricellular proteins thrombospondin 2 and tenascin C and cross-linking enzyme lysyl oxidase, decrease in expression during early pregnancy. A potential consequence of these altered parameters known to influence collagen structure is increased dispersion of the cervical ECM and reduced crosslinks as pregnancy progresses. Collagen fibril size also increases during pregnancy as the fibers become more loosely packed and larger in diameter (Akins, Luby-Phelps, & Mahendroo, 2010). Biomechanical studies also support the theory of collagen fiber reorganization during pregnancy (Read, Word, Ruscheinsky, Timmons, & Mahendroo, 2007). Cervical stiffness is significantly decreased on day 12 of pregnancy and maximal stretch increased. A maximal loss of cervical tissue stiffness occurs prior to delivery.

Other molecules abundant in the cervical stroma are small leucine rich proteoglycans, or SLRPs. These secreted proteins are comprised of a core protein and one or more glycosaminoglycan chains (Merline, Schaefer, & Schaefer, 2009). The glycosaminoglycan chain of the class 1 SLRP decorin is known to regulate interfibrillar spacing by interacting with nearby collagen fibers (Scott, 1988). SLRPs act to regulate intrafibrillar bridges to help organize individual fibrils making up collagen fibers. Without class 1 SLRP decorin (Dcn), cervical collagen fibrils are abnormal in the nonpregnant state and until day 12 of gestation

(Nallasamy et al., 2017b). Interestingly, the abnormal fibrils disappear until the postpartum tissue repair period. Abnormal fibrils in non-pregnant ovariectomized Dcn $-/-$ mice are rescued upon progesterone treatment. In that same group, cervical tissue biomechanical parameters such as maximum stiffness, tissue strength, and yield stress are significantly decreased compared to wild type ovariectomized mice. These measurements highlight the impact of dynamic alterations in collagen and collagen-associated proteins on the biomechanical properties of the tissue.

Elastin

Elastic fibers are composed of tropoelastin protein crosslinked in and around a microfibrillar scaffold (Wagenseil & Mecham, 2007). The main function of elastic fibers is to provide elasticity in the form of energy storage for the tissue during mechanical strain. The synthesis, processing, and assembly of elastic fibers occur during times of development, and the mature fibers are thought to be permanent with limited repair possible. Elastic fibers comprise about 1.5% of the connective tissue portion of the human cervix (Leppert, Keller, Cerreta, Hosannah, & Mandl, 1983). The elastic fibers in the cervix are thin (2-4 μ m wide) (Leppert, 1995; Leppert & Yu, 1991). These fibers are mainly concentrated in the sub-epithelial portions of both the endocervical canal and the ectocervix with lower abundance seen in the midstroma. Reduced elastic fibers in the human cervix have been suggested to contribute to cervical insufficiency, although not until recently supported by experimental evidence that will be presented later in this dissertation (Leppert, Yu, Keller, Cerreta, & Mandl, 1987).

The importance of elastic fibers to the mechanical function of the cervix, and the demonstration that elastic fibers undergo a gradual reorganization from early to late pregnancy was recently reported in studies using mice deficient in the small proteoglycan decorin (Nallasamy et al., 2017a). Mice lacking decorin have defects in assembly of both collagen and elastic fibers. In an ovariectomized decorin knockout model, abnormal elastic fibers are rescued with estrogen treatment. Interestingly, these phenotypic changes also correlate with rescued tissue stiffness, strength, and yield stress parameters compared to wild type ovariectomized estrogen treated animals. These studies demonstrate elastic fibers' contributions to the biomechanical function of the cervix.

1.3.5 Physiologic Cervical Softening

The cervical tissue must balance the need for tissue competency (ability to preserve threshold of rigidity for fetal maintenance in the uterus) and tissue remodeling to ensure that, when gestation comes to an end, an appropriately compliant canal can allow for the fetus to exit the womb. The early stages of cervical remodeling have been termed softening. This occurs around day 12 in the mouse when the first measurable decline in cervical tissue stiffness occurs (Read et al., 2007). Noted changes in collagen crosslinking, which occur during the final maturation process of collagen assembly, have been correlated with the biomechanical change. A decline in the degree of crosslinking and a decrease in crosslinking enzyme activity also occur around day 12 in the mouse (Akins et al., 2011; Ozasa, Tominaga, Nishimura, & Takeda, 1981). Expression of matricellular proteins such as thrombospondin 2 and tenascin C also decline during softening, although the exact role of these molecules in this process has not been determined (Akins et al., 2011).

1.3.6 Physiologic Cervical Ripening

In the late remodeling phase known as ripening, changes in the cervix proceed in a more rapid, robust fashion when compared to softening. As mentioned previously, maximal changes in collagen fiber morphological parameters coincide with maximal declines in cervical stiffness shortly before delivery. Immune cells such as monocytes and eosinophils influx the tissue (Holt, Timmons, Akgul, Akins, & Mahendroo, 2011). Serum progesterone levels, in the mouse, decline and estrogen increases (B. C. Timmons et al., 2014). Prostaglandins, often used clinically to induce cervical ripening, are not necessary for term cervical ripening and delivery. Canonical parturition genes including HA synthase 2 (*Has2*), connexin 26 (*Gjb2*), oxytocin receptor (*Oxtr*), and steroid 5 α reductase type 1 (*5ar1*) are upregulated at the end of pregnancy in the cervix.

1.3.7 Postpartum Tissue Repair

Effective tissue repair postpartum is integral to repetitive reproductive success of a species. The rapid nature of this process is specifically important in the rodent, where ovulation and subsequent fertilization of oocytes can take place the same day as delivery of pups. Activated immune cells including macrophages and neutrophils are present at increased numbers in the mouse cervix 1 day postpartum compared to a day 18 ripened cervix (Holt et al., 2011). Based on known functions of these immune cells in other systems, it is hypothesized that in the cervix during postpartum tissue repair, they are likely involved in extracellular matrix degradation and reorganization. A number of inflammatory and chemokine/cytokine genes including *Ccl6*, *Ccl11*, *Cxcl5*, *Il1b*, *Ccr1*, and *Tlr4* are also upregulated postpartum (B. C. Timmons, Mitchell, Gilpin, & Mahendroo, 2007). Genes

important for ECM synthesis and processing, including thrombospondin 2 (*Thbs2*), versican (*Vcan*), procollagen lysine, 2-oxoglutarate 5-dioxygenase 2 (*Plod2*), matrix metalloproteinase 19 (*Mmp19*), and serine peptidase inhibitor, clade B, member 2 (*Serpib2*) are upregulated shortly postpartum as well. Hyaluronan is also more abundant in the postpartum cervix (Ruscheinsky, De la Motte, & Mahendroo, 2008). As measured by biomechanics, the postpartum cervix becomes stiffer during the tissue repair process, when compared to samples collected at the end of pregnancy (Barone, Feola, Moalli, & Abramowitch, 2012; Buhimschi, Sora, Zhao, & Buhimschi, 2009; B. Timmons, Akins, & Mahendroo, 2010).

In another system, tissue repair has an important function in decreasing cancer metastasis. Work done in parous rat breast stroma demonstrates that collagen architecture after pregnancy slows the growth of tumors and decreases tumor cell invasion properties when compared to collagen in nulliparous stroma (Maller et al., 2013). These data demonstrate a distinction between never pregnant (virgin) and parous non-pregnant tissues. The postpartum cervical tissue repair process likely does not return a parous nonpregnant cervix to a virgin state and may have a number of protective functions in physiology.

1.3.8 LPS-Mediated Preterm Birth

Understanding the physiologic basis of parturition lends itself to comparisons and contrasts of pathological perturbations of the process, including preterm birth. Although nearly 60% of all preterm births lack a clinically identifiable cause, 25% can be attributed to infection.

Inflammasomes are part of the innate immune system responsible for activating a number of proinflammatory processes in response to the sensing of pathogens (figure 1.2) (Guo, Callaway, & Ting, 2015). Recent studies implicate inflammasomes as mediators of both sterile inflammation leading to spontaneous labor at term and pathological inflammation leading to preterm delivery both in women with antiphospholipid syndrome and women with acute histologic chorioamnionitis (Gomez-Lopez et al., 2017; Mulla et al., 2013; Romero et al., 2016). Endogenous danger signals, termed damage-associated molecular patterns (DAMPs), resulting from cellular stresses can trigger sterile inflammation. Pathogens, which are recognized by pattern recognition receptors (PRRs), and subsequent DAMP induction can induce pathological inflammation. Components of inflammasomes are expressed in the chorioamnion of women at term, and there is evidence of increased caspase-1 activation and mature IL1B in tissues from women at term and in labor compared to non-laboring term tissues (Romero et al., 2016). In response to pathogens recognized by a number of PRRs, human fetal membrane explants can mount an immune response (i.e. secrete cytokines), indicating these tissues express machinery needed for inflammasome activation (Hoang et al., 2014). Chorioamnion membranes from women with acute histologic chorioamnionitis at term show increased PRR gene expression, protein abundance, and downstream inflammasome activation as measured via caspase-dependent IL1B production *in vivo* that is not present in tissues from women without the pathologic finding (Gomez-Lopez et al., 2017).

To study infection-mediated preterm birth, a well-established model of inflammation is used. Intrauterine lipopolysaccharide (LPS) is administered in mid to late pregnancy in the mouse, which has a 19 day gestation (figure 1.3) (Elovitz, Wang, Chien, Rychlik, & Phillippe, 2003) . Previously published works highlight the distinct cervical features involved in LPS-mediated preterm birth in mice compared to cervical ripening at term. These studies demonstrate that the physiological changes in the tissue occurring in response to a number of hormonal and non-hormonal cues at the end of pregnancy are not fast-forwarded, or completed on a more limited timescale, in LPS-mediated preterm birth (Gonzalez, Xu, Chai, Ofori, & Elovitz, 2009; Holt et al., 2011). Rather, a unique set of features help define cervical remodeling in response to an infection or to inflammation, more generally.

Declining serum progesterone at the end of pregnancy, a process not seen in women, occurs at term and in response to LPS in the mouse (Mathur, Landgrebe, & Williamson, 1980; B. C. Timmons et al., 2014). Interestingly, however, serum levels of estradiol do not increase to the same degree in LPS-mediated preterm birth as they do at term. This difference in the serum progesterone to estrogen ratio—P:E is 80 at term and 528 in LPS preterm—indicates distinct hormone environments in the two groups.

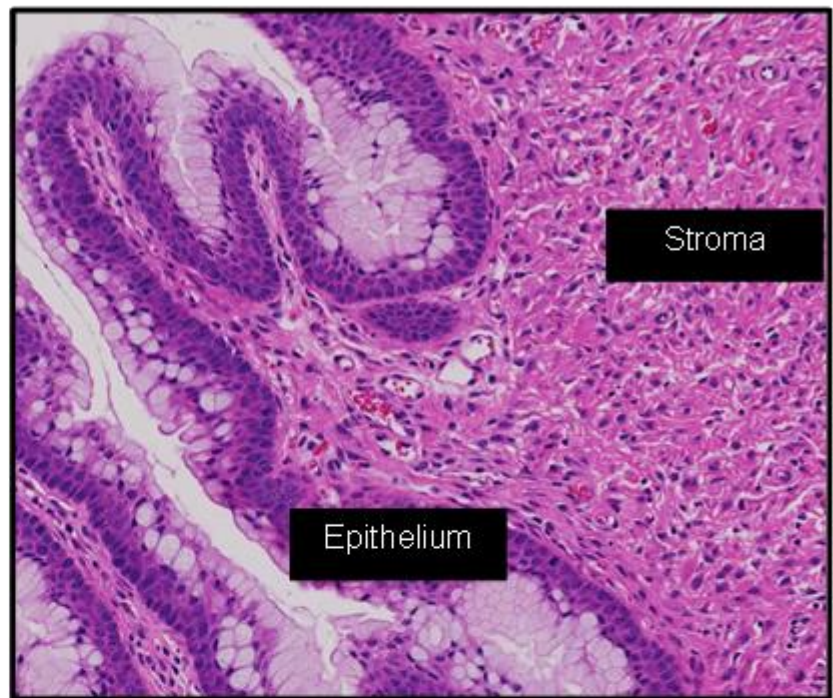
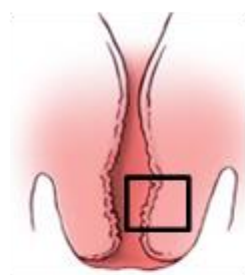
Endogenous prostaglandins, specifically PGE₂, PGF₂α, PGD₂, and 6-keto-PGF₁α, are increased in the cervix in LPS-mediated preterm birth and not increased in term cervical ripening. In fact, prostaglandins are essential for LPS-mediated preterm cervical compliance changes and dispensable for term cervical ripening (B. C. Timmons et al., 2014).

Additionally, a distinct population of immune cells is present in the cervix during LPS-mediated preterm birth compared to term. Whereas an influx of activated immune cells such as neutrophils and macrophages does not occur during a normal pregnancy until the postpartum tissue repair phase, these cells are present at increased numbers 6 hours after intrauterine LPS treatment on day 15 of mouse gestation, when compared to cells in the cervix of non-treated day 15 mice (Holt et al., 2011).

1.4 Goal of Research

The goal of this research is to use genomic approaches to add to the field's understanding of the unique transcriptome induced in the pregnant cervix in response to inflammation and to identify the subsequent structural changes in the extracellular matrix that allow for the increase in tissue compliance during preterm birth. More specifically, the purpose of this research is to identify novel and exclusive pathways in LPS-mediated preterm birth. Here I use RNA-seq to unbiasedly interrogate the inflammation-specific transcriptome in comparison to both a nontreated day 15 group and also cervical ripening at term (day 18). Given recent demonstration that elastic fibers contribute to the biomechanical function of the pregnant cervix, I sought to understand how the ultrastructure of elastic fibers is impacted upon LPS treatment. Taken together, these data provide unique insights into the distinct mechanisms of premature cervical remodeling in response to infection and may help explain increased risk of preterm birth after previous preterm births.

A.



B.

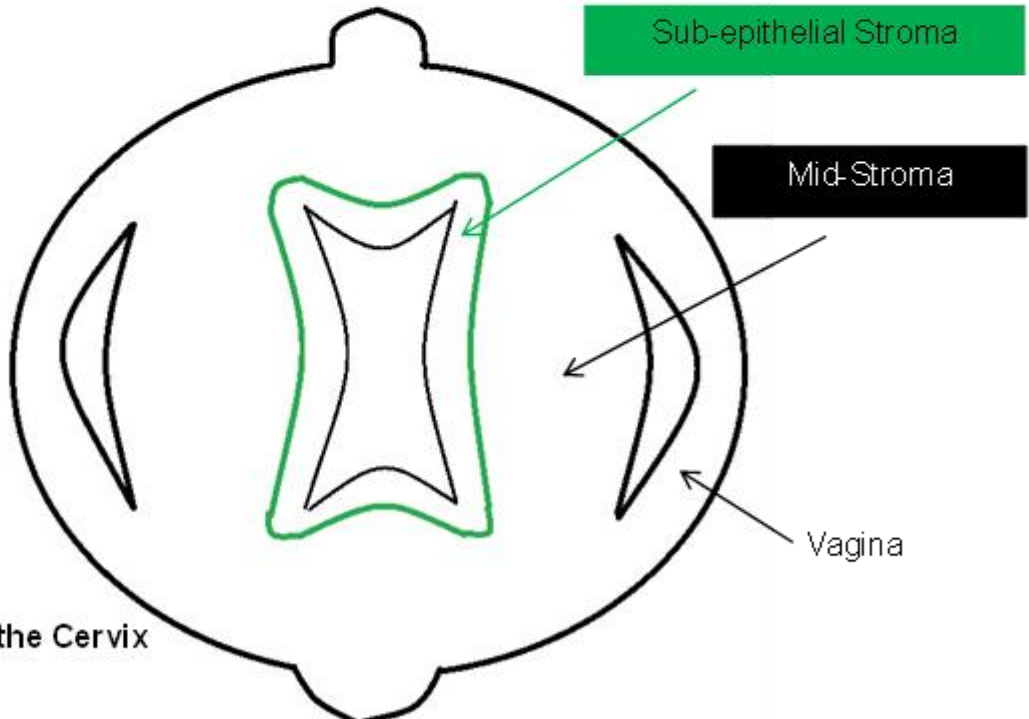
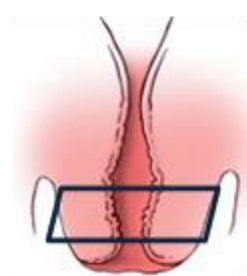


Figure 1-2 Regions of the Cervix

(A) Schematic depicting longitudinally sectioned cervix and H&E stained stromal and epithelial cell compartments. (B) Schematic depicting transversely sectioned cervix and regions of the stroma.

Inflammasome Activation

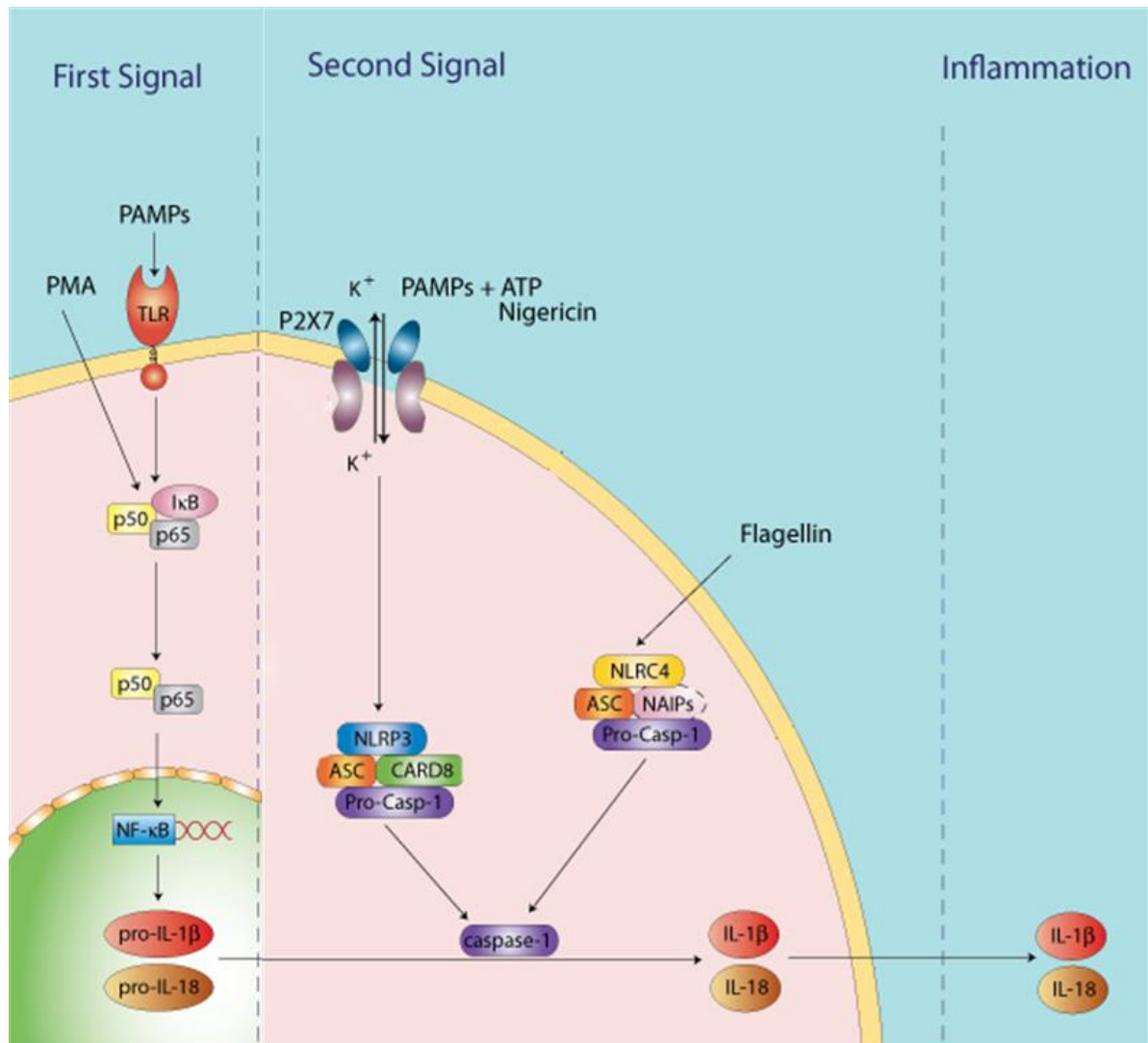
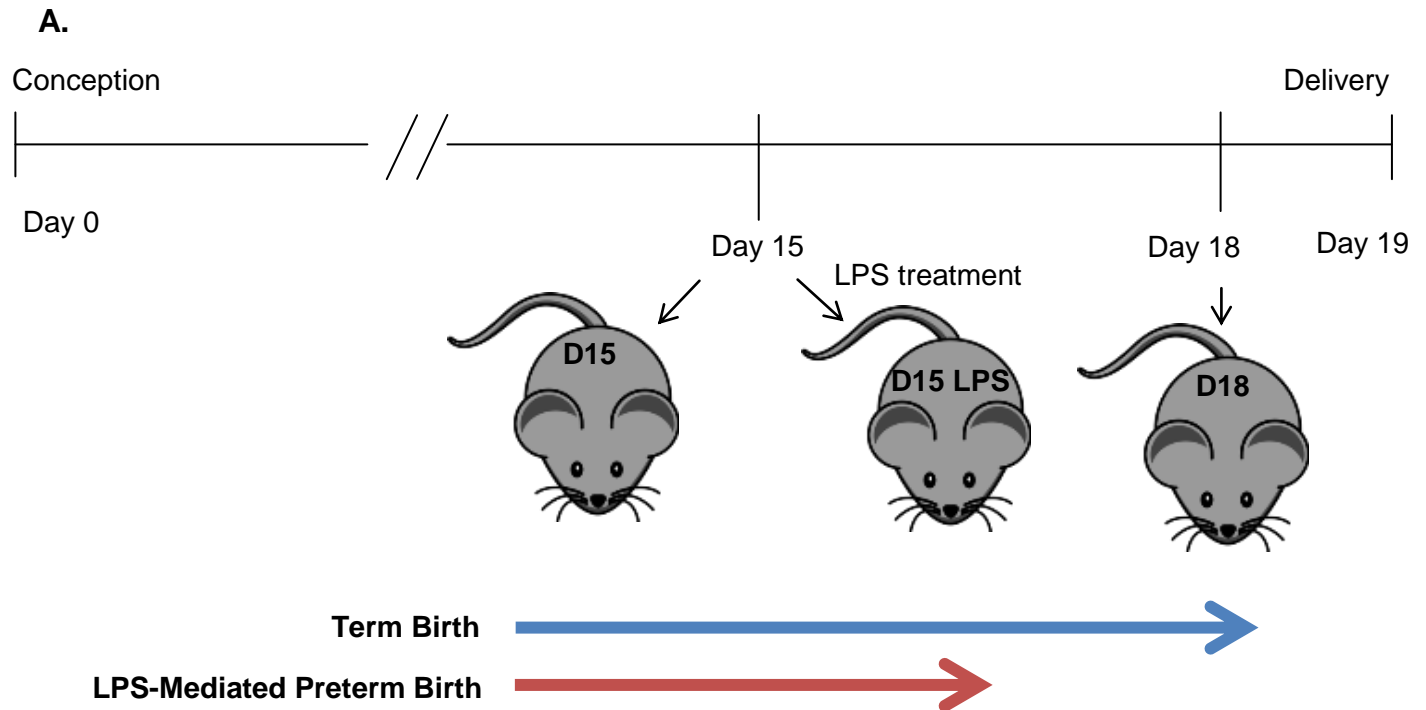


Figure 1.2. Inflammasome activation requires “second signal” for cleavage and activation of caspases and subsequent cytokine maturation.

Schematic demonstrating generalized steps to inflammasome activation. Pathogen-associated molecular patterns (PAMPs), such as are recognized by their specific receptor (Toll-like receptors, NOD-like receptors, RIG-I-like receptors, AIM2-like receptors). Downstream activation of gene transcription involving NF- κ B leads to upregulation of a number of proinflammatory genes—in this diagram, cytokine genes *Il1b* and *Il18*. A second signal, such as a DAMP (damage associated molecular pattern molecules), commonly cell-derived endogenous molecules including HMGB1, S100, ATP, uric acid, and RNA or DNA, are recognized by their specific receptors (including P2X7, Nlrp3, Nlr4, etc.). These receptors then incorporate into the inflammasome proper, a cytosolic protein complex which includes a number of adapter proteins and a pro-caspase protein that becomes cleaved upon activation. This activated caspase then processes and matures the cytokines previously produced by the first proinflammatory signal. Image modified from Invitrogen. (Anders & Schaefer, 2014; Tang, Kang, Coyne, Zeh, & Lotze, 2012).



B.

	LPS-Mediated Preterm	Term
Serum progesterone to estrogen ratio	P:E 528	P:E 80
Dependence on prostaglandins	YES	NO
Immune cell populations	neutrophils & macrophages	monocytes & eosinophils

Figure 1.3. Comparisons of LPS-Mediated Preterm and Term Birth

(A) Schematic depicting mouse gestation (19 days), LPS treatment on day 15 (infection-mediated preterm birth model, and term (day 18). **(B)** Table depicting unique features of LPS-mediated preterm and term birth.

CHAPTER TWO

Cervical Transcriptome Signature in Term & LPS-Mediated Preterm Birth

2.1 Introduction

Cervical changes in response to infection are quite different than those that occur during cervical ripening at term. These include differences in immune cell populations, concentrations of circulating steroid hormones, and the necessity of prostaglandins. Despite these marked differences, the compliance of the mouse cervix 6 hours after LPS treatment on gestation day 15 is similar to the compliance of the term ripened cervix at gestation day 18 (B. C. Timmons et al., 2014).

At the transcription level, parturition has been well characterized. Broadly, parturition has been studied as a process initiated in an inflammatory fashion, with decreased progesterone function allowing for activation of NF- κ B in a number of reproductive tissues including the uterus and fetal membranes (Haddad et al., 2006; Osman et al., 2003). In the cervix, however, an induction of proinflammatory actions including influx of activated immune cells such as neutrophils and macrophages and upregulated inflammatory gene expression, does not occur during cervical ripening but instead after the initiation of labor and delivery (Gonzalez et al., 2009; Hassan et al., 2006).

As highlighted in chapter 1, the reduced function of progesterone and its subsequent influence on gene expression is impacted by microRNAs. In the cervix more specifically, however, a limited number of studies have been carried out to highlight microRNA function

in the context of pregnancy and parturition. In the context of labor at term, microRNAs 223, 34b, and 34c have been identified as upregulated in the cervixes of women at term in labor versus term women not in labor (Hassan et al., 2010). Analyses of microRNAs in the cervix of women have identified differential expression of a number of microRNAs, including miR-143, 145, 199a & b, and miR-140 as upregulated in subjects who later delivered preterm compared to those that later delivered at term (Elovitz et al., 2014). Given the method of extraction for RNA isolation likely enriches for epithelial cells on the ectocervix, it is not surprising that these microRNAs in other contexts have been shown to target a number of molecules involved in epithelial barrier function. Another study of cervical microRNAs measured expression of miRs in relation to length of gestation (Sanders et al., 2015). Higher miR 30-e, 142, 148b, 29b, and 223 expression is associated with decreased length of gestation. mRNA targets of these miRs are reported to involve cellular functions including DNA replication, recombination, and repair, and amino acid metabolism.

With respect to the proinflammatory cytokine IL1B, a nonessential role for its function has been uncovered in the context of physiological pregnancy and parturition. *Il1b* null, IL1B converting enzyme (CASP1) null, and IL-1 receptor type 1 null mice all have normal fertility and parturition, indicating a nonessential role for IL1B cytokine and signaling pathway in pregnancy physiology (Leon, Conn, Glaccum, & Kluger, 1996; P. Li et al., 1995; Nadeau-Vallee et al., 2016; Zheng et al., 1995). In the context of intraamniotic infection, it has been known for nearly three decades that IL1B is associated with preterm labor (Romero, Brody, et al., 1989; Romero, Durum, et al., 1989). A number of animal studies, including in the mouse, rabbit, and nonhuman primate, demonstrate that IL1B is

sufficient to induce labor with systemic, intrauterine, or intraamniotic administration (Nadeau-Vallee et al., 2016; Romero, Mazor, & Tartakovsky, 1991; Sadowsky, Adams, Gravett, Witkin, & Novy, 2006; Yoshimura & Hirsch, 2005). Attenuation of IL1B induced preterm birth via recombinant endogenous IL1B receptor antagonist demonstrates that IL1B acts through the IL1B receptor (Romero & Tartakovsky, 1992). The mechanism of action is hypothesized to be the cytokine's induction of prostaglandins in reproductive tissues (Bartlett, Sawdy, & Mann, 1999; Romero, Brody, et al., 1989). Another study indicates the existence and importance of other pathways in addition to IL1B signaling in inflammation-mediated preterm birth. When used in an intrauterine model of infection-mediated preterm birth, namely intrauterine LPS, Anakinra (Kineret), a IL1B receptor antagonist commonly used clinically to treat rheumatoid arthritis, does not prevent preterm birth (Leitner et al., 2014).

Given that changes in the cervix that are the tissue's response to infection involve different features that are unique to an overall inflammatory cervical milieu in LPS-mediated preterm birth, studies were undertaken to better understand the molecular mechanisms underlying the processes by which the cervix responds to infection and inflammation and how these responses lead to preterm delivery. RNA sequencing was used to interrogate the protein coding and long noncoding RNA transcriptome (polyA RNA-seq). Small RNA-seq was also carried out to identify microRNAs that may be regulating polyA targets. Using RNA-seq, an unbiased approach to analyze gene expression, allowed for comparisons and contrasts of the changes that occur in the cervix in response to inflammation to those changes that occur at the end of pregnancy physiologically. This approach expands our understanding

of how the cervix physiologically prepares for delivery and how the cervix responds at the transcription level to inflammation. Ideally, development of therapies to prevent preterm birth, once at-risk women have been identified, will abrogate pathologic processes and allow for appropriately timed parturition to occur.

The goal of this project was to identify novel and exclusive cervical pathways in inflammation-mediated preterm birth.

2.2 Results

2.2.1 RNA-seq identifies unique transcriptomes in LPS-mediated preterm and term cervical ripening.

To determine changes in gene expression during LPS-mediated preterm birth, we compared day 15 LPS cervixes to untreated day 15 cervixes (figure 2.1A). To determine gene expression changes during term cervical ripening, we compared day 18 to day 15. To ensure the changes in gene expression observed upon LPS treatment were due to the LPS and not due to the survival surgery, sham surgery to day 15 comparisons were also included. Overall gene expression patterns between LPS preterm (day 15 vs day 15 LPS) and term (day 15 vs day 18) were quite distinct (figure 2.1B). The number of differentially expressed genes exclusive to day 15 LPS vs day 15 (2918 genes) was impressive, compared to day 18 vs day 15 (475 genes) (figure 2.1C). Relatively few genes (267) were common between the two groups and differentially expressed as compared to day 15. A similar number of genes was up-regulated in the day 15 LPS group compared to gestation day 15 and down-regulated in the same group, while the majority of differentially expressed genes were up-regulated in the

day 18 group (figure 2.1D). In agreement with previous reports using qPCR, gene expression of canonical parturition genes including connexin 26 (*Gjb2*), hyaluronan synthase (*Has2*), and steroid 5 α reductase type I (*Srd5a1*), as measured using RNA-seq, are upregulated at term and not changing in day 15 LPS (table 2.1) (Holt et al., 2011). Reciprocally, proinflammatory genes previously reported via qPCR to be upregulated upon LPS treatment on day 15 and not changing at term—in particular cyclooxygenase 2 (*Ptgs2*), prostaglandin E synthase (*Ptges*), interleukin 6 (*Il6*), interleukin 1 alpha (*Il1a*), and C-X-C motif chemokine ligand 2 (*Cxcl2*)— are identified as upregulated via RNA-seq in day 15 LPS and not on day 18 compared to day 15 (table 2.2) (Holt et al., 2011).

Sham surgery (day 15 sham) compared to day 15 (untreated) induced relatively few gene expression changes compared to the LPS preterm and day 18 term samples. About 200 upregulated and nearly 20 downregulated genes were observed in sham vs day 15 (figure 2.1D). Genes within the upregulated category upon sham surgery are parts of “single-organism metabolic process” and “response to stress” biological processes and “endopeptidase regulator activity” and “peptidase regulator activity” molecular functions. Downregulated genes are “unclassified” when run through the Gene Ontology biological process and molecular functions databases. The sham surgery group is a model of sterile inflammation, and a threshold for preterm birth is not reached.

2.2.2 Gene ontology analyses identify exclusive pathways in LPS-mediated preterm birth.

To gain insight into potential pathways driving premature cervical changes and term cervical ripening, Gene Ontology (GO) Analyses were performed. The most enriched

processes from the group of genes upregulated in LPS preterm exclusively included immune, defense, and inflammatory responses and response to wounding (figure 2.2A). Analyses of genes upregulated exclusively at term identified the *biological processes lipid catabolic process, female pregnancy, epidermis development, and ectoderm development* as the most enriched. Biological processes from genes upregulated both in LPS preterm and term include *positive regulation of developmental process, keratinization, positive regulation of biological process, and positive regulation of cellular processes* (figure 2.2A). Further in-depth comparisons of GO pathways based on Molecular Function, Biological Processes and KEGG Pathways specific to the LPS preterm group identify a common theme consistent with pathogen sensing, inflammasome components, and downstream endpoints of inflammasome activation (figure 2.2B). Inflammasomes are also reported to induce prostaglandins, which have been previously established as essential mediators of LPS-induced preterm birth (B. C. Timmons et al., 2014). Given the critical role of inflammasome activation in host defense against pathogens, sterile insults, and host-derived molecules via activation of downstream proinflammatory events, we focused our studies on inflammasome activation in the cervix as a novel pathway specific to LPS-mediated preterm birth.

2.2.3 Components of the inflammasome are upregulated in LPS-mediated preterm birth.

Genes encoding components of the inflammasome activation pathway were identified in the RNA-seq dataset as upregulated in LPS preterm and not changing at term (figure 2.3A). These include the pattern recognition receptors *Nod 2, Nrlc4, Nrlc5, Nrlp3*, activator protein *Gbp5*, executioner proteins *Casp1* and *Casp4*, and cytokine *Il1b*. Gene expression analysis by quantitative PCR corroborate RNA-seq results for the majority of genes and

show an increase in gene expression in inflammation preterm (day 15 LPS vs day 15) and no change at term (day 18 vs day 15) for *Gbp5*, *Nlrc5*, *Nod2*, *Casp4* and *Il1b* (figure 2.3B).

Using quantitative PCR, transcripts encoding *Nlrp3* and *Nlrp4* were not significantly induced in the LPS-mediated preterm birth group while transcripts encoding *Casp1* were induced at term.

2.2.4 Cervical caspase activity is unchanged in LPS-mediated preterm birth

A functional consequence of inflammasome complex formation is caspase 1 and/or 4 activation. These caspases are synthesized as inactive proteins that are then cleaved by the inflammasome complex to be activated (Cerretti et al., 1992; Thornberry et al., 1992). Caspase 1 and caspase 4 (also known as mouse caspase 11) are the major inflammatory caspases known to cleave and activate IL1B and IL18, which are cytokines that can be secreted and invoke inflammatory responses in other cells (Fantuzzi, 2001; Gracie, Robertson, & McInnes, 2003). Fluorescent Caspase Assay kits were used to assess activity of caspases 1 and 4 in whole tissue lysates from day 15 untreated, day 15 sham, day 15 LPS, and day 18 mouse cervixes. Activity of caspase 1 was similar in all groups—relatively low—and unchanged with LPS treatment and on day 18 compared to day 15 (figure 2.4A). Recombinant human caspase-1 at 0.5 and 1.0 unit concentrations were used as positive controls, and a dose dependent increase in activity was observed. Caspase 4 activity was similar in all groups—relatively low—and unchanged with LPS treatment or on day 18 compared to day 15 in both assays (figure 2.4B). The positive controls (recombinant human caspase 4) for the caspase 4 activity assay did not show a concentration-dependent increase in fluorescence (activity), suggesting a potential technical problem with the assay.

The processing and maturation of IL1B is a consequence of caspase 1 or 4 activation. While activity of both caspase 1 and 4 were low and unchanging in the cervixes of mice treated with LPS, IL1B protein in mouse cervical lysates was measured as a read out of caspase activation. IL1B levels were measured in whole cervical tissue lysates from untreated day 15 mice, day 15 sham mice, day 15 LPS mice, and day 18 mice. IL1B was measurable in each of the day 15 LPS samples tested and amounts were significantly increased compared to non-treated day 15 (figure 2.4C). How a measurable increase in IL1B is occurring without measurable changes in caspase 1 and/or 4 activities will be discussed in the next section.

2.2.5 Inflammasome Activation in Epithelial Cells

In addition to determining if inflammasome activation is derived from immune cells in the cervix in response to intrauterine LPS treatment, the hypothesis that cervical epithelial cells may elicit immune surveillance responses through inflammasome activation was also tested. Evidence of inflammasome activation and an immune surveillance function of epithelial cells would add to our understanding of the epithelium as an immune protective barrier for the cervical tissue and the upper reproductive tract (Akgul, 2014). Inflammasome activation has been shown to be important in other mucosal epithelia, such as the intestines, where epithelial cells are in contact with bacterial flora, much like the mucosal epithelia of the cervix is in contact with vaginal flora (Sellin, Maslowski, Maloy, & Hardt, 2015). For example, without cytosolic protein NLRC4, an important receptor for flagellin sensing in inflammasome activation, *Nlrc4* knockout mice are more susceptible than wildtype mice to

C. rodentium, a bacterium similar to enterohemorrhagic *E. coli*, which indicates the importance of the molecule in innate immunity (Nordlander, Pott, & Maloy, 2014).

Human immortalized cervical epithelial cells were used to evaluate the potential activation of inflammasomes in response to TLR agonists and second signals ATP & flagellin. Two cell lines were used in these studies. End1 cells were derived from the endocervical canal and Ect1 cells from the ectocervix. Neither cell type express toll-like receptor 4 (TLR4) and thus are not responsive to TLR4 ligand LPS. Instead, these cells express TLR2, and proinflammatory responses can be induced in response to its ligand, synthetic triacylated lipopeptide Pam3CSK4 (PamCSK) (figure 2.5).

To induce true inflammasome activation, cells require not only an inflammatory priming but also a “second hit,” or a more specific danger signal (figure 1.2) (Jo, Kim, Shin, & Sasakawa, 2016; Schroder & Tschopp, 2010). Ect1 cells were chosen for these initial experiments because they express NLRP3 while End1 cells do not (high or undetermined cT values upon qPCR experimentation with validated primers). It was determined that ATP would be used to test the cells’ capacity for Nlrp3 induction and flagellin for Nlrc4 experiments (Lee et al., 2012; Miao et al., 2006; Zhao et al., 2011).

With PamCSK treatment alone, genes involved in inflammasome activation, from pathogen sensing (including *NLRP3* and *NOD2*) to downstream inflammatory response (including *IL8*, and *PTGS2*), are upregulated in Ect1 cells (figure 2.6). Only *PTGS2* is further upregulated with PamCSK priming and subsequent flagellin treatment, compared to priming alone.

Much like in mouse tissue lysate experiments, very low caspase 1 activity is detected in Ect1 and End1 cell lysates primed with PamCSK and subsequently treated with ATP or flagellin (figure 2.7). In Ect1 cells, caspase 4 activity was similarly low and unchanging in all treatment groups. End1 cells were not tested for caspase 4 activity.

Results from a human IL1B ELISA kit demonstrate that even untreated Ect1 and End1 cells at basal conditions have measurable intracellular IL1B (figure 2.8). This amount increases significantly with PamCSK, PamCSK + ATP, and PamCSK + flagellin. These data demonstrate human epithelial cells can produce IL1B in response to proinflammatory stimuli.

The cell's ability to secrete processed (mature) IL1B is a functional readout of inflammasome activation (Brough et al., 2003; Brough & Rothwell, 2007; Lopez-Castejon & Brough, 2011)). To measuring the abundance of IL1B in the cell culture media (predicted to be secreted mature IL1B), no detectable protein was found, even with concentration of the culture supernatant and appropriate immune cell media control. Future experiments using western blotting, a method to separate pro and mature forms of IL1B based on size, will be carried out in cell lysates. These experiments will help determine if the epithelial cells are able to produce mature IL1B in response to proinflammatory stimuli but lack the means to secrete the protein.

2.2.6 Cervical Small RNAs Induced in LPS-Mediated Preterm & Term Birth

In addition to polyA RNA-seq, small RNA-seq was carried out to determine the expression of cervical microRNAs (miRs) in day 15 mouse samples and to pinpoint how expression of these microRNAs change with sham or LPS treatment and at term (day 18). The goal of small RNA-seq was to identify miRs that may target mRNAs identified as

differentially expressed in the polyA RNA-seq dataset. Small RNA-seq identified 33 and 22 microRNAs differentially expressed (downregulated greater than 0.75 and upregulated greater than 1.5, $q < 0.05$) in day 15 LPS and day 18 respectively, compared to nontreated day 15 cervixes (figure 2.9A). As will be discussed below, because few LPS-induced miRNAs from this data set were validated using qPCR, microarray analyses were undertaken. The microarray analyses provided fewer differentially expressed microRNAs in day 15 LPS compared to untreated day 15 (figure 2.9B). Interestingly relatively few microRNAs were identified by both methods as being differentially expressed (figure 2.9C). All differentially regulated microRNAs, as measured by small RNA-seq and microarray analyses, are highlighted in tables 2-3, 2-4, 2-5, and 2-6.

2.2.7 miR-210 and The Hifs

Small RNA-seq identified miR-210 as significantly upregulated at term and downregulated upon LPS treatment in the pregnant mouse cervix. This miR is a member of a group of genes called “hypoxomiRs” that are induced during hypoxia and important for a variety of processes in such an environment (Wang et al., 2014). In fact, expression of this microRNA has been shown to be regulated by direct HIF1A binding at the gene promoter (Cicchillitti et al., 2012). PolyA RNA-seq identified *Hif1a* as significantly upregulated both in day 15 LPS and day 18 groups compared to day 15 (table 2-7). A target of miR-210 is *Hif3a*, a negative regulator of hypoxia responses (Maynard et al., 2005). *Hif3a* is downregulated significantly in day 18 and in day 15 LPS, compared to untreated day 15 and as seen via RNA-seq (table 2-7). qPCR data corroborate the upregulation of both *Hif1a* and miR-210 as well as a trend toward downregulation of the target *Hif3a* at term (figure 2.10 A,

B). In disagreement with RNA-seq data, qPCR data indicate a significant upregulation of *Hif3a* in response to LPS.

2.2.8 Other miRs in Term and LPS-mediated Preterm Birth

Another miR identified as significantly upregulated at term, both in the small RNA-seq and microarray data sets, is miR-203. This microRNA was chosen for validation purposes, and qPCR results corroborate the upregulation on day 18 and not in day 15 LPS (figure 2.10B).

MicroRNAs such as miR-155 and miR-144, identified as upregulated via small RNA-seq in day 15 LPS vs day 15, did not demonstrate significant upregulation in qPCR (table 2-7, figure 2.10C).

2.2.9 mechanomiRs & ECM-targeting miRs

Given the limited reproducibility and therefore functionality of the microRNA analyses completed as part of this project, literature searches provided a second avenue for microRNA selection. The first experiment undertaken involved selection of a housekeeping miR for a new qPCR platform (discussed in methods). miR-26a was selected for its relatively high expression level (~21.5 Ct values) and stability of expression throughout a normal pregnancy time course (figure 2.11).

Two mechanically sensitive microRNAs, miR-98 and let-7e, were identified in a screen of mouse muscular dystrophies (Mohamed, Hajira, Lopez, & Boriek, 2015). Expression of these microRNAs was examined in both a normal pregnancy time course of the mouse cervix and also in response to sham (day 15 sham) and LPS (day 15 LPS) treatments (figure 2.12A, B). Expression of neither mechanomiR was changed significantly

throughout pregnancy, and only let-7e was downregulated in response to LPS (figure 2.12B, table 2-8).

MicroRNAs 195 and the 29 family (a, b, and c) have been shown to regulate the expression of a number of ECM proteins during times of vascular and cardiac dysfunction (Kumarswamy & Thum, 2013; van Rooij et al., 2008; Zampetaki et al., 2014). The expression pattern of these microRNAs was elucidated using qPCR (figure 2.13). No significant changes in gene expression compared to non-pregnant cervix tissues was observed in the normal pregnancy time course (figure 2.13 A), and no significant changes in LPS treated samples were observed, compared to day 15 untreated (figure 2.13 B).

2.3 Discussion

This study builds upon previous findings that demonstrate distinct features of the cervical remodeling process in response to inflammation are not present at term (Gonzalez et al., 2009; Holt et al., 2011; B. C. Timmons et al., 2014). The distinct transcriptome signatures uncovered in this study add to the field's understanding of the differences between LPS-mediated and term cervical remodeling. In particular, LPS does not alter expression of many genes regulated in term cervical ripening, while pathways related to and downstream of inflammatory responses were most dramatically induced upon LPS treatment. While much valuable information remains to be extracted from the RNA-seq data sets, in the present study, these data have been leveraged to identify transcriptional pathways that may direct features of LPS-mediated preterm cervical remodeling—including prostaglandin synthesis—

that have previously been identified (B. C. Timmons et al., 2014). The inflammasome pathway in the cervix is exclusive to LPS-mediated preterm birth.

As mentioned in the introduction, recent studies implicate inflammasomes as mediators of both sterile inflammation leading to spontaneous labor at term and pathological inflammation leading to preterm delivery both in women with antiphospholipid syndrome and women with acute histologic chorioamnionitis (Gomez-Lopez et al., 2017; Mulla et al., 2013; Romero et al., 2016). In response to pathogens recognized by a number of PRRs, human fetal membrane explants can mount an impressive immune response (i.e. secrete cytokines), indicating these tissues express machinery needed for inflammasome activation (Hoang et al., 2014). Chorioamnion membranes from women with acute histologic chorioamnionitis at term show increased inflammasome activation as measured via caspase-dependent IL1B production *in vivo* that is not present in tissues from women without the pathologic finding (Gomez-Lopez et al., 2017).

In contrast to evidence in the fetal membranes that inflammasome-mediated increases in IL1B play a role in fetal membrane signaling for the initiation of labor both at term and with pathogen-mediated inflammation, our transcriptome data in the mouse confine the potential for inflammasome activation to the LPS-treated group and not term ripening. These data suggest specific employment of inflammasome-directed proinflammatory responses in the fetal membranes, at term or preterm, is consistent with the absence of functional necessity of the membranes after delivery; in contrast, the cervix must undergo rapid, precise tissue repair postpartum to ensure protection of the reproductive tract and allow for successful future pregnancies.

Inflammasome-mediated activation of caspases is potentially a key regulatory step in directing downstream processes that collectively facilitate LPS-mediated premature cervical remodeling. These include the rapid influx of signaling lipids such as eicosanoids, activation of the programmed cell death pathway pyroptosis, and expression of proteases induced by mature IL1B. The “eicosanoid storm,” of which prostaglandins are a subset, is independent of the other inflammasome outputs, namely cytokine maturation and pyroptosis (Rathinam & Fitzgerald, 2016; von Moltke et al., 2012). It has been previously demonstrated that prostaglandins are necessary for LPS-mediated preterm cervical remodeling and preterm birth and not required for cervical remodeling and birth at term (B. C. Timmons et al., 2014). Pyroptosis, an inflammatory cell death program, is a caspase-dependent process initiated upon inflammasome activation (Fink & Cookson, 2006). As illustrated in figure 2.2B, a number of cell death-related pathways were identified by RNA-seq as enriched upon LPS treatment compared to day 15 and not at term. Programmed cell death is a defense mechanism against infection that includes non-lytic forms of cell death, termed apoptosis, as well as highly inflammatory lytic cell death pathways, termed necroptosis and pyroptosis. The expression pattern of genes belonging to each of these pathways supports the upregulation of necroptosis and pyroptosis predominantly, with little evidence for activation of the apoptotic pathway in LPS-mediated preterm birth. While previous studies report a role for apoptosis in cervical ripening at term, both the transcriptional profile generated in this study and preliminary experiments (data not shown) demonstrating absence of increased TUNEL staining to assess DNA fragmentation as a marker for apoptosis in the cervix of LPS treated mice suggest programmed cell death pathways other than apoptosis may be relevant

(Leppert, 1998). Although not specifically investigated in this study, these auxiliary pathways may be induced in a caspase-dependent manner.

As a readout of inflammasome activation in the cervix of LPS-treated mice, IL1B protein abundance is increased. The set of caspase activity assay experiments presented here do not demonstrate increased activity in the cervix in response to LPS, and leave open the question of how IL1B processing occurs, if at all, in the cervix. The caspase activity studies were far from exhaustive, and using these data to conclude no increase in caspase activity would be misleading. Further caspase activity assays will need to be undertaken to investigate changes due to LPS.

There exist inflammasome-independent pathways for IL1B maturation, including through activity of serine proteases from neutrophils and macrophages (Coeshott et al., 1999; Dinarello, Simon, & van der Meer, 2012; Sugawara et al., 2001). Meprin α and Meprin β , metallopeptidases, can also cleave pro-IL1B into its mature and active 17kDa form (Herzog et al., 2009). Further experimentation involving these proteases, a subset of which are upregulated upon LPS as will be discussed in the next chapter, and their potential role in IL1B maturation in the cervix during LPS-mediated preterm birth will need to be completed.

In terms of IL1B, the ELISA kit used in these studies is likely not specific for the mature, processed, and physiologically active form of the protein. Western blots that allow for size separation of pro (unprocessed) and mature IL1B were undertaken but the results highly variable, unreliable, and not convincing that there was any measurable mature form in the mouse cervix.

On the whole, this study identifies a unique polyA and small RNA cervical transcriptome in LPS-mediated preterm birth that is distinct from cervical ripening at term. Genes involved in inflammasome activation are upregulated in response to LPS and not at term, indicating this is a novel and exclusive cervical pathway in LPS-mediated preterm birth. A measurable increase in IL1B, a potential output of the inflammasome, occurs in cervixes of mice treated with LPS compared to cervixes from untreated day 15 mice. This increase is not seen at term. Cell culture studies completed in human cervical epithelial cell lines, while preliminary, suggest that primary sources of inflammasomes are cervical immune cells rather than epithelial cells. These cells contain the machinery (i.e. receptors, caspases, and cytokines) needed for activation of the inflammasome and lack just the ability to secrete the IL1B. Laser capture microscopy might one day allow for inflammasome experiments in an isolated mouse epithelial cell population.

An eicosanoid storm, or rapid influx of prostaglandins, also occurs in the cervix in LPS-mediated preterm birth exclusively, and this pathway is also known to be induced in response to inflammasome activation (Rathinam & Fitzgerald, 2016; von Moltke et al., 2012). Further studies to identify which cell death pathways are induced in response to LPS will add to our understanding of the myriad pathways mediated by LPS and inflammasome activation.

Although not definitely proven in cell culture using immortalized human cervical cells, it is still possible that cervical epithelial cells elicit inflammasome activation in response to inflammation.

Looking at the big picture, the original intention of the project was to identify differentially expressed microRNAs and their polyA targets to gain insight into cervical gene regulation driving LPS-mediated preterm birth, all the while understanding similarities to and differences from cervical ripening at term. AgoHITSClip, a way to catch microRNAs in the act of targeting of polyA transcripts, was also planned for further validation of targeting relationships (Chi, Zang, Mele, & Darnell, 2009). This project hit a snag with the relatively few reliable, reproducible microRNAs identified as differentially expressed in LPS-treated day 15 and day 18 cervixes, compared to day 15 untreated cervixes (figure 2.10C). qPCR studies to corroborate differential expression of microRNAs in LPS were far from fruitful while some microRNAs (miR-210 and miR-203) had similarly significant changes in expression using qPCR and in small RNA-seq/microarray.

As with any project, completion allows for contemplation of improvements on the experimental set up, which will be discussed next. The timing of sample collection and presence of unique cell populations in the tissues may be improved upon for clearer results in the RNA-seq data set. Additionally, had the experiment been designed using the most recent understanding of the biology—namely LPS-mediated preterm birth's dependence on prostaglandins—the RNA-seq results may have been more informative and less confirmatory of what is already known (namely that inflammation occurs in response to LPS).

The initial data collected in this study were transcriptomic signatures of term and inflammation-mediated preterm mouse cervixes. Uncovering novel and exclusive cervical pathways in LPS-mediated preterm birth was a more specific sub-aim of the project. Regarding methods, samples for day 15 LPS were taken at the 6 hour mark following

survival surgery for the injection of intrauterine LPS. At this time point, it has been shown that the cervix is equally compliant in comparison to term ripened cervixes and that LPS-treated mice will deliver within 1-3 hours post collection (7-9 hours post-surgery) (B. C. Timmons et al., 2014). To elucidate *gene expression profiles* driving changes in the cervix occurring in response to LPS, looking at the 6 hour time point is too late (considering the *changes* have already occurred and the cervix is prepped for delivery). Mouse cervix samples collected at 1, 2, and 4 hours after intrauterine application of LPS have demonstrated an early and time-dependent increase in proinflammatory gene expression (data in chapter 3), demonstrating that further experiments using those time points are warranted. The cervical transcriptomes generated here for both term and LPS-mediated preterm birth may provide insight into pathways driving postpartum tissue repair as well, both physiologic after a birth at term and potentially pathologically and preterm in response to LPS—a complex process currently understudied in the field but discussed later.

The second concern with the project revolves around the unique cell populations residing in the cervix at time of tissue collection. With the likelihood that the dataset captures transcripts from immune cells in addition to epithelial and stromal cells, comparing the transcriptomes of neutrophils and macrophages, both of which have been shown to be present at increased number upon LPS treatment compared to day 15 and day 18, to transcripts from monocytes and eosinophils (more abundant on day 18 vs day 15) is akin to whole transcriptome comparisons between apples and oranges. Knowing from which cell populations transcripts are originating would aid in development of mechanistic strategies

(i.e. cell culture modeling) for interrogating the necessity of such processes in physiologic and pathologic cervical changes at term and in response to LPS.

Finally, in designing the RNA-seq study of the transcriptomic signatures driving cervical ripening at term and cervical changes in response to LPS leading to preterm birth, utilization of the knowledge that pathways induced or somehow connected to prostaglandins could have narrowed the biological question being asked. In my hands, day 15 pregnant mice treated with intraperitoneal (IP) LPS deliver preterm between 10-12 hours post-injection (data not shown). Others have shown in their own hands that this preterm birth, and maximal decline in cervical stiffness, can be rescued with oral gavage of Cox-2 inhibitor SC-236 (B. C. Timmons et al., 2014). Use of this SC-236 inhibitor, which blocks the rate limiting step of prostaglandin synthesis, demonstrates the necessity of prostaglandins in LPS-mediated preterm birth (Gross et al., 2000) . Using RNA-seq to elucidate the gene expression differences between IP-LPS (preterm delivery) and IP-LPS + SC236 (no preterm delivery) could have aided in furthering our understanding of prostaglandin-mediated pathways involved in extracellular matrix reorganization in response to LPS and leading to preterm delivery. This likely would have produced a smaller list of differentially expressed transcripts and less dataset noise.

2.4 Materials and Methods

2.4.1 Mice

All animal studies were conducted in accordance with the standards of humane animal care as described in the NIH Guide for the Care and Use of Laboratory Animals. The research protocols were approved by the IACUC office at the University of Texas Southwestern Medical Center. Mice were housed under a 12 h-light/12 h- dark cycle at 22°C. Virgin C57B6/129sv 2-6 month old female mice were caged with fertile males of the same strain for 6 hours. The presence of a vaginal plug at the end of the 6 hours was considered as day 0 of pregnancy, with birth of the pups generally occurring early morning day 19.

2.4.2 Inflammation Preterm Labor Model

Intrauterine injection of LPS (day 15 LPS) was used to induce preterm labor as previously described (Holt et al., 2011). Briefly, mice on day 15 of pregnancy were anesthetized between 0700-0900, and 30uL sterile water (sham) or 5mg/mL LPS (*E. coli* O55:B5 Sigma, St. Louis, MO) was injected intrauterine. Cervical tissues were collected 6 hours after surgery and before the onset of labor, which occurs approximately 7-9 hours after LPS administration.

2.4.3 RNA Sequencing

RNA was isolated using an miRNeasy kit from Qiagen (Hilden, Germany). Quantity was determined using a Nanodrop and quality determined using a Bio-Rad Experion. RNAs with RNA Quality Index (RQI) scores above 9 were used to make cDNA libraries. Eight total cDNA libraries from four different time points/treatment groups (day 15, day 15 sham, day 15 LPS, and day 18) were prepared, with duplicate libraries for biological replicates containing 4 cervixes each. 1.25 µg RNA from each cervix was pooled for 5µg of starting RNA in each library. Library preparation was carried out as described previously (Zhong et

al., 2011). 100 base pair, paired end sequencing was carried out on an Illumina sequencer to a depth of 100 million reads. As indicated in supplemental table 4, the total reads for each library was in the range of 8-10 million reads with 94-95% mappable raw reads. We developed a computational pipeline to determine the differentially expressed genes between the conditions, which included the following steps: reads were aligned to the *mm9* genome using the spliced read aligner TopHat version v.2.0.4, transcriptome assembly was carried out using Cufflinks v.2.0.2 with default parameters, filtered transcripts were merged into distinct non overlapping sets using Cuffmerge, and Cuffdiff was used to calculate the differential expression genes between the conditions (Kim et al., 2013; Trapnell et al., 2010).

2.4.4 Transcriptome Data Analysis

The differentially expressed genes extracted from the above analysis were then used in downstream analyses. Venn Diagrams were generated using Venn Diagram Plotter version 1.5.5228.29250 for the differentially expressed genes in different conditions. Gene Ontology Analyses and KEGG pathways were determined using DAVID, a web tool for functional annotation and gene enrichment analysis for the genes that are specifically expressed at Day 15 LPS treatment as compared to Day 18. Heatmaps were generated using Java TreeView for the significantly expressed genes in at least one condition to analyze the effect in the specified condition (Dennis et al., 2003).

2.4.5 RNA isolation and quantitative PCR

Total RNA was isolated as previously described (Nallasamy et al., 2017a). cDNA synthesis was carried out using 0.5µg total RNA and 5x iScript Reverse Transcription Supermix (Bio-Rad, Hercules, CA). Quantitative PCR primers used in this study were

designed and purchased from Invitrogen. Target gene expression was normalized to the expression of housekeeping gene *Ppib* using the $2^{-\Delta\Delta Ct}$ relative gene expression method (User Bulletin no. 2; Applied BioSystems).

2.4.6 Caspase Activity Assays

Whole mouse cervixes were dissected as described above and flash frozen before being stored at -80. For caspase 1 activity, tissues were homogenized in RIPA buffer + Protease Inhibitors (Sigma). For caspase 4 activity, tissues were homogenized in lysis buffer provided by Abcam in assay kits. Lysates were left on ice for 30 minutes then spun at max speed for 10 minutes before supernatant was taken for protein concentration (BCA) assay. 75ug of lysate for caspase 1 and 36ug of lysate for caspase 4, in technical replicate was used for fluorescence activity and kit protocols followed (Abcam catalog #s ab39412 caspase 1 and ab65658 caspase 4). Values were subtracted from blank no substrate buffer control.

2.4.7 IL1B ELISA

Flash frozen cervical tissues were homogenized in 300uL Abcam lysis buffer and left on ice for 30 minutes before centrifugation at 4° C for 10 minutes (cat no. 65658, Abcam, UK). Protein concentration was determined (BCA assay, Thermo Scientific, Rockford, IL). IL1B protein was measured via Mouse IL-1 beta/IL-1F2 DuoSet ELISA (R&D Systems DY401-5) in technical replicates of 100uL supernatant for day 15, day 15 sham, and day 18 samples while a 3x dilution (33uL lysate + 66uL lysis buffer) was used for day 15 LPS samples to maintain the measurements in assay range.

2.4.8 Cell Culture Inflammasome Induction

Ect1 (human ectocervical epithelial HPV-16 E6/E7 transformed cat # CRL-2614) and End1 (human endocervical epithelial E6/E7 transformed cat # CRL-2615) cells were obtained from ATCC. Cells were cultured under standard conditions in Keratinocyte Serum-Free Medium (KSFM) with supplements as recommended, and media were changed every 72 hours. Cells were cultured in 75mL flasks and allowed to grow to 80% confluence before splitting with trypsin. Cells were then cultured in 6 well plates for 48 hours and 80% confluence reached. Cells were washed and cultured with KSFM media without supplements overnight. On the morning of the experiment, cells were washed and again cultured with KSFM.

Time and concentration course results using qPCR primers for proinflammatory genes are shown in figure 2-14. 1.5ug/mL PamCSK (Invitrogen cat code tlr1-pms) at 1.5 hours were the chosen concentration and timing for inflammatory priming. At completion of the priming, cells were washed with warm PBS and new, supplement-free medium was placed in the wells atop the cells. For inflammasome induction, 2mM treatment with ATP (sigma cat # A6419) for 40 minutes and transfection of 20ng flagellin (sigma cat # SRP8029) was performed (Lee et al., 2012; Miao et al., 2006). For transfections, Xfect Protein Transfection Kit (Clontech cat # 631327) and beta-galactosidase staining kit (Clontech cat # 631326) were used according to manufacturer's instructions. Blue beta-gal staining indicated successful transfection.

For molecular biology studies, 300uL RNASTat 60 was placed on cells with previously aspirated media. Cells were scraped and RNA isolation proceeded as noted

above. qPCR was also carried out as noted above using human primers and 36b4 as the housekeeping gene.

2.4.9 Small RNA-seq

Small RNA-seq was carried out using 50 base pair single-end sequencing on an Illumina sequencer as above. Reaper was used for trimming adapters, Tally for removing redundancies, Bowtie for alignment to *mm10*, and EdgeR for differential expression.

2.4.10 Microarray

MicroRNA expression was measured using an Affymetrix GeneChip miRNA 3.0 Array (Thermo Fisher Scientific, Santa Clara, CA; Genomics & Microarray Core Facility, UT Southwestern, Dallas, TX). Results were analyzed using Expression Console software version 1.3.1.187. Differential expression was determined by Partek software analyses (St. Louis, MO).

2.4.11 Initial Validation of Small RNA-seq & Microarray: qPCR Studies

Initial attempts to validate differentially expressed microRNAs from small RNA-seq and microarray studies utilized TaqMan MicroRNA Reverse Transcription Kit (cat # 4366596; Applied BioSystems, Foster City, CA) and microRNA specific primers from TaqMan MicroRNA Assays (cat # 4427975) and protocol was followed as written. qPCR was carried out also using microRNA specific primers and TaqMan Master Mix (cat # 4324018). Gene expression was normalized to U6 housekeeping gene and relative gene expression determined by 2^{-ddCt} as above.

2.4.12 MechanomiR & ECM Targeting miR qPCR Studies

Due to the timing of its availability and the universal (non-miR specific as above) reverse transcription step, TaqMan Advanced miRNA Assays were used for these qPCR studies. cDNA synthesis was carried out using the TaqMan Advanced miRNA cDNA Synthesis Kit (cat # A28007) and qPCR completed using gene specific primers (cat # A25576) and the TaqMan Fast Advanced Master Mix (cat # 4444963). Gene expression was normalized to miR-26a expression and relative gene expression determined via $2^{-\Delta\Delta Ct}$ method as above.

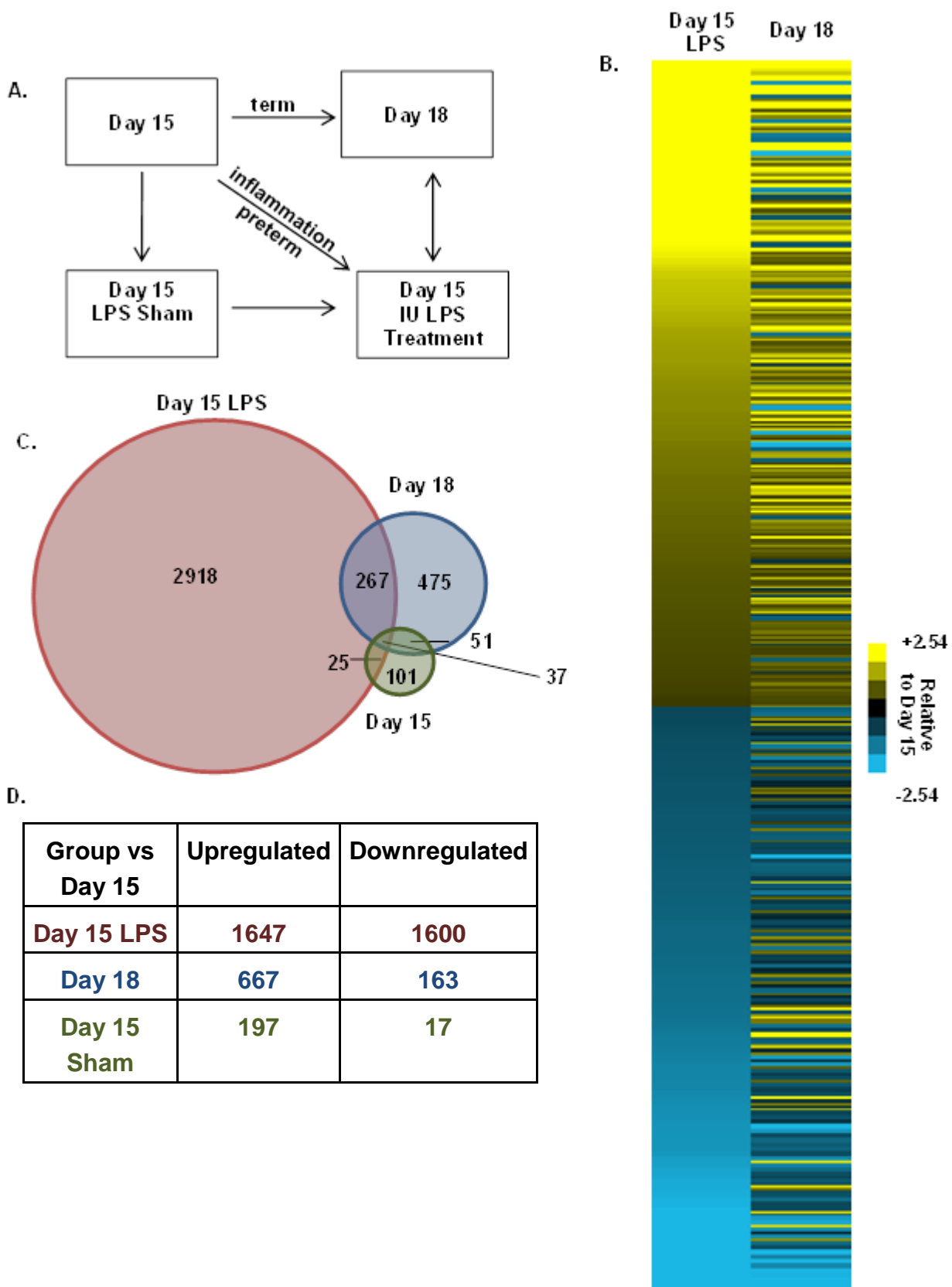


Figure 2.1. RNA-seq analyses of the pregnant mouse cervix demonstrate unique transcriptome profiles in term and LPS-mediated preterm cervical remodeling.

(A) Schematic indicating time points (day 15 and day 18) and treatment groups (sham and intrauterine LPS) used in RNA-seq. Two libraries of four cervixes each were constructed for each of the 4 conditions. (B) Heatmap of all differentially expressed transcripts in day 15 LPS and day 18 cervixes, both compared to untreated day 15 samples. (C) Venn diagram with the total number of differentially expressed transcripts in each group (day 15 sham, day 15 LPS, and day 18) compared to day 15. (D) Table with numbers of upregulated and downregulated transcripts in each condition (day 15 sham, day 15 LPS, and day 18) compared to day 15.

Table 2-1: Fold change of canonical parturition genes, measured by RNA-seq.

Gene	Fold change vs Day 15	
	Day 15 LPS	Day 18
<i>Gjb2</i>	no change	5.96
<i>Has2</i>	no change	2.12
<i>Srd5a1</i>	no change	2.39

Table 2-2: Fold change of proinflammatory genes, measured by RNA-seq

Gene	Fold change vs Day 15	
	Day 15 LPS	Day 18
<i>Cxcl2</i>	176.71	no change
<i>Il1a</i>	35.64	no change
<i>Il6</i>	141.31	no change
<i>Ptges</i>	2.56	no change
<i>Ptgs2</i>	28.43	no change

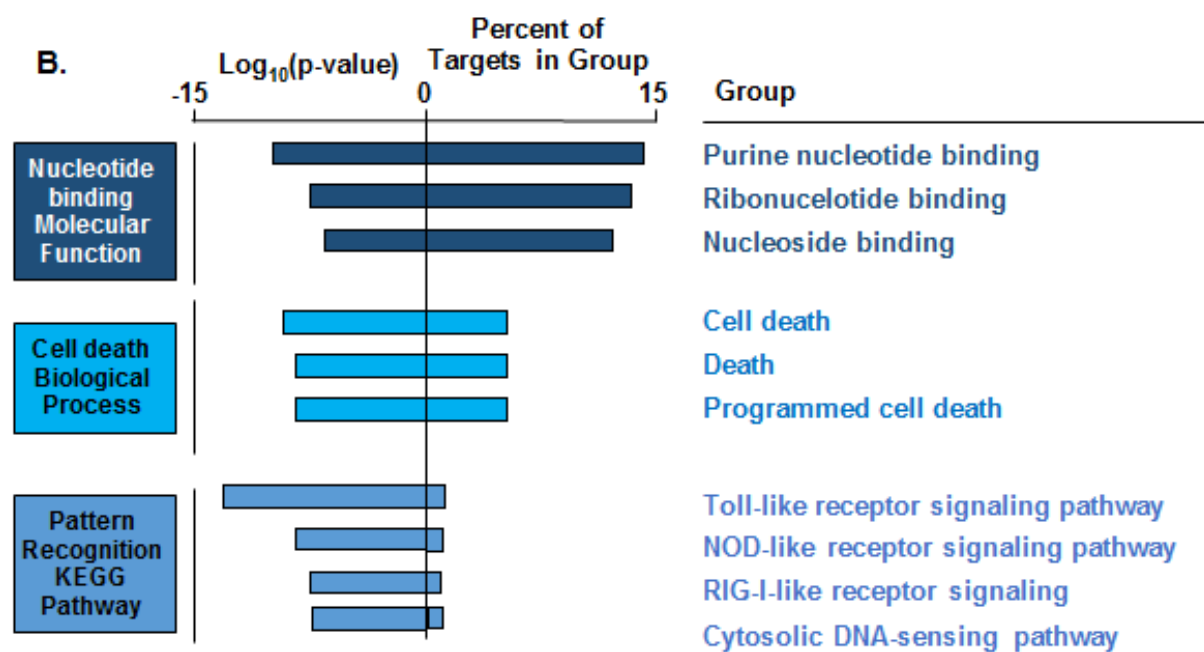
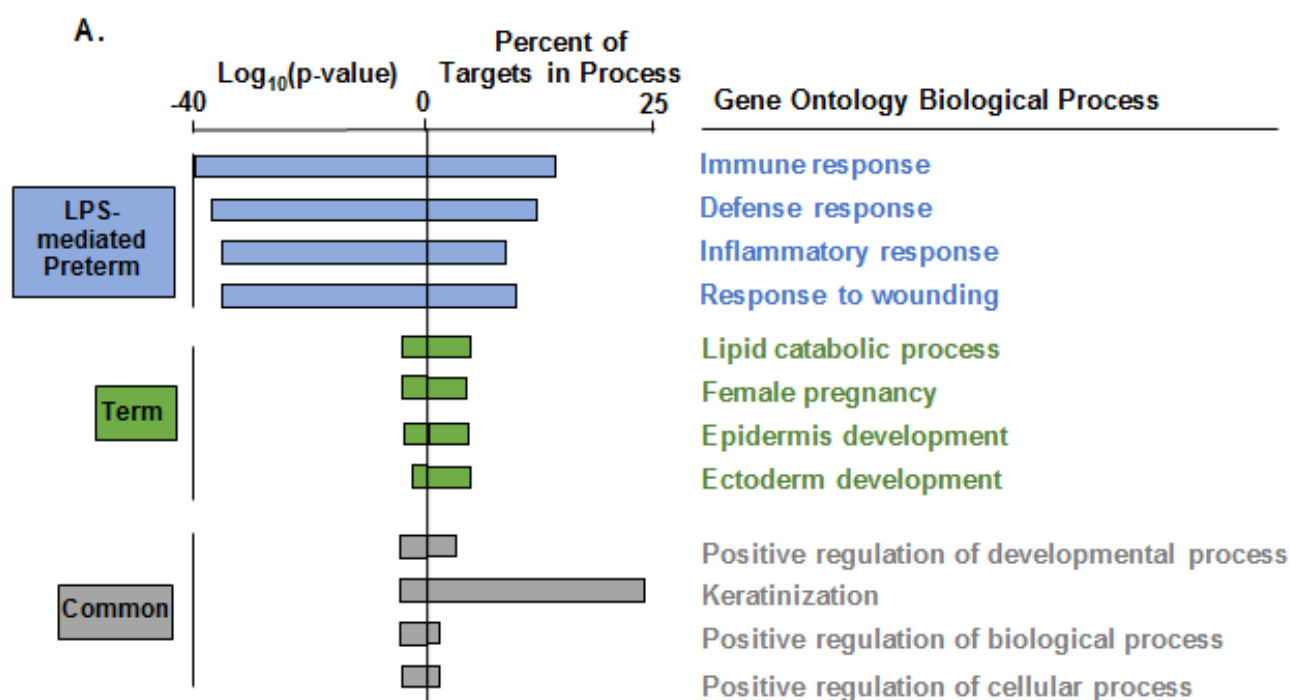
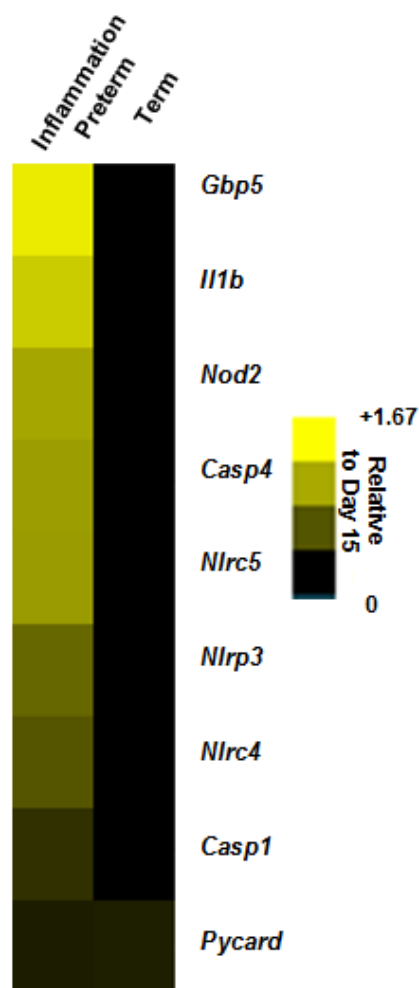


Figure 2.2. Gene Ontology and KEGG pathway analyses of term and LPS-mediated preterm cervical remodeling.

(A) Gene ontology analyses demonstrate enrichment of unique biological processes in term and LPS-mediated preterm birth. The most statistically significant process with genes expressed exclusively in each of the groups and those commonly expressed between them (common) are presented. Percentages indicate the percentage of genes in the process represented in the data set. (B) Gene ontology analyses (nucleotide binding related molecular functions and cell death biological processes) and KEGG analysis (pattern recognition receptor related pathways) of genes expressed in LPS preterm exclusively. Components of inflammasome activation fall within several of the indicated pathways and processes.

A. Inflammasome Components

B.

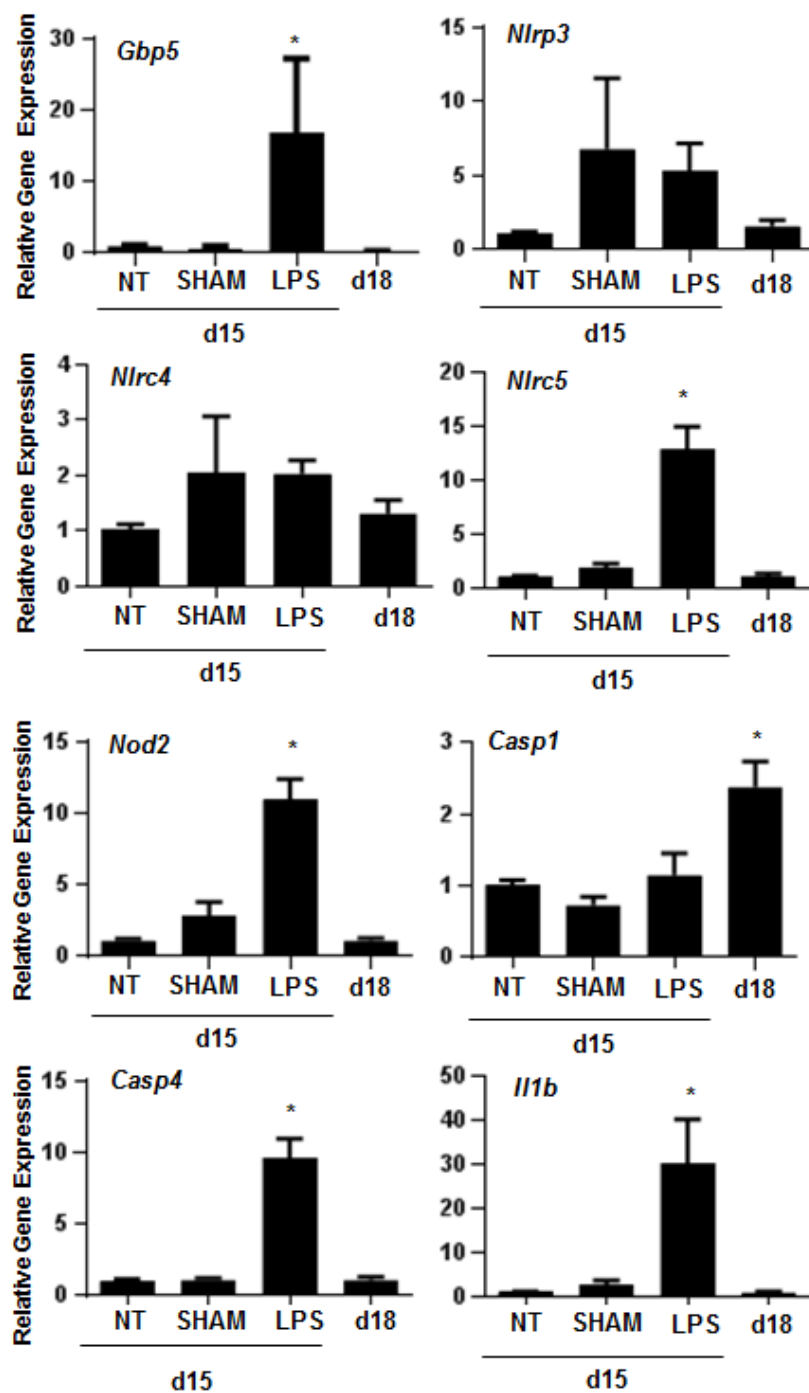


Figure 2.3. Components of the inflammasome are upregulated in LPS-mediated preterm birth exclusively.

(A) Heatmap of select inflammasome-related genes and their expression pattern in day 15 LPS cervixes vs day 15 cervixes (LPS preterm) and in day 18 cervixes vs day 15 cervixes (term). (B) qPCR results of selected inflammasome genes showing relative gene expression on day 15, day 15 sham, day 15 LPS, and day 18. The values expressed are mean \pm SEM. (n=5-7 cervixes per group, One way ANOVA * P<0.05 relative to day 15).

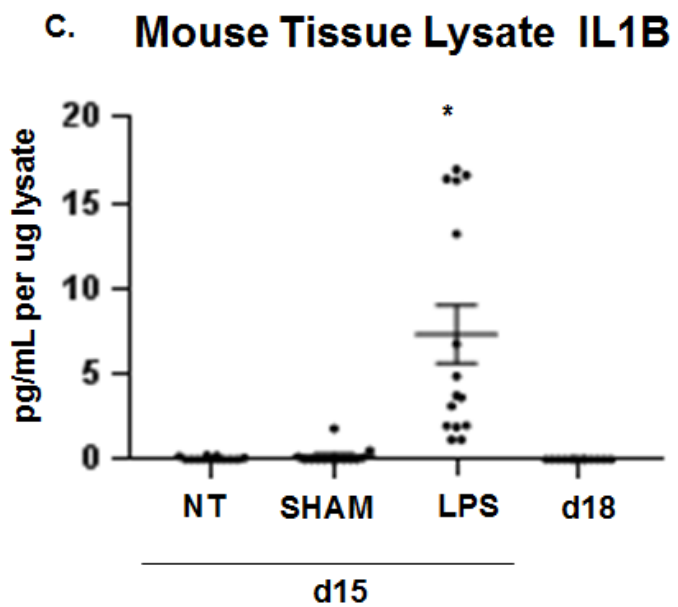
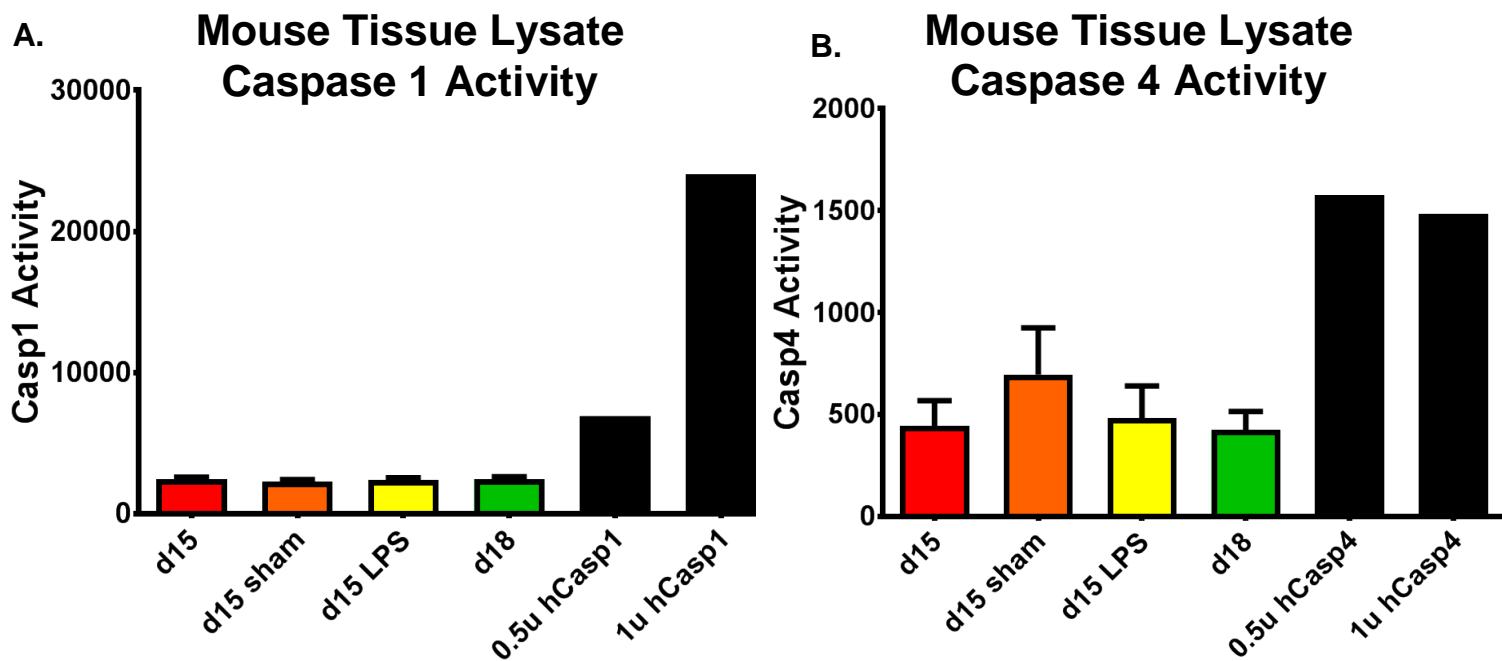


Figure 2.4. Cervical caspase 1 and 4 activities are unchanged in LPS-mediated preterm birth

(A) Activity assay results for caspase 1 activity in day 15 (untreated), day 15 sham, day 15 LPS, and day 18 cervixes. Recombinant human Caspase 1 was used for positive control.

Values are mean \pm SEM. (n=4-5 cervixes per group). Experiment completed once. (B)

Activity assay results for caspase 4 activity in day 15 (untreated), day 15 sham, day 15 LPS, and day 18 cervixes. Recombinant human Caspase 4 was used for positive control. Values

are mean \pm SEM. (n=4-5 cervixes per group). Experiment completed once (C) ELISA

results for IL1B in whole tissue lysates from the cervix of day 15, day 15 sham, day 15 LPS, and day 18 mice. Three separate experiments were performed with a total of 13-15 total

cervixes per group. (One way ANOVA * $P < 0.05$ relative to day 15)

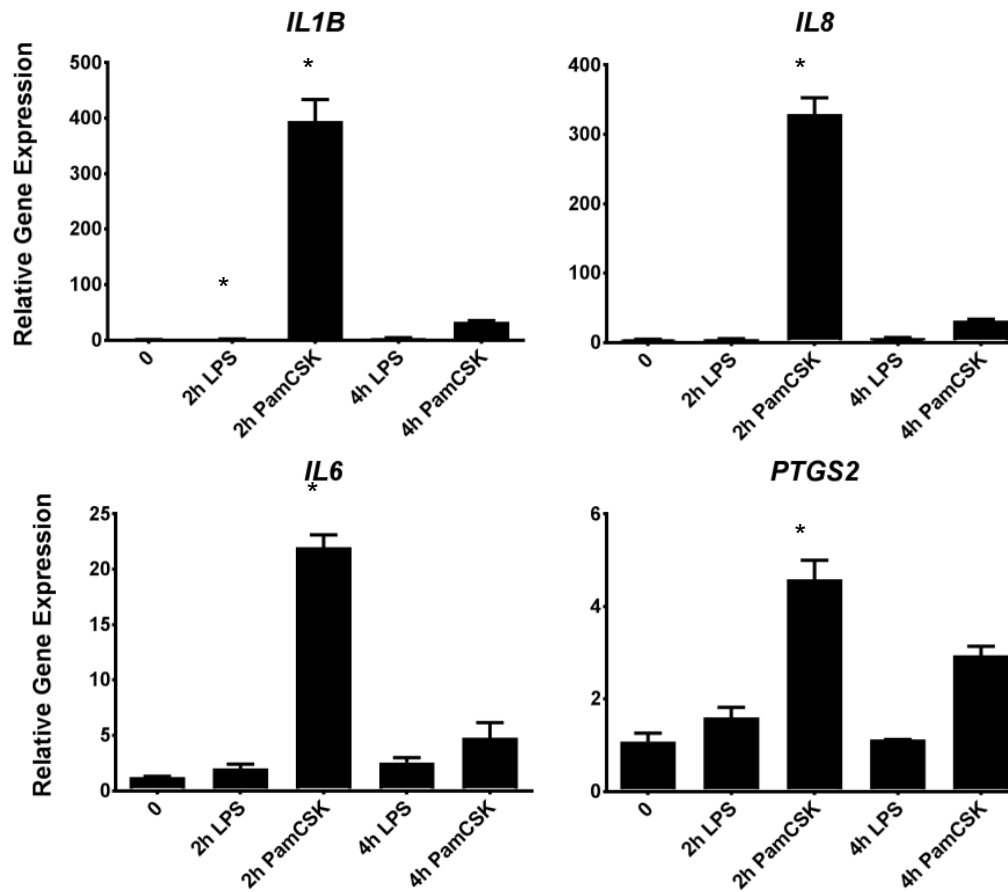


Figure 2.5. End1 cell proinflammatory responses to LPS and PamCSK

qPCR results of selected proinflammatory genes showing relative gene expression in End1 cells when treated with TLR4 ligand LPS and TLR2/TLR1 ligand PamCSK for 2 and 4 hours. The values expressed are mean \pm SEM. (n=2-4 separate wells per group, one experiment). One way ANOVA * P<0.05 relative to vehicle (0).

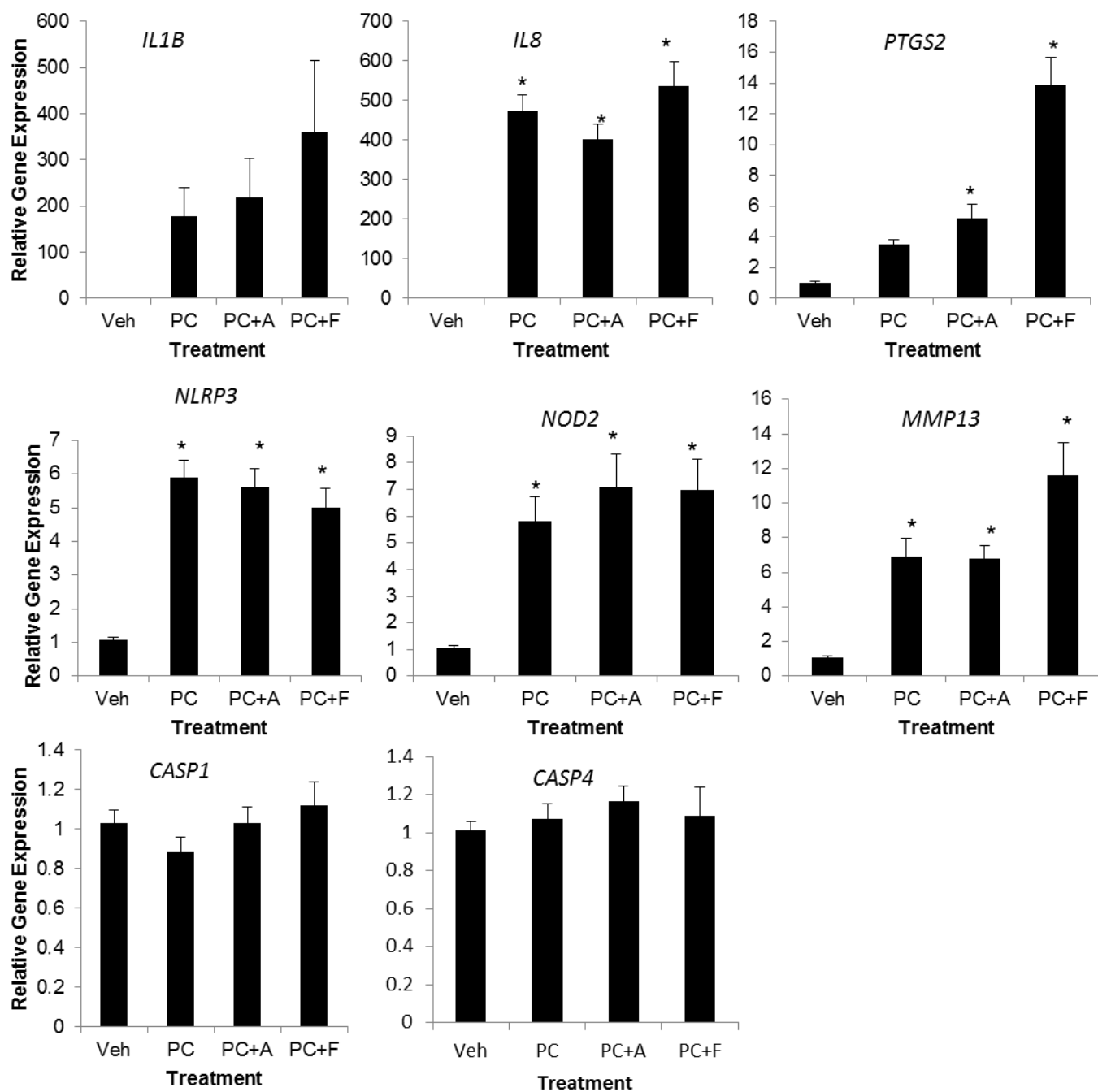


Figure 2.6. Ect1 cell response to PamCSK and ATP or flagellin treatment

qPCR results of selected inflammasome genes showing relative gene expression in Ect1 cells when untreated (NT), treated with PamCSK (PC) and ATP for flagellin (flag). The values expressed are mean \pm SEM. One way ANOVA * $P < 0.05$ relative to vehicle (veh). (n=13 separate wells per group, three different experiments).

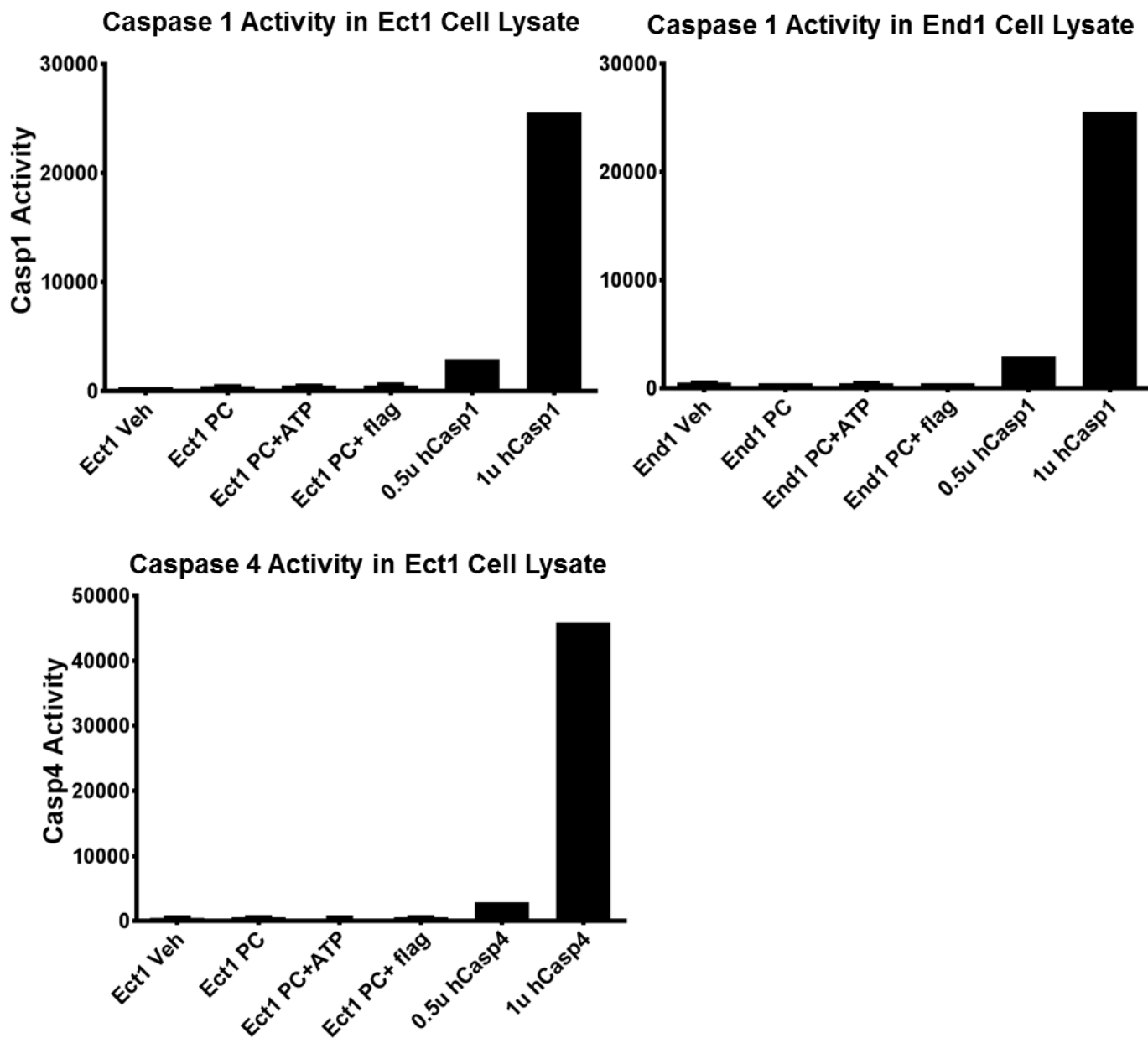


Figure 2.7. Low and unchanging caspase activity Ect1 and End1 cells in response to PamCSK and ATP or flagellin treatment

(A) Activity assay results for caspase 1 activity in Ect1 and End1 cell lysates. Recombinant human Caspase 1 was used for positive control. Values are mean \pm SEM. Ect1 cells n=3 replicates per group, two wells combined for each replicate, one experiment. End1 cells n=3-4 per group, single wells used, one experiment. (B) Activity assay results for caspase 4 activity in Ect1 cell lysates. Recombinant human Caspase 4 was used for positive control. Values are mean \pm SEM. Ect1 cells n=3 replicates per group, single wells used, one experiment.

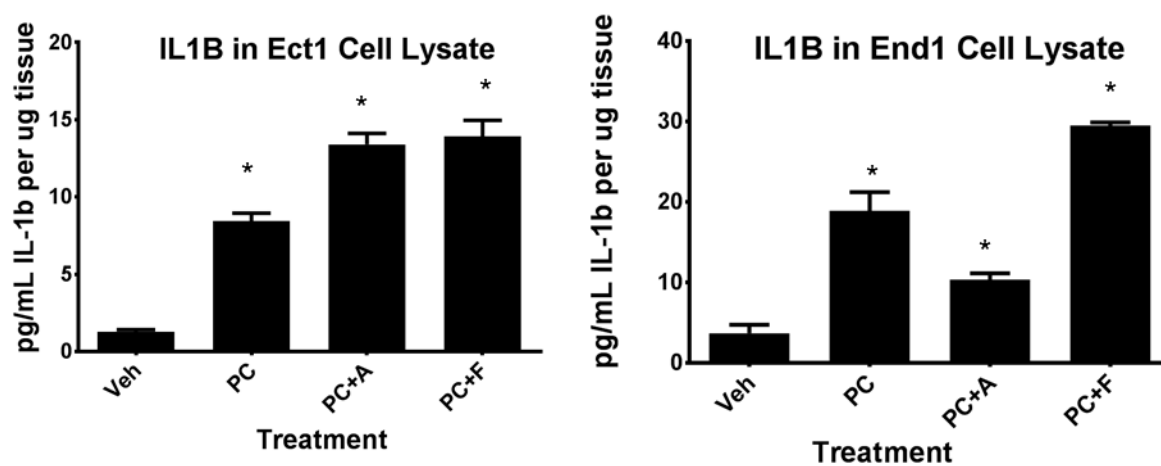
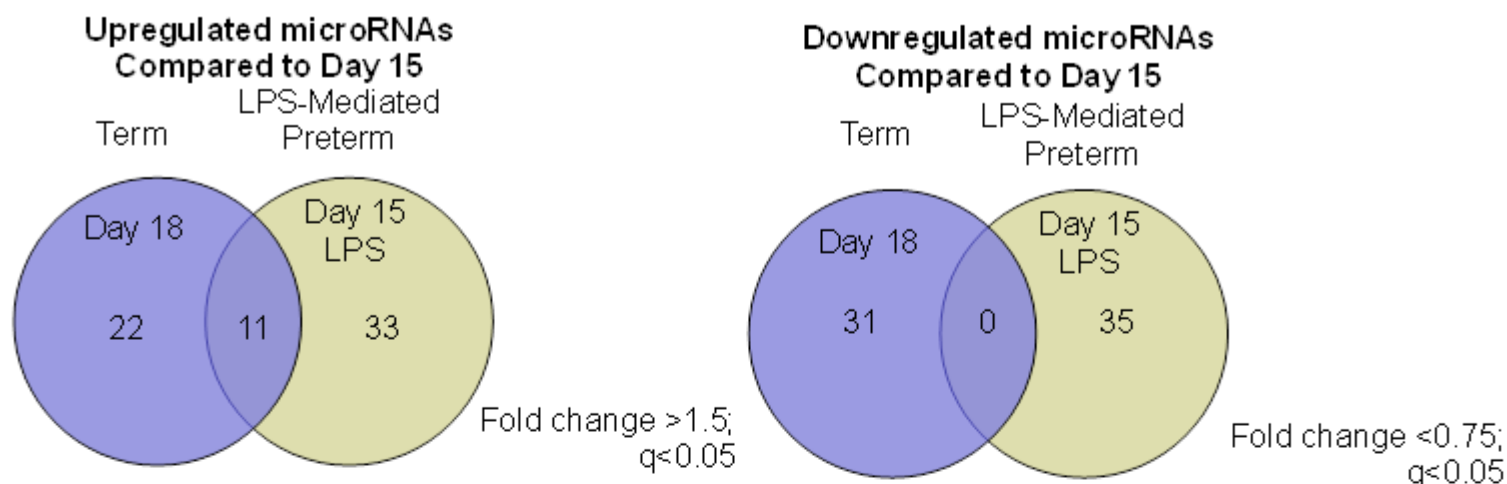


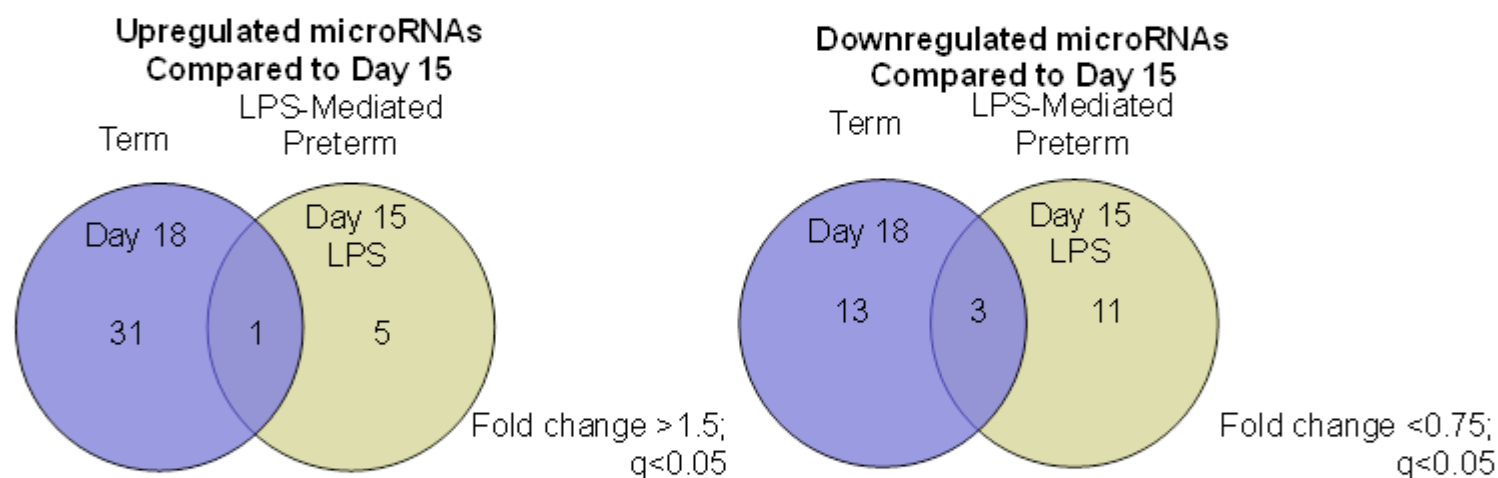
Figure 2.8. Intracellular IL1B in Ect1 and End1 lysate

ELISA results for human IL1B in whole cell lysates from Ect1 and End1 cells. Vehicle (veh) was compared to PamCSK (PC) treatment and PC + ATP or flagellin (PC+flag) groups. The values expressed are mean \pm SEM. (n=3-4 separate wells per group, One way ANOVA * $P < 0.05$ relative to vehicle (veh), one experiment).

Figure 2-10



B. MicroRNAs from Microarray Analyses



C. MicroRNAs Common Between Small RNA-seq and Microarray Analyses Comparisons to day 15

Downregulated in day 15 LPS	Upregulated in day 15 LPS
miR-423	miR-34c

Downregulated in day 18	Upregulated in day 18
None	miR-361
	miR-203
	miR-200b

Figure 2.9. Cervical microRNAs in term and LPS-mediated preterm birth

(A) Venn diagrams depicting the number of differentially expressed microRNAs in the cervix from small RNA-seq analyses in term (day 18 vs day 15) and LPS-mediated preterm (day 15 LPS vs day 15) birth. (B) Venn diagrams depicting the number of differentially expressed microRNAs in the cervix from microarray analyses in term (day 18 vs day 15) and LPS-mediated preterm (day 15 LPS vs day 15) birth. (C) Tables depicting microRNAs identified as differentially regulated in both small RNA-seq and microarray analyses for LPS-mediated preterm (day 15 LPS vs day 15) and term (day18 vs day 15).

Table 2-3: Downregulated MicroRNAs in Day 15 LPS vs Day 15 Cervices

Day 15 LPS vs Day 15 Downregulated Small RNA-seq	Fold Change	P-value
mmu-mir-129-1,mmu-mir-129-1-3p	0.396	0.014
mmu-mir-145a,mmu-mir-145a-5p	0.483	0.032
mmu-mir-150,mmu-mir-150-5p	0.389	0.023
mmu-mir-16-1,mmu-mir-16-5p	0.504	0.034
mmu-mir-16-2,mmu-mir-16-5p	0.503	0.034
mmu-mir-181b-1,mmu-mir-181b-1-3p	0.475	0.050
mmu-mir-1947,mmu-mir-1947-5p	0.376	0.040
mmu-mir-210,mmu-mir-210-5p	0.074	0.000
mmu-mir-25,mmu-mir-25-5p	0.388	0.004
mmu-mir-26a-1,mmu-mir-26a-1-3p	0.313	0.003
mmu-mir-299a,mmu-mir-299a-3p	0.354	0.011
mmu-mir-31,mmu-mir-31-5p	0.126	0.000
mmu-mir-34c,mmu-mir-34c-3p	0.318	0.007
mmu-mir-409,mmu-mir-409-3p	0.457	0.007
mmu-mir-423,mmu-mir-423-3p	0.277	0.001
mmu-mir-615,mmu-mir-615-3p	0.393	0.036

Day 15 LPS vs Day 15 Downregulated Microarray	Fold Change	P-value
hp_mmu-mir-1956_st	0.343647	0.047
hp_mmu-mir-384_st	0.336575	0.028
mmu-miR-135a-1-star_st	0.189727	0.021
mmu-miR-181c-star_st	0.221442	0.048
mmu-miR-1839-3p_st	0.165511	0.045
mmu-miR-187_st	0.311866	0.042
mmu-miR-1981_st	0.346758	0.011
mmu-miR-378-star_st	0.280486	0.000
mmu-miR-3971_st	0.278355	0.047
mmu-miR-423-5p_st	0.346277	0.031
mmu-miR-5114_st	0.173981	0.016
mmu-miR-539-3p_st	0.302708	0.023
mmu-miR-7b-star_st	0.207186	0.007
mmu-miR-874_st	0.297302	0.024

Table 2-4: Upregulated MicroRNAs in Day 15 LPS vs. Day 15 Cervices

Day 15 LPS vs Day 15 Upregulated Small RNA-seq	Fold Change	P-value
mmu-mir-362,mmu-mir-362-3p	2.965	0.005
mmu-let-7k,mmu-let-7k	3.136	0.046
mmu-mir-1306,mmu-mir-1306-5p	3.150	0.046
mmu-mir-27a,mmu-mir-27a-5p	3.311	0.000
mmu-mir-144,mmu-mir-144-3p	4.130	0.000
mmu-mir-155,mmu-mir-155-5p	4.220	0.000
mmu-mir-215,mmu-mir-215-5p	4.577	0.000
mmu-mir-146a,mmu-mir-146a-3p	5.294	0.015
mmu-mir-423,mmu-mir-423-5p	5.884	0.000
mmu-mir-145a,mmu-mir-145a-3p	6.493	0.000
mmu-mir-15a,mmu-mir-15a-3p	6.905	0.000
mmu-mir-16-2,mmu-mir-16-2-3p	7.813	0.049
mmu-mir-141,mmu-mir-141-3p	14.569	0.026
mmu-mir-30c-1,mmu-mir-30c-1-3p	16.903	0.000
mmu-mir-155,mmu-mir-155-3p	20.254	0.000
mmu-mir-467b,mmu-mir-467b-5p	2.074	0.078
mmu-mir-222,mmu-mir-222-5p	2.109	0.080
mmu-mir-34a,mmu-mir-34a-3p	2.142	0.127
mmu-mir-196b,mmu-mir-196b-3p	2.146	0.093
mmu-mir-455,mmu-mir-455-5p	2.212	0.026
mmu-mir-221,mmu-mir-221-3p	2.216	0.059
mmu-mir-223,mmu-mir-223-3p	2.221	0.097
mmu-mir-3103,mmu-mir-3103-3p	2.244	0.072
mmu-mir-500,mmu-mir-500-3p	2.265	0.016
mmu-mir-92b,mmu-mir-92b-3p	2.322	0.016
mmu-mir-374c,mmu-mir-374c-3p	2.380	0.121
mmu-mir-666,mmu-mir-666-5p	2.395	0.018
mmu-mir-5129,mmu-mir-5129-3p	2.410	0.039
mmu-mir-136,mmu-mir-136-3p	2.420	0.010
mmu-mir-592,mmu-mir-592-5p	2.457	0.243
mmu-mir-3473d,mmu-mir-3473d	2.483	0.035
mmu-mir-434,mmu-mir-434-3p	2.510	0.007
mmu-mir-147,mmu-mir-147-3p	2.528	0.016
mmu-mir-205,mmu-mir-205-3p	2.598	0.005
mmu-mir-377,mmu-mir-377-3p	2.643	0.047
mmu-mir-132,mmu-mir-132-3p	2.665	0.005
mmu-mir-196a-1,mmu-mir-196a-1-3p	2.738	0.018
mmu-mir-149,mmu-mir-149-5p	2.763	0.300
mmu-mir-154,mmu-mir-154-5p	2.826	0.010
mmu-mir-30c-2,mmu-mir-30c-2-3p	2.841	0.002
mmu-mir-362,mmu-mir-362-3p	2.965	0.005
mmu-let-7k,mmu-let-7k	3.136	0.046
mmu-mir-1306,mmu-mir-1306-5p	3.150	0.046
mmu-mir-27a,mmu-mir-27a-5p	3.311	0.000
mmu-mir-144,mmu-mir-144-3p	4.130	0.000
mmu-mir-155,mmu-mir-155-5p	4.220	0.000
mmu-mir-215,mmu-mir-215-5p	4.577	0.000
mmu-mir-146a,mmu-mir-146a-3p	5.294	0.015
mmu-mir-34b,mmu-mir-34b-5p	5.550	0.065
mmu-mir-423,mmu-mir-423-5p	5.884	0.000
mmu-mir-145a,mmu-mir-145a-3p	6.493	0.000
mmu-mir-15a,mmu-mir-15a-3p	6.905	0.000
mmu-mir-16-2,mmu-mir-16-2-3p	7.813	0.049
mmu-mir-34c,mmu-mir-34c-5p	10.297	0.082
mmu-mir-27a,mmu-mir-27a-3p	11.007	0.078
mmu-mir-141,mmu-mir-141-3p	14.569	0.026
mmu-mir-30c-1,mmu-mir-30c-1-3p	16.903	0.000
mmu-mir-155,mmu-mir-155-3p	20.254	0.000
mmu-mir-145b,mmu-mir-145b	213.190	0.001

Day 15 LPS vs Day 15 Upregulated Microarray	Fold Change	P-value
mmu-miR-3075_st	3.368	0.008
mmu-miR-16-1-star_st	2.576	0.020
mmu-miR-466c-5p_st	2.481	0.035
mmu-miR-34c-star_st	2.343	0.031
mmu-miR-344f-5p_st	2.047	0.010
mmu-miR-467g_st	1.811	0.008

Table 2-5: Downregulated MicroRNAs in Day 18 vs. Day 15 Cervices

Day 18 vs Day 15 Downregulated	Fold Change	P-Value
Small RNA-seq		
mmu-mir-26b,mmu-miR-26b-3p	0.064	0.000
mmu-mir-143,mmu-miR-143-3p	0.163	0.000
mmu-mir-218-1,mmu-miR-218-1-3p	0.217	0.039
mmu-mir-297a-3,mmu-miR-297a-3p	0.294	0.008
mmu-mir-297a-4,mmu-miR-297a-3p	0.294	0.008
mmu-mir-297b,mmu-miR-297b-3p	0.294	0.008
mmu-mir-297c,mmu-miR-297c-3p	0.294	0.008
mmu-mir-490,mmu-miR-490-3p	0.312	0.008
mmu-mir-467a-1,mmu-miR-467a-3p	0.366	0.024
mmu-mir-467a-10,mmu-miR-467a-3p	0.366	0.024
mmu-mir-467a-2,mmu-miR-467a-3p	0.366	0.024
mmu-mir-467a-3,mmu-miR-467a-3p	0.366	0.024
mmu-mir-467a-4,mmu-miR-467a-3p	0.366	0.024
mmu-mir-467a-5,mmu-miR-467a-3p	0.366	0.024
mmu-mir-467a-6,mmu-miR-467a-3p	0.366	0.024
mmu-mir-467a-7,mmu-miR-467a-3p	0.366	0.024
mmu-mir-467a-8,mmu-miR-467a-3p	0.366	0.024
mmu-mir-467a-9,mmu-miR-467a-3p	0.366	0.024
mmu-mir-467d,mmu-miR-467d-3p	0.366	0.024
mmu-mir-3102,mmu-miR-3102-3p.2-3p	0.367	0.013
mmu-let-7k,mmu-let-7k	0.391	0.048
mmu-mir-190a,mmu-miR-190a-5p	0.411	0.010
mmu-mir-3068,mmu-miR-3068-5p	0.422	0.040
mmu-mir-101c,mmu-miR-101c	0.422	0.016
mmu-mir-21a,mmu-miR-21a-5p	0.445	0.005
mmu-mir-299b,mmu-miR-299b-3p	0.491	0.025
mmu-mir-26b,mmu-miR-26b-5p	0.498	0.017
mmu-let-7g,mmu-let-7g-3p	0.522	0.040
mmu-let-7f-2,mmu-let-7f-5p	0.526	0.028
mmu-let-7f-1,mmu-let-7f-5p	0.527	0.029
mmu-let-7d,mmu-let-7d-5p	0.556	0.049

Day 18 vs Day 15 Downregulated	Fold Change	P-value
Microarray		
hp_mmu-mir-5121_st	0.349412	0.013
mmu-miR-93_st	0.343171	0.046
hp_mmu-mir-140_st	0.325561	0.006
mmu-miR-199a-5p_st	0.323088	0.031
mmu-miR-93-star_st	0.322641	0.013
mmu-miR-25-star_st	0.32197	0.045
hp_mmu-mir-1956_st	0.289975	0.019
hp_mmu-mir-5120_st	0.284993	0.016
hp_mmu-mir-500_st	0.280292	0.016
hp_mmu-mir-2137_st	0.272249	0.000
hp_mmu-mir-465a_x_st	0.264255	0.009
mmu-miR-135a-1-star_st	0.262429	0.050
mmu-miR-2137_st	0.23423	0.009
mmu-miR-181c-star_st	0.136503	0.019
mcmv-miR-M23-1-5p_st	0.129857	0.008
mmu-miR-690_st	0.051797	0.022

Table 2-6: Upregulated MicroRNAs in Day 18 vs. Day 15 Cervices

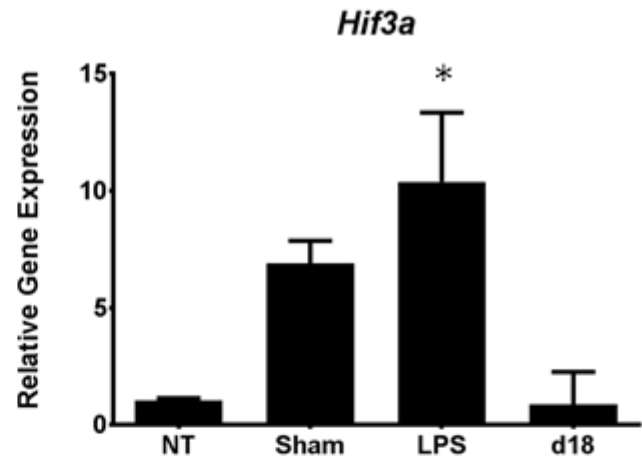
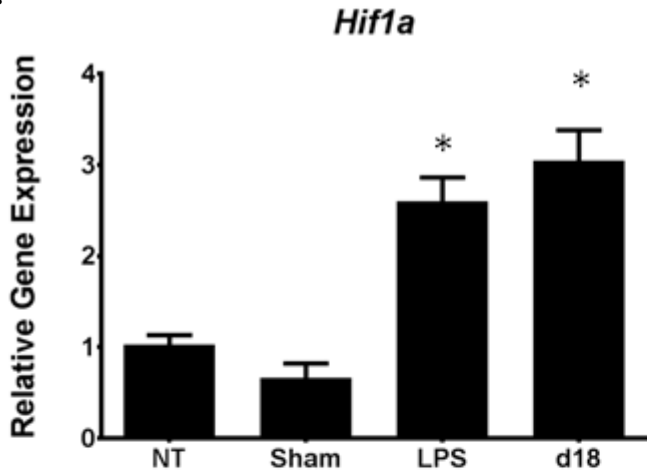
Day 18 vs Day 15 Upregulated Small RNA-seq	Fold Change	P-value
mmu-mir-200b,mmu-miR-200b-3p	1.926	0.029
mmu-mir-425,mmu-miR-425-5p	2.238	0.045
mmu-mir-30c-1,mmu-miR-30c-1-3p	2.245	0.038
mmu-let-7d,mmu-let-7d-3p	2.279	0.019
mmu-mir-154,mmu-miR-154-5p	2.303	0.042
mmu-mir-378a,mmu-miR-378a-5p	2.317	0.033
mmu-mir-30c-2,mmu-miR-30c-2-3p	2.352	0.008
mmu-mir-664,mmu-miR-664-5p	2.357	0.035
mmu-mir-200a,mmu-miR-200a-3p	2.393	0.007
mmu-mir-149,mmu-miR-149-5p	2.421	0.050
mmu-mir-365-2,mmu-miR-365-2-5p	2.430	0.021
mmu-mir-503,mmu-miR-503-5p	2.486	0.032
mmu-mir-323,mmu-miR-323-3p	2.495	0.032
mmu-mir-449a,mmu-miR-449a-5p	2.505	0.032
mmu-mir-1934,mmu-miR-1934-5p	2.575	0.017
mmu-mir-1199,mmu-miR-1199-5p	2.589	0.030
mmu-mir-132,mmu-miR-132-3p	2.663	0.007
mmu-mir-1983,mmu-miR-1983	2.843	0.010
mmu-mir-22,mmu-miR-22-3p	2.916	0.001
mmu-mir-200c,mmu-miR-200c-5p	3.067	0.009
mmu-mir-210,mmu-miR-210-5p	3.110	0.002
mmu-mir-501,mmu-miR-501-3p	3.687	0.001
mmu-mir-361,mmu-miR-361-3p	4.122	0.003
mmu-mir-145b,mmu-miR-145b	4.380	0.004
mmu-mir-802,mmu-miR-802-3p	5.258	0.014
mmu-mir-136,mmu-miR-136-5p	6.175	0.000
mmu-mir-34b,mmu-miR-34b-5p	7.324	0.000
mmu-mir-203,mmu-miR-203-3p	7.401	0.001
mmu-mir-141,mmu-miR-141-3p	12.690	0.043
mmu-mir-34c,mmu-miR-34c-5p	12.712	0.000
mmu-mir-592,mmu-miR-592-5p	12.884	0.000
mmu-mir-27a,mmu-miR-27a-3p	14.165	0.000
mmu-mir-5099,mmu-miR-5099	24.541	0.012

Day 18 vs Day 15 Upregulated Microarray	Fold Change	P-value
mmu-miR-1a_st	5.392	0.018
mmu-miR-669f-3p_st	4.476	0.020
mmu-miR-466f_st	4.423	0.037
mmu-miR-669o-3p_st	3.848	0.015
mmu-miR-466c-5p_st	3.634	0.011
mmu-miR-669k-star_st	3.535	0.033
mmu-miR-29b-1-star_st	3.485	0.031
mmu-miR-224_st	3.265	0.045
mmu-miR-374_st	3.045	0.042
mghv-mir-M1-3-star_st	2.695	0.016
mmu-miR-361-star_st	2.514	0.044
mmu-miR-1899_st	2.502	0.036
mmu-let-7f_st	2.448	0.013
mmu-miR-33-star_st	2.445	0.012
mmu-miR-467e-star_st	2.421	0.003
mmu-miR-466c-3p_st	2.415	0.025
mmu-miR-344g-5p_st	2.404	0.030
mmu-miR-1907_st	2.388	0.026
mmu-miR-1968_st	2.360	0.008
mmu-miR-1935_st	2.340	0.036
mmu-miR-203_st	2.108	0.013
mmu-miR-467c-star_st	2.062	0.018
mmu-miR-466f-5p_st	2.036	0.028
mmu-miR-211_st	2.006	0.005
mmu-miR-487b-star_st	2.003	0.020
mmu-miR-3082-5p_st	1.999	0.043
mmu-miR-3095-3p_st	1.993	0.039
mmu-miR-466j_st	1.928	0.013
mmu-miR-669p_st	1.898	0.043
hp_mmu-mir-449b_st	1.891	0.007
mmu-let-7g_st	1.829	0.018
mmu-miR-200b_st	1.763	0.036

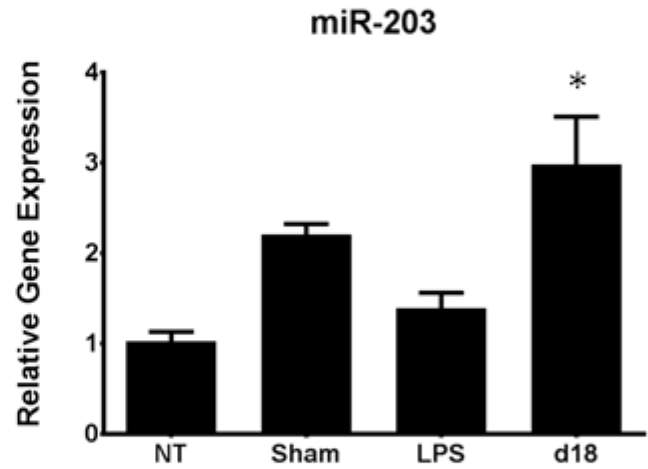
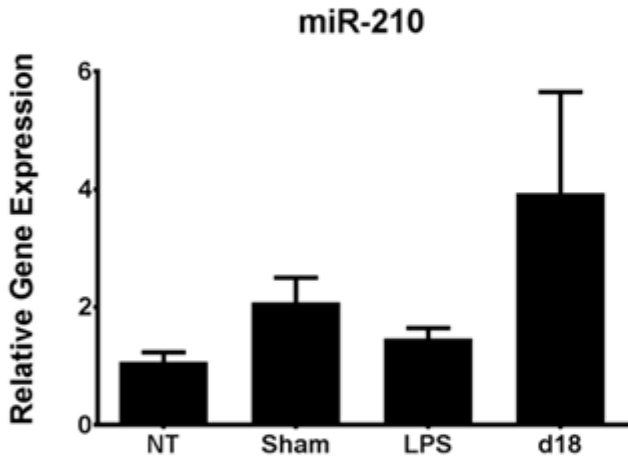
Table 2-7: Differentially Expressed Cervical MicroRNAs & mRNA Targets in Term and LPS-Mediated Preterm Birth

	Fold change day 15 LPS vs day 15	Fold change day 18 vs day 15
<i>Hif1a</i>	3.613	2.251
miR-210-5p (data from small RNA-seq)	0.074	3.110
<i>Hif3a</i>	0.467	0.486
miR-203	No change	7.401
miR-155-5p	4.22	No change
miR-144-3p	4.130	No change

A.



B.



C.

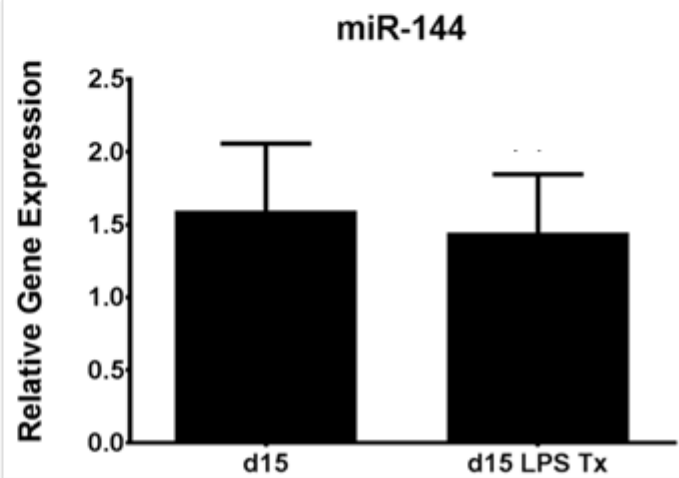
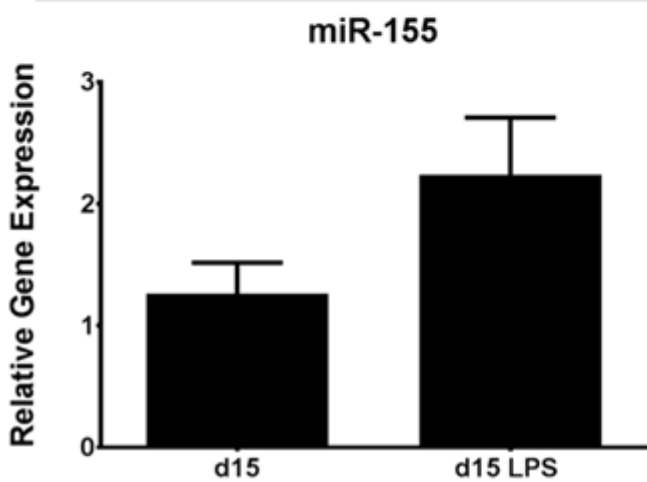


Figure 2.10. Cervical microRNAs in term and LPS-mediated preterm birth

(A) qPCR results of hypoxia inducible factor 1a and 3a genes showing relative gene expression on day 15, day 15 sham, day 15 LPS, and day 18. The values expressed are mean \pm SEM. (n=3-8 cervices per group, One way ANOVA * P<0.05 relative to day 15). (B) qPCR results of selected microRNAs showing relative expression on day 15, day 15 sham, day 15 LPS, and day 18. The values expressed are mean \pm SEM. (n= 6-7 cervices per group, One way ANOVA * P<0.05 relative to day 15). (C) qPCR results of selected microRNAs showing relative expression on day 15 and day 15 LPS. The values expressed are mean \pm SEM. (n= 5-12 cervices per group, no significance using student's t-test).

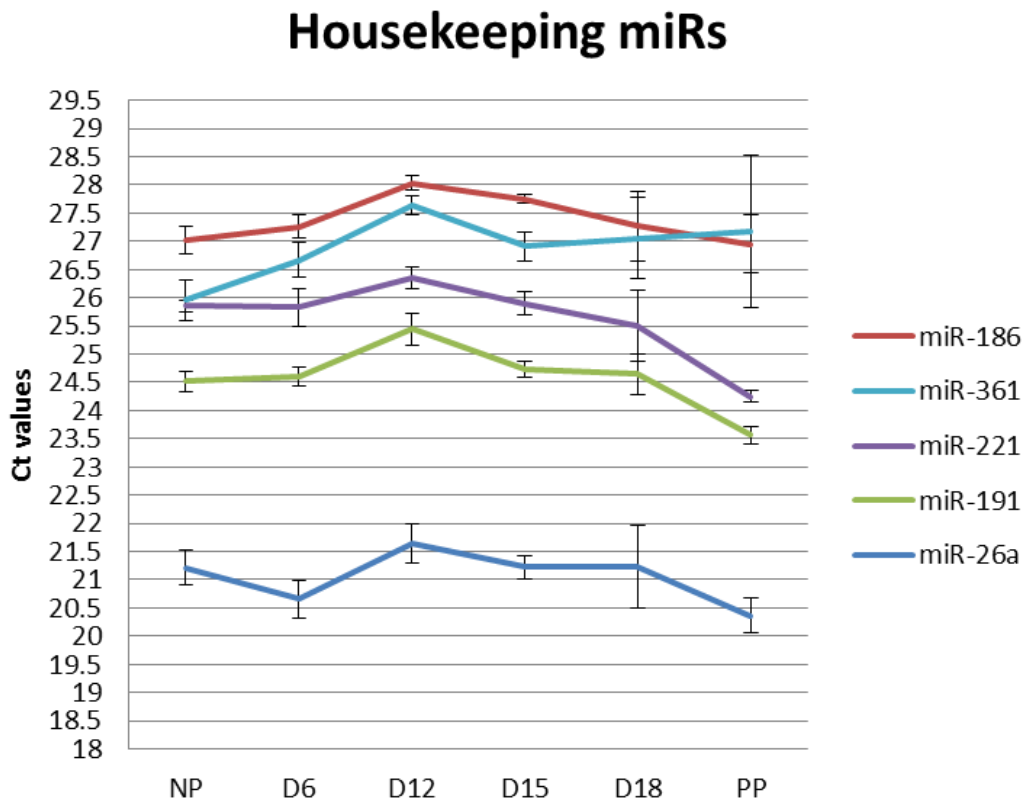


Figure 2.11. Housekeeping gene candidates for microRNA qPCR

qPCR results of housekeeping mature microRNAs genes showing how their expression changes throughout a normal pregnancy time course in the cervix. The values expressed are mean Ct values \pm SEM. (n=3 cervixes per time point per group).

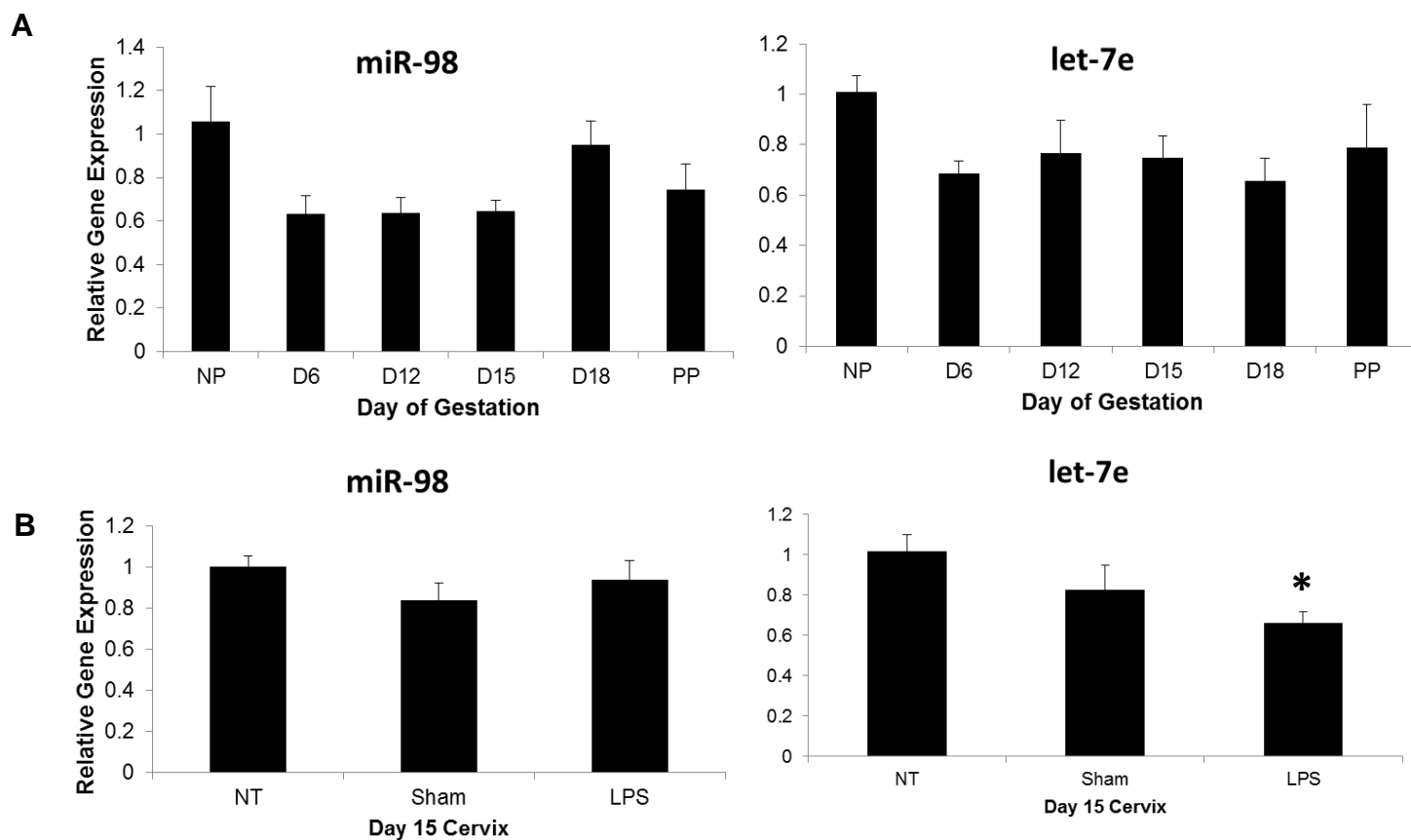


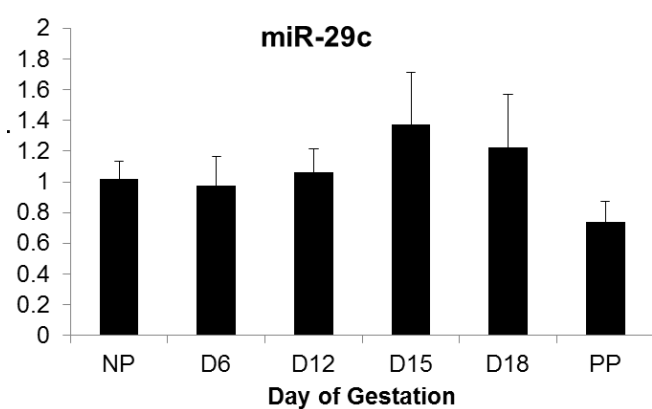
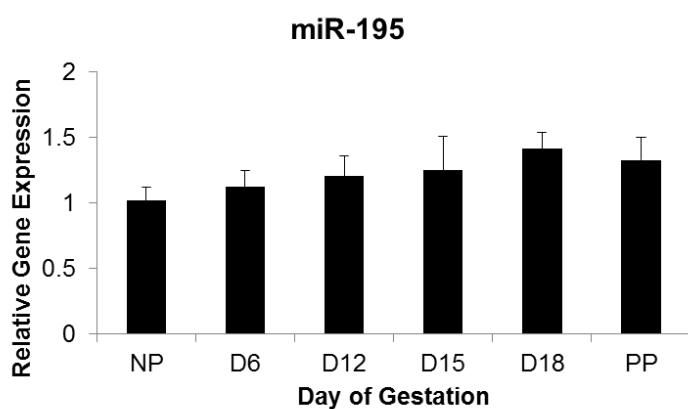
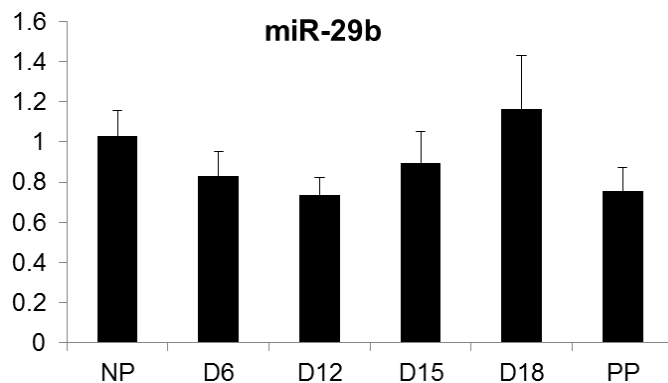
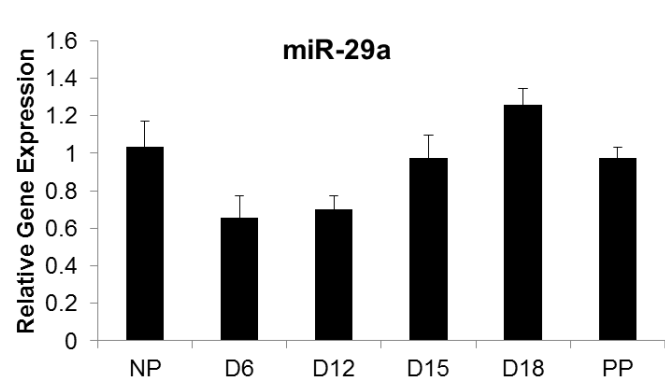
Figure 2.12. Expression of mechanomiRs throughout pregnancy & in response to LPS

(A) qPCR results of “mechanomiRs” genes showing expression changes throughout a normal pregnancy time course in the cervix. The values expressed are mean \pm SEM. (n=5-6 cervices per time point per group, significance using One way ANOVA * P<0.05 highlighted in table 2-8, one experiment). (B) qPCR results of “mechanomiR” genes showing expression changes in day 15 sham and day 15 LPS compared to day 15. The values expressed are mean \pm SEM. (n=5 cervices per time point per group, One way ANOVA * P<0.05 relative to day 15, one experiment)

Table 2-8: Mechanically Regulated & ECM-Targeting MicroRNAs

	microRNA	Δ pregnancy	Δ LPS
mechanomiRs	miR-98	Decreased at d6, 12, and 15 vs non-pregnant	No change
	let-7e	Decreased at all time points vs non-pregnant	Decreased in LPS vs Sham
ECM targeting miRs	miR-195	No change	No change
	miR-29a	Decreased at d6, 12 vs non-pregnant	No change
	miR-29b	Decreased at d12 vs non-pregnant	No change
	miR-29c	Increased at d15, 18 vs non-pregnant	No change

A



B

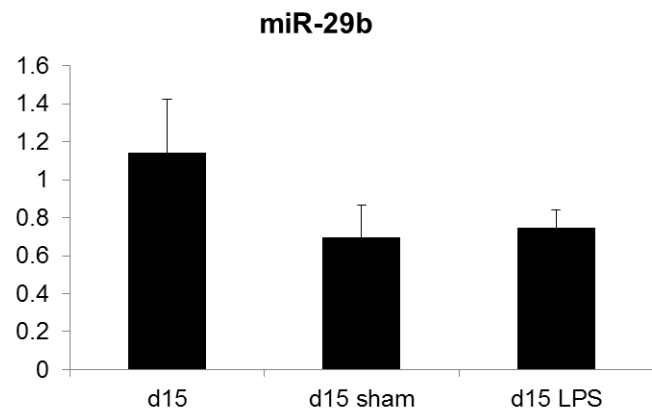
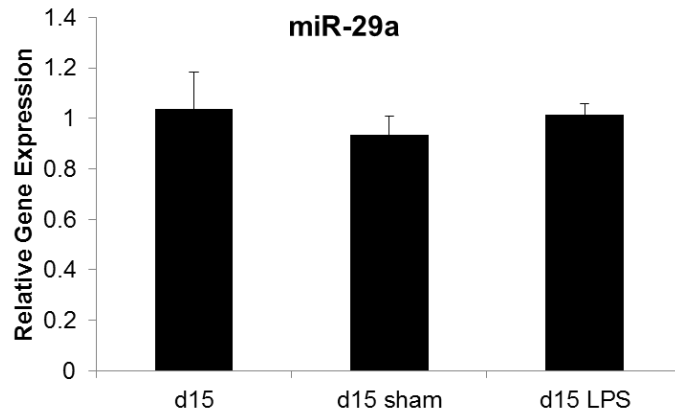
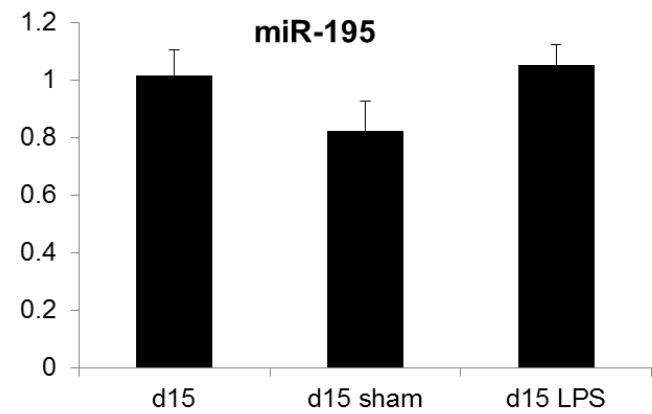
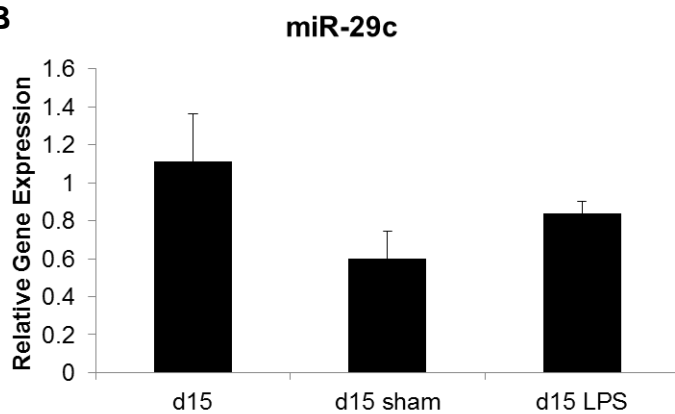
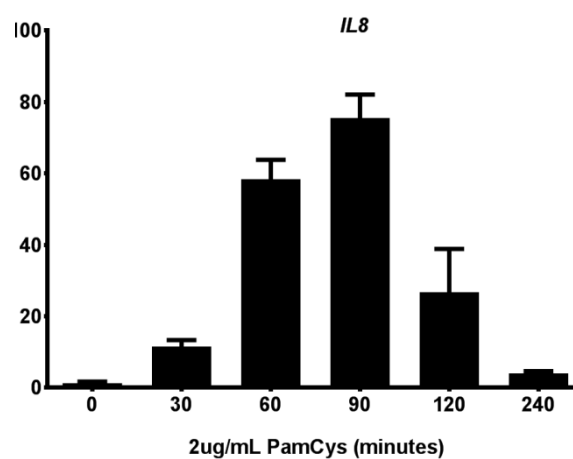
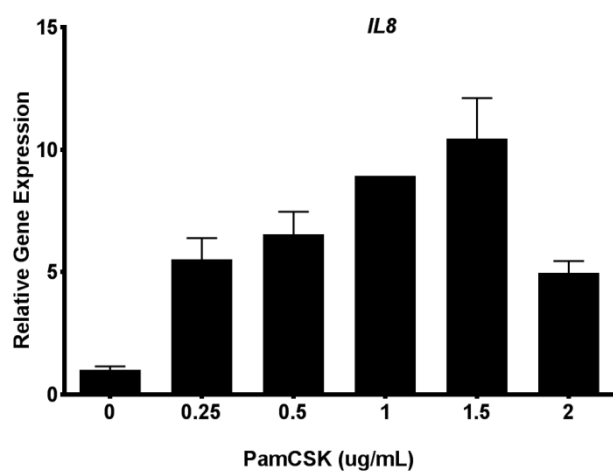
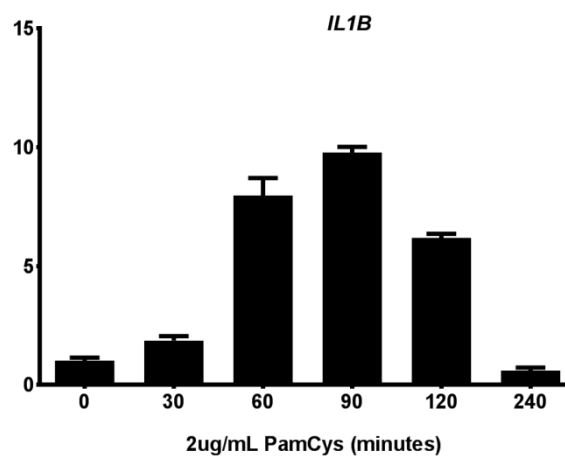
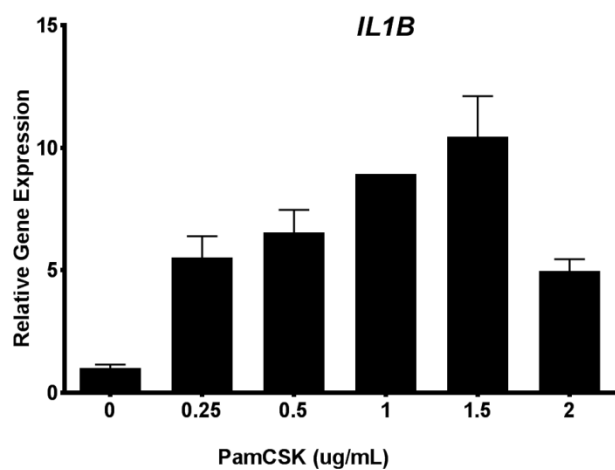


Figure 2.13. Expression of ECM-targeting microRNAs throughout pregnancy & in response to LPS

(A) qPCR results of mature microRNAs showing expression changes throughout a normal pregnancy time course in the cervix. The values expressed are mean \pm SEM. (n=6 cervixes per time point per group, significance using One way ANOVA * P<0.05 highlighted in table 2-8, one experiment). (B) qPCR results of mature microRNAs showing expression changes in day 15 sham and day 15 LPS compared to day 15. The values expressed are mean \pm SEM. (n=5-6 cervixes per time point per group, no significance when using One-way ANOVA)

A. End1 Cell PamCSK Concentration and Timecourses



B. Ect1 Cell PamCSK Concentration Course

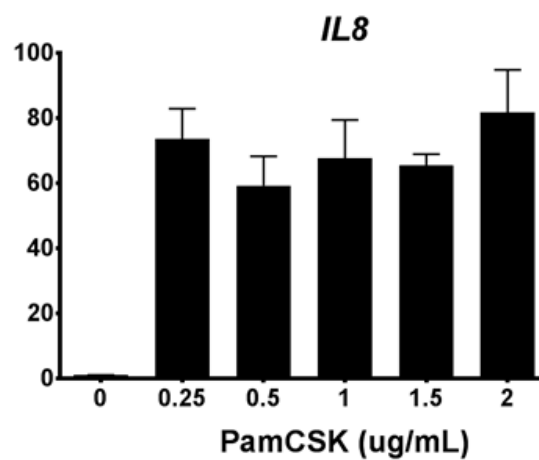
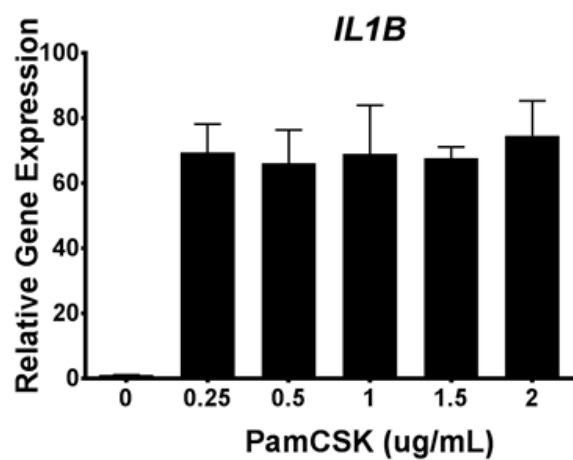


Figure 2.14. Ect1 Cell Response to PamCSK and ATP or Flagellin Treatment

(A) qPCR results of selected proinflammatory genes showing relative gene expression in End1 cells when with varying concentrations of PamCSK at 2 hours and at varying lengths of time using 2ug/mL PamCSK. Vehicle treated (0ug/mL), treated with PamCSK (PC) and ATP (PC+A) or flagellin (PC+F). The values expressed are mean \pm SEM. No statistical significance when using one-way ANOVA.

CHAPTER THREE

Transcriptional Signatures of Inflammation Influencing Cervical ECM

3.1 Introduction

As was discussed in the previous chapters, there are unique features at play in LPS-mediated preterm birth that are not seen physiologically at term on day 18 of mouse pregnancy. These features include unique cervical immune cell populations, different steroid hormone profiles, dependence on prostaglandins in the infection model and not at term, and the distinct cervical transcriptome profiles described in chapter 2. This chapter focuses on how these features specific to inflammation-mediated preterm birth influence the cervical extracellular matrix in such a way that is once again unique to this mechanism of preterm birth and not seen physiologically at the end of pregnancy.

Throughout normal pregnancy, collagen fibers undergo a dramatic structural reorganization. Collagen fibers, which can be visualized by second harmonic generation (SHG), increase in diameter and transition from straight and thin to thick and curved (Akins et al., 2011; Akins et al., 2010; Zhang et al., 2012). Collagen fibrils are the building blocks of collagen fiber. Using transmission electron microscopy (TEM), it has been noted that fibril diameter increases during pregnancy and an overall dispersal of fibrils occurs in term ripening on gestation day 18 in the mouse.

Similar assessments of collagen fibers by SHG and fibrils by TEM in cervixes from mice treated with LPS on gestation day 15 demonstrate that structural reorganization of

collagen is not achieved as described for term ripening. Specifically, there is no increase in collagen fibril dispersal and no increase in collagen fiber diameter. Unique to cervixes from LPS treated mice on day 15 of gestation is an increase in areas lacking SHG signal, termed pores, in the stromal regions adjacent to the cervical epithelium (Nallasamy et al, manuscript in preparation).

Given the similarities in cervical compliance observed in day 15 LPS and day 18 cervixes despite only modest changes in collagen reorganization in the LPS group, the role of other structural proteins in the ECM was investigated (B. C. Timmons et al., 2014). Recently published work highlights the contribution of elastic fibers, which are most concentrated in the sub-epithelial stroma of the cervix, to the biomechanical functions of the tissue (Nallasamy et al., 2017a). These small yet mighty fibers lend a viscoelastic property to tissues and account for between 0.9-1.54% of the connective tissue fraction of the human cervix (Leppert et al., 1983). Elastic fibers are composed of elastin protein crosslinked in and around a microfibrillar scaffold consisting of fibrillin 1 and 2, plus a number of other matricellular proteins (Wagenseil & Mecham, 2007). The synthesis of components of the elastic fiber is thought to be constrained to times of development, with coordinated assembly of elastic fibers happening at the later stages (Kelleher, McLean, & Mecham, 2004). It has been hypothesized that upon injury, elastic fibers are rarely able to repair, owing to the lack of ability to coordinate the synthesis of such a variety of molecules needed for appropriate reassembly (Shifren & Mecham, 2006). While studies in the human cervix suggest elastic fiber content does not change in term pregnancy, there is evidence that elastic fiber content, as determined by desmosine and isodesmosine measurements, is reduced with cervical

dysfunction in pregnancy (Leppert et al., 1987). Cervical insufficiency, once termed cervical incompetency, has been associated with decreased cervical content of desmosine and isodesmosine, residues of elastin crosslinked in and around the microfibrillar scaffold.

Using RNA-seq and subsequent analyses of Gene Ontology (GO) biological processes and molecular functions, a common set of proteases were identified as being upregulated in the cervix both at term and in infection-mediated preterm birth. Interestingly, there is also a subset of proteases upregulated exclusively in response to LPS, and not at term, that target a number of ECM molecules, not the least of which are major structural proteins collagen and elastin. **This chapter highlights the findings from this project whose goal was to identify how the cervical ECM is impacted upon intrauterine LPS treatment, leading to decreased cervical stiffness and subsequent preterm birth.**

Morphology and ultrastructure of elastic fibers were investigated alongside experiments to determine the mechanism of inflammation-mediated changes in these parameters.

3.2 Results

3.2.1 Expression of proteases in the cervix is upregulated in LPS-mediated preterm birth

As highlighted in chapter 2, an RNA-seq project was undertaken to define the cervical transcriptome signatures of term ripening and LPS-mediated preterm birth. In addition to genes involved in inflammasome activation, another group of genes identified as upregulated in LPS-mediated premature cervical remodeling is proteases (figure 3.1). RNA-seq data set analysis identified two GO terms—proteolysis and peptidase activity—as

significantly enriched in genes exclusive to day 15 LPS vs day 15 (figure 3.1A). The data set contains a large number of genes (107 and 75 respectively) within these pathways. These genes, including matrix metalloproteinase (*mmp*), a disintegrin and metalloproteinase with thrombospondin type 1 motifs (*adamts*), and cathepsin (*cts*) proteases, target and modify components of the ECM. Known functions of these proteases include post-synthesis processing of mature ECM molecules including collagen, degradation during physiologic turnover processes (i.e. pregnancy), and pathologic breakdown due to inflammation (i.e. arthritis) (Asquith et al., 2011; Colige et al., 2002; Rajabi, Solomon, & Poole, 1991). The heatmap in figure 3.1B depicts fold change values of genes encoding *ADAMTS*, *MMP*, and *CTS* proteases identified as differentially regulated in LPS preterm or term compared to non-treated day 15. Gene expression analyses using RT-qPCR for select genes *Mmp13*, *Mmp12*, *Ctsl*, *Ctsc*, *Adamts5*, and *Adamts15* identified significantly increased expression of *Mmp13* and *Adamts5* in cervixes from day 15 LPS treated mice. (figure 3.1C). While the observed increase in *Ctsl* did not achieve statistical significance, subsequent studies shown in figure 3.11 indicate a temporal increase in *Ctsl* expression. We have previously reported increased expression of *Mmp8*, *Adamts1*, and *Adamts4* in the cervix of day 15 LPS treated mice. Both *Adamts1* and *Adamts4* are also upregulated in term ripening at gestation day 18, and their known targets are proteoglycans (Holt et al., 2011; Sandy et al., 2001). The upregulation of proteases that target the main structural components collagen and elastic fibers in response to pathological inflammation but not in the normal catabolic processes led to assessment of the cervical ECM structure in the day 15 LPS treated mice.

3.2.2 Cervical elastic fiber ultrastructure is disrupted in LPS-mediated preterm birth.

Recently published studies from our lab demonstrating elastic fibers' contributions to the biomechanical function of the cervix, in conjunction with the RNA-seq dataset indicating upregulation of proteases that target collagen and elastic fibers specifically in the LPS-mediated preterm birth group, led to the evaluation of the structure of elastic fibers (Nallasamy et al., 2017b). Three staining and imaging modalities were used to visualize elastic fibers.

In the first imaging experiments, transverse sections from day 15, day 15 sham, day 15 LPS, and day 18 mouse cervixes were stained using Hart's variation of Verhoeff Van Gieson staining (figure 3.2). As has been well documented previously, the elastic fibers, stained black using this technique, are interdigitated at a perpendicular angle to the basal epithelium on day 15 of pregnancy in the cervix. The morphology of the fibers varies at different locations in the tissue but overall elastic fiber staining is most concentrated in the subepithelial stroma with shorter and generally fewer fibers in the mid-stroma. Similar localization, relative abundance, and morphologies were seen in day 15 sham, day 15 LPS, and day 18 cervixes compared to day 15 samples.

An antibody generated against tropoelastin was utilized for immunofluorescence staining for more directed studies of elastin. Similar to the Verhoeff Van Gieson staining as mentioned above, elastin staining on day 15 appeared concentrated in the subepithelial stroma region of the cervix in long fibers with less staining and less fiber-like staining in the midstroma (figure 3.3). When compared to elastin in the cervix of an untreated day 15 mouse, elastin staining in day 15 LPS appears similarly localized in the sub-epithelial stroma yet more punctate with fewer linearly arranged strands. Elastin staining in sham treated

animals shows similar morphology to day 15 untreated, with the appearance of long strands of elastin.

To gain further evidence for potential structural abnormalities in cervical elastic fibers of day 15 LPS mice, elastic fiber ultrastructure was evaluated by transmission electron microscopy (TEM). Elastic fibers in the sub-epithelial stroma region of the cervix were evaluated in day 15, day 15 sham, day 15 LPS, and day 18 mice. The majority of elastic fibers in the day 15 LPS group appeared disrupted with less darkly stained elastin integrated into the scaffold, resulting in increased visibility of the microfibrillar scaffold component of the elastic fiber (figure 3.4). Cervical elastic fibers from day 15 sham animals were similar in structure and density to untreated day 15. No such disruption of elastic fiber ultrastructure occurs at term. Comparing day 18 to day 15, elastic fibers appear intact with the darkly stained elastin covering the microfibrillar scaffold.

3.2.3 Cervical tissue resilience decreased at 75% yield force in LPS-mediated preterm birth but not at term

In collaboration with Dr. Kristin Myers lab in the Department of Mechanical Engineering at Columbia University, the recoverability of mouse cervical tissues was tested using biomechanical parameters (figure 3.5A). It has been shown that altered elastic fibers, specifically due to a fibulin-5 deficiency in the mouse, negatively impacts the fibers' ability to store energy (Ferruzzi, Bersi, Uman, Yanagisawa, & Humphrey, 2015). Instead of using load-to-break mechanical tests that have previously demonstrated reduced cervical stiffness in day 15 LPS versus day 15, load-unload-recovery studies were undertaken to better understand the ability of the tissue, with respect to both collagen and elastic fibers, to return

to its original shape after stress (House & Socrate, 2006; B. C. Timmons et al., 2014). At 75% yield force, day 15 LPS cervixes have reduced recoverability compared to day 15 samples (figure 3.5B). Day 18 samples have similar recoverability to day 15 samples. These preliminary findings suggest potential disruption of elastic fibers upon LPS treatment that weakens the cervical tissue's ability to recover after repetitive stress.

3.2.4 Neither solubility nor extractability of cervical elastin is altered in LPS-mediated preterm birth

Given the observation that less elastin appeared to be integrated in the microfibrillar scaffold on day 15 LPS compared to day 15, we sought to measure the amount of solubilized elastin in the cervix. In its mature form, elastin integrated into elastic fibers is highly insoluble and resistant to most heat and acid treatments (Mecham, 2008). We hypothesized that a larger amount of "liberated" (unintegrated) elastin that had been solubilized would be measurable in day 15 cervixes from mice treated with LPS compared to samples from untreated day 15 mice. Two sequential extractions were performed, the first with PBS and the second with urea, in order to extract soluble elastin. PBS is anticipated to extract the most soluble elastin, and urea is expected to extract less soluble elastin. The antibody used in these experiments recognizes dimerized tropoelastin (144kDa) and monomer tropoelastin (72kDa) (figure 3.6A). Both monomer and dimer forms of elastin were detectable in both PBS and urea fractions in day 15, day 15 sham, day 15 LPS, and day 18 samples. Results from four independent experiments in which one set of samples from each of the four groups mentioned above was used do not indicate increased amounts of soluble elastin in day 15 LPS samples compared to day 15 samples.

As a second attempt to measure changes in soluble elastin, a commercial kit in which elastin is extracted by hot oxalic acid was used. Two separate experiments were completed, each using three unique samples per group. Extractability was measured and compared to starting weight of tissue (figure 3.6B). There was no measurable change in extractability of cervical elastin in LPS-mediated preterm or term birth, compared to untreated day 15 samples.

3.2.5 No increase in TGF β signaling with disrupted matrix

As an indirect way of demonstrating disrupted cervical ECM structure upon LPS treatment, TGF β signaling was tested. It has been reported that TGF β is sequestered in the microfibrillar scaffold in the ECM nearby to cells, with latent TGF β binding proteins (LTBPs) acting as mediator molecules during secretion of TGF β from cells and integration into the matrix (Dallas et al., 2000; Massam-Wu et al., 2010; Saharinen, Hyytiainen, Taipale, & Keski-Oja, 1999). Gene expression of *Ltbp1*, *Ltbp3*, and *Ltbp4* was tested using qPCR. *Ltbp3* was upregulated in day 15 sham and downregulated in day 15 LPS, both compared to day 15 (figure 3.7A). Likewise, *Ltbp4* was downregulated in day 15 LPS compared to day 15. To analyze potential changes in TGF β signaling, phosphorylation of SMAD2/3 proteins was investigated using western blotting (Abdollah et al., 1997). Levels of phospho-SMAD2/3 have been found to be highest in the nonpregnant cervix and to decline during pregnancy, with a return to nonpregnant abundance postpartum [communications with S. Nallasamy]. To test the hypothesis that ECM degradation in cervixes of mice treated with intrauterine LPS causes increased TGF β signaling, western blotting was completed using day 15, day 15 sham, and day 15 LPS samples. Three separate experiments identified low levels

of phosphorylated SMAD2/3 with 2 of 3 blots showing a modest increase in pSMAD2/3 with LPS treatment compared to day 15 (figure 3.7B). These changes in phosphorylation were minimal compared to the phosphorylation in the nonpregnant state. The overall finding from these experiments is that the measured changes in biomechanical resilience of the tissues in addition to the observed elastic fiber disruption, both in the day 15 LPS cervix, are not accompanied by abnormal TGF β signaling.

3.2.6 Investigations of cervical protease activity in LPS-mediated preterm birth

The ultimate goal of this segment of the project was to identify the mechanisms by which the cervical elastic fibers become disrupted in LPS-mediated preterm birth. To investigate this mechanism, a number of protease activity assays were undertaken (figure 3.8A). Fluorescently conjugated ECM substrates including elastin, gelatin, and type 1 collagen, were used for both *in situ* zymography (figure 3.8B) and whole tissue lysate experiments (figure 3.9). With activity of endogenous proteases, substrates were expected to be cleaved and able to fluoresce. A high amount of background fluorescence was detected in both day 15 and day 15 LPS samples when using the substrates in the *in situ* zymography technique. No detectable increase in fluorescence was seen in day 15 LPS versus day 15. When the fluorescent substrates were used in a well-based tissue lysate extract format, both positive (purified enzyme) and negative (purified enzyme + inhibitor) gave expected results (figure 3.9A). When purified enzyme was spiked into tissue extracts during and after the isolation protocol, a demonstrable decline in enzymatic activity was observed (figure 3.9B). No measureable change in fluorescence (enzyme activity) could be measured in day 15 LPS compared to day 15 (figure 3.9C). It was hypothesized that either something in the isolation

protocol (chemical) or the tissue lysate (endogenous inhibitor) impacted or quenched the fluorescence generated by the exogenous enzyme and that this endogenous inhibitor may also be preventing endogenous enzymes from cleaving the fluorescent substrate.

Given the recent demonstration that neutrophils are present and clustered at a greater density in the cervix upon LPS treatment compared to untreated day 15 samples, another assay was used to determine activity of endogenous proteases against a chemical substrate with specific cleavage sites recognized by neutrophil elastases (Nallasamy et al, manuscript in preparation). Upon cleavage, the chemical substrate increases the optical density of the sample and in a 96 well format, relative absorbance can be measured. No measurable increase in absorbance was seen in day 15 LPS compared to day 15 samples (data not shown). To determine if an endogenous inhibitor may be present in tissue lysates and potentially affecting protease activity, cervix samples collected 1, 2, and 4 hours after IU LPS treatment were used with spike-in of exogenous enzyme (figure 3.10). In all samples with addition of exogenous purified enzyme, a demonstrable decline in enzymatic activity compared to enzyme alone was observed.

3.2.7 Regulation of cervical protease expression in LPS-mediated preterm birth

To investigate the regulation of cervical protease gene expression, literature searches in addition to RNA-seq Gene Ontology analyses highlighted the potential for inflammasome activation of proteases as a viable mechanism for ECM disruption. The process by which infection and inflammation induce upregulation of these particular collagen and elastin targeting proteases in the cervix may be similar to the pathophysiology of the proinflammatory disease osteoarthritis in which IL1B has been shown to directly upregulate

proteases such as collagenase *Mmp13* (Mengshol, Vincenti, Coon, Barchowsky, & Brinckerhoff, 2000). Consistent with this hypothesis, upregulation of the *Il1b* transcript is concurrent with or precedes the upregulation of proteases such as *Adamts4*, *Mmp13*, *Ctsl* (figure 3.11). Two methods were used to test the hypothesis that IL1B directly regulates proteases. In the first, recombinant mature (17kDa) mouse IL1B was injected intrauterine, and uterine and cervical gene expression was measured via qPCR. At the 4 and 8 hour time points post-injection, proinflammatory markers *Il1b*, *Il6*, *Ptgs2*, and *Tnf* along with proteases *Adamts4* and *Mmp13* were analyzed in the uterus (figure 3.12) and the cervix (figure 3.13). In the uterus upon IL1B treatment, there was a trend for increased expression of proinflammatory and proteases, although the induction was not statistically significant compared to untreated controls. In the cervix, *Ptgs2* gene expression was significantly upregulated 4 hours after intrauterine application of IL1B compared to untreated samples. Transcripts of proinflammatory *Tnf* and protease *Mmp13* were also upregulated in the cervix 8 hours after intrauterine IL1B treatment.

Using IL1B receptor antagonist Anakinra (Kineret), the necessity of IL1B signaling to downstream protease expression was investigated during inflammation-mediated preterm birth. In the first set of experiments, Anakinra was injected intraperitoneally (IP) in combination with IP or IU LPS. Figure 3.13A illustrates the dosage regimen for Anakinra, based on the known potency and half-life in humans (Dinarello et al., 2012; Girard, Tremblay, Lepage, & Sebire, 2010; Leitner et al., 2014). Using a standard dose of LPS IP, proinflammatory markers *Il1b* and *Il6* were significantly upregulated in the cervix compared to day 15 (figure 3.14B). Proteases *Mmp13* and *Adamts4* were similarly upregulated.

Expression of these genes was not influenced further by the administration of Anakinra (figure 3.14B). Administration of IP Anakinra to LPS treated mice did not blunt the expression of described genes.

In a pilot study with small sample size using the IU LPS administration route, a variety of concentrations of LPS were used (figure 3.15). Even at the lowest dosage of LPS (50ug), Anakinra was unable to decrease the expression of proinflammatory and protease genes.

To utilize a more localized administration of Anakinra, IU Anakinra pre-treatment 15 minutes before IU LPS injection in combination with IU Anakinra was utilized. This treatment regimen was not enough, however, to overcome proinflammatory induction and upregulated protease gene expression induction in the uterus (figure 3.16) or the cervix (figure 3.17) at the 2 or 4 hour time point after LPS injection.

3.3 Discussion

RNA-seq identified upregulation of a number of proteases in the cervix, both at term and in response to infection. Members of the ADAMTS protease family including *Adamts1* and *Adamts4* are upregulated in the cervix both at term and in LPS-mediated preterm birth. These proteases are known to target proteoglycans and likely contribute to the normal cervical ECM turnover required for physiological remodeling (Kelwick, Desanlis, Wheeler, & Edwards, 2015; Sandy et al., 2001).

The cervical transcriptional signature of LPS treated mice includes robust upregulation of proteases, including *Mmp13*, *Mmp8*, and *Ctsl*, that target the major structural proteins of the cervix, namely collagen and components of the elastic fiber (figure 3.1). The process by which infection and inflammation induce upregulation of these particular collagen and elastin targeting proteases in the cervix may be similar to the pathophysiology of the proinflammatory disease osteoarthritis in which IL1B has been shown to directly upregulate proteases such as collagenase *Mmp13* (Mengshol et al., 2000). Consistent with this hypothesis, upregulation of the *Il1b* transcript precedes the upregulation of proteases such as *Mmp13* and *Ctsl*. Cathepsin L, a protease targeting both elastin and collagen, is a lysosomal and secreted enzyme that has yet to be appreciated in the context of cervical remodeling (figure 3.11) (Hashimoto, Kondo, & Katunuma, 2015; Kirschke, Kembhavi, Bohley, & Barrett, 1982; Mason, Johnson, Barrett, & Chapman, 1986). Its expression is exclusive to day 15 LPS cervixes and is not upregulated at term, indicating further studies are warranted to investigate its potential role in the cervical elastic fiber disruption seen in LPS-mediated preterm birth.

Investigations into how the cervical ECM is altered in a proinflammatory environment assumed to be rich in proteases utilized three main staining and imaging techniques. Initial forays into elastin imaging using Hart's variation of Verhoeff Van Gieson staining did not demonstrate any observable changes in elastin morphology in day 15 LPS versus day 15 (figure 3.2). Immunofluorescence using an antibody specific for exons 6-17 of tropoelastin demonstrated increased punctate morphology and fewer long fibers in day 15 LPS compared to day 15 (figure 3.3). This result suggested a potential disruption in elastic

fibers. Perhaps more antibody binding is occurring in day 15 LPS due to more epitope availability, owing to disrupted elastic fiber. Transmission electron microscopy most clearly allowed for the visualization of disrupted elastic fiber ultrastructure (figure 3.4).

These described findings above along with biomechanics data demonstrating reduced tissue resiliency in day 15 LPS compared to day 15 (figure 3.5) provided rationale to further investigate biochemical parameters of elastic fibers. Given that less darkly stained elastin was observed qualitatively using TEM, it was surprising that overall elastin solubility and extractability appeared unchanged in day 15 LPS versus day 15 using the methods described above (figure 3.6). A true measure of functionally integrated elastin would come from crosslinking measurements, which were not performed as part of this study, but will likely be completed in the future, depending on reagent availability for our collaborators.

TGF β signaling, via measurements of phospho-SMAD2/3, did not demonstrate an increase in activity in day 15 LPS versus day 15. Other TGF β signaling pathways, including the MAPK cascade, could be induced with disrupted microfibrillar/elastic fiber ultrastructure but were not investigated here.

While Gene Ontology analysis results, demonstrating upregulated protease gene expression, and the observed disrupted ECM architecture suggest that protease-mediated disruption of the cervical ECM contributes to the premature loss of cervical stiffness in LPS-mediated preterm birth, we were unable to provide functional evidence to support this hypothesis. Generally un-optimizable protocols, specifically the demonstration that some aspect of whole tissue extracts inhibits exogenous protease activity, plagued these mechanistic studies. Potential explanations include the heterogeneity of whole tissue lysates

(both from a cell type perspective and the abundance ECM present in the cervix).

Employment of an optimized purification protocol to enrich for proteases, as was done for the EnzChek assays, did not prevent activity of endogenous inhibitors. Given the localization of disrupted elastic fibers and collagen fiber spacing changes in the subepithelial stromal region of the cervix, *in situ* zymography was anticipated to localize intensified fluorescent signal in the region of the cervical stroma nearest to the epithelial cells in day 15 LPS samples versus day 15 samples in which fluorescent signal was expected to be minimal. No such increase in fluorescence was seen, however.

Determination of the role of IL1B in the upregulation of protease gene expression was undertaken in two separate sets of experiments. To determine the sufficiency of IL1B to induce the proteases demonstrated to be upregulated in response to LPS, intrauterine application of IL1B was performed much like IU LPS on day 15 of pregnancy (figure 3-12). The uterine proinflammatory response to IL1B treatment was highly variable with overall trends toward proinflammatory induction at both 4 and 8 hour time points. Cervical induction of proinflammatory *Tnf* and protease *Mmp13* occurred at the 8 hour time point with *Ptgs2* induction seen at 4 hours. It is likely that additional uterine-derived stimuli, induced by LPS, are able to activate proteases in the cervix. Our lack of understanding of the actual signaling that happens with IU LPS to lead to cervical remodeling likely hinders our understanding of gene expression changes. To determine necessity of IL1B signaling to upregulated protease gene expression, IL1B receptor antagonist Anakinra (Kineret) was utilized in conjunction with LPS (figure 3-17). No change in uterine or cervical proinflammatory or protease gene expression with Anakinra treatment was seen, pointing to

the likelihood of multiple compensatory mechanisms in place, such that blocking a single pathway is not sufficient to block the proinflammatory cascade.

The goal of the experiments described in this chapter was to expand our understanding of structural changes within the ECM that allow for the loss of mechanical integrity of the cervix with LPS exposure and to interrogate transcriptome pathways identified in the RNA-seq datasets as a means to understand the molecular events in the cervix driving LPS-mediated preterm birth. Proteases commonly upregulated at term (*Adamts 1 & 4*) are also upregulated in the cervix upon LPS treatment. There is an additional subset of proteases including other ADAMTS proteins, matrix metalloproteinases, and cathepsins, each of which are known to target collagen and elastin for degradation, that are upregulated exclusively in LPS. Evidence of altered ECM organization, which we hypothesize is a consequence of the protease upregulation, includes increased collagen porosity in the sub-epithelial stroma specifically and disrupted ultrastructure of elastic fibers, which are located in the same stromal area near to the epithelium of the central os. The variety of techniques undertaken to link inflammasome activation and downstream ECM disruption fell short of determining a mechanistic link between the two.

Future studies will focus on understanding potential disruptions to another important member of the elastic fiber, namely the microfibrillar scaffold consisting of fibrillin 1 and 2. There may be proteases, upregulated specifically in response to infection, that target fibrillin 1 and/or 2 and somehow disrupt the normal elastic fiber ultrastructure and therefore function.

Much of what has been learned from these experiments can inform future investigations of the unique cervical ECM landscape of infection-mediated preterm birth.

The sub-epithelial stroma appears to be a ‘hot bed’ of activity—ECM alterations in collagen and elastin are localized here upon LPS treatment, immune cells cluster here (Nallasamy et al, manuscript in preparation), and preliminary results from our lab demonstrate the ability of epithelial cells, in addition to immune cells, to express proteases in response to LPS. Understanding how these regionalized changes specifically influence biomechanical parameters of the tissues may one day aid in the development of clinically relevant modalities, given that epithelial cells are the most diagnostically and therapeutically accessible cells of the cervix.

The protease and ECM data provide a launching point for studies into the ECM repair process following a birth at term and also following a preterm birth mediated by infection and inflammation. Much is yet to be understood about postpartum tissue repair, which undoubtedly is influenced by an inflammatory milieu. This cervical repair in the postpartum period may be pathologically altered following an infection-mediated preterm birth, leading to compromised cervical function in subsequent pregnancies. After all, the most robust risk factor for a preterm delivery is an obstetrical history of preterm birth (Ferrero et al., 2016). The postpartum studies undertaken as part of this thesis will be discussed in chapter 4.

3.4 Materials and Methods

3.4.1 Mice

All animal studies were conducted in accordance with the standards of humane animal care as described in the NIH Guide for the Care and Use of Laboratory Animals. The

research protocols were approved by the IACUC office at the University of Texas Southwestern Medical Center. Mice were housed under a 12 h-light/12 h- dark cycle at 22°C. Virgin C57B6/129sv 2-6 month old female mice were caged with fertile males of the same strain for 6 hours. The presence of a vaginal plug at the end of the 6 hours was considered as day 0 of pregnancy, with birth of the pups generally occurring early morning day 19.

3.4.2 Inflammation Preterm Labor Model

Intrauterine injection of LPS (day 15 LPS) was used to induce preterm labor as previously described (Holt et al., 2011). Briefly, mice on day 15 of pregnancy were anesthetized between 0700-0900, and 30uL sterile water (sham) or 5mg/mL LPS (E. coli O55:B5 Sigma, St. Louis, MO) was injected intrauterine. Cervical tissues were collected 1, 2, 4, or 6 hours after surgery and before the onset of labor, which occurs approximately 7-9 hours after LPS administration.

3.4.3 RNA Sequencing

RNA was isolated using an miRNeasy kit from Qiagen (Hilden, Germany). Quantity was determined using a Nanodrop and quality determined using a Bio-Rad Experion. RNAs with RNA Quality Index (RQI) scores above 9 were used to make cDNA libraries. Eight total cDNA libraries from four different time points/treatment groups (day 15, day 15 sham, day 15 LPS, and day 18) were prepared, with duplicate libraries for biological replicates containing 4 cervixes each. 1.25 µg RNA from each cervix was pooled for 5µg of starting RNA in each library. Library preparation was carried out as described previously (Zhong et al., 2011). 100 base pair, paired end sequencing was carried out on an Illumina sequencer to a depth of 100 million reads. We developed a computational pipeline to determine the

differentially expressed genes between the conditions, which included the following steps: reads were aligned to the *mm9* genome using the spliced read aligner TopHat version v.2.0.4, transcriptome assembly was carried out using Cufflinks v.2.0.2 with default parameters, filtered transcripts were merged into distinct non overlapping sets using Cuffmerge, and Cuffdiff was used to calculate the differential expression genes between the conditions (Kim et al., 2013; Trapnell et al., 2010).

3.4.4 Transcriptome Data Analysis

The differentially expressed genes extracted from the above analysis were then used in downstream analyses. Venn Diagrams were generated using Venn Diagram Plotter version 1.5.5228.29250 for the differentially expressed genes in different conditions. Gene Ontology Analyses and KEGG pathways were determined using DAVID, a web tool for functional annotation and gene enrichment analysis for the genes that are specifically expressed at Day 15 LPS treatment as compared to Day 18. Heatmaps were generated using Java TreeView for the significantly expressed genes in at least one condition to analyze the effect in the specified condition (Dennis et al., 2003).

3.4.5 RNA isolation and quantitative PCR

Total RNA was isolated as previously described (Nallasamy et al., 2017a). cDNA synthesis was carried out using 0.5µg total RNA and 5x iScript Reverse Transcription Supermix (Bio-Rad, Hercules, CA). Quantitative PCR primers used in this study were designed and purchased from Invitrogen. Target gene expression was normalized to the expression of housekeeping gene *Ppib* using the $2^{-\Delta\Delta Ct}$ relative gene expression method (User Bulletin no. 2; Applied BioSystems).

3.4.6 Elastin staining

Mice were anesthetized with avertin and perfused with heparinized saline and 4% PFA on day 15, day 15 sham, day 15 LPS, and day 18. Cervical tissues were fixed for 48 hours at 4 degrees with fresh PFA before paraffin embedding and sectioning at 5 microns.

Hart's Variation of Verhoeff van Gieson staining was carried out on transverse sectioned cervixes as previously described (Sheehan DC, 1980). Stained sections were imaged using a Hamamatsu NanoZoomer 2.0-HT digital slide scanner. Images were taken at 40x and NDP.view 2.4.26 from Hamamatsu Photonics K.K. software used to export 20x views.

Immunofluorescence studies were carried out as previously described (Nallasamy et al., 2017a). Briefly, paraffin sections were deparaffinized in ethanol baths and rinsed in PBS. Antigen retrieval was carried out using 6M Guanidine HCl and iodoacetate. Sections were blocked for 30 minutes with normal goat serum (NGS) before primary antibody (1:250 dilution, Elastin Products Company cat #PR385, Owensville, MO) incubation in NGS overnight 4°C. Sections were washed in PBS then incubated with Alexa Fluor 546 goat anti-rabbit antibody (1:500, Invitrogen cat# A-11035, Carlsbad, CA) in NGS for 30 minutes at room temperature in the dark. Coverslips were mounted atop sections with DAPI Prolong Gold (Life Technologies, Eugene, OR) and imaged using a Zeiss LSM880 microscope.

TEM was carried out as previously described (Nallasamy et al., 2017a). Briefly, pregnant mice were perfused with heparinized saline then glutaraldehyde and paraformaldehyde fixatives in sodium cacodylate buffer. Cervical tissue was removed and fixed in glutaraldehyde in sodium cacodylate buffer overnight at 4°C. The cervix was then

sliced in transverse sections and processed as previously described (Nallasamy et al., 2017a).

A Tecnai G2 spirit transmission electron microscope at 120 kV and a side mounted SIS

Morada 11 megapixel CCD camera were used for image acquisition.

3.4.7 Biomechanical Testing

Mice from day 15, day 15 LPS, and day 18 groups were sacrificed and cervical tissue collected without removal of uterine and vaginal tissue. Samples were flash frozen and sent on dry ice overnight to collaborators at Columbia University, New York. Biomechanics testing was carried out in cyclical load-unload-recover tensile testing after equilibration of samples in PBS + EDTA for 2-4 hours (communications with Kyoko Yoshida). The first load level was 90% of the average transition stress, the second 150% of average transition stress, and the third and final at 75% of average yield force prior to breaking.

3.4.8 Elastin solubility testing

Elastin solubility was tested as previously described (Nallasamy et al., 2017a). Briefly, whole tissues were frozen pulverized and suspended in PBS with protease inhibitors and EDTA (Thermo Scientific) and extracted for 24 hours on a rotator at 4°C. The next day, samples were centrifuged at max speed for 15 minutes at 4°C and supernatant kept at -20°C while pellet was resuspended in 6M Urea, homogenized, and extracted for 24 hours on a rotator at 4°C. The next day, samples were centrifuged at max speed for 15 minutes at 4°C and supernatant kept at -20°C and pellet discarded. PBS and urea extracts were dialyzed in distilled water for 6 hours, changing water every 2 hours, before lyophilization was used to concentrate extracts. Protein concentration was estimated using a Bradford protein assay (Thermo Scientific). 20ug of protein was used for western blotting. After running samples

alongside protein standards (Precision Plus Protein Kaleidoscope, Bio-Rad) at 100V for 90 minutes on a 4-20% 10 well gel (Bio-Rad), extracts were transferred to a nitrocellulose membrane at 100V for 60 minutes at 4°C. Blot was washed with TBST, blocked in 5% nonfat dry milk (NFDM) for 1 hour at room temp, and probed with a primary antibody against tropoelastin, as used in immunofluorescence above, at 1:1000 dilution in 5% NFDM overnight at 4°C. The next morning, blots were washed 3x in TBST and probed with 1:10,000 goat anti-rabbit HRP conjugated antibody (Bio-Rad) for 1 hour at room temp. Blots were washed 3x in TBST before being rinsed in ECL (GE Healthcare) and imaged.

3.4.9 Elastin extractability testing

To test the extractability of elastin in whole tissue, Fastin Elastin Assay (biocolor life science assays) was used. Briefly, individual cervix samples from day 15, day 15 sham, day 15 LPS, and day 18 groups were weighed and 750uL 0.25M oxalic acid added to each sample. Tubes were placed in a metal heating block for 60 minutes at 100°C. Samples were then removed from heat, allowed to cool to room temperature, and centrifuged at 10,000 rpm for 10 minutes. Supernatants were retained at -20°C for future experimentation. Pellet was once again extracted using hot oxalic acid as above, samples centrifuged, and supernatant stored. Remaining pellet was again extracted as above, centrifuged, and supernatant kept as final sample. Pellet was discarded. Equal volume of elastin precipitating reagent was added to each supernatant and briefly vortexed. Samples were kept at room temperature for 15 minutes to allow for precipitation. Tubes were centrifuged at 10,000 rpm for 10 minutes and tubed drained of liquid. 1mL Dye Reagent was added to each tube and vortexed. Samples were shaken for 90 minutes and centrifuged at 10,000 rpm for 10 minutes. Tubes were

drained for unbound dye and 250uL Dye Dissociation Reagent. Tubes were set at room temperature for 10 minutes and vortexed briefly. Contents of tubes were transferred to 96 well plate and measured using a microplate reader at 513nm. Blanks were made using test solution solvent and standards using alpha-elastin.

3.4.10 TGF β Signaling

Relative abundance of SMAD2/3 and phosphorylated (p)SMAD2/3 was measured using western blotting. Two cervices per group (day 15, day 15 sham, and day 15 LPS) were used per lane and experiment repeated with unique samples 3 times. Frozen tissues were homogenized in RIPA buffer with protease and phosphatase inhibitors, protein concentrations estimated using Bradford assay as above, and 20ug sample loaded and western run as above. Primary antibodies against pSMAD2/3 and SMAD2/3 (Cell signaling cat # 8828) were used at 1:1000 concentrations in 5% BSA overnight at 4°C and completed as above.

3.4.11 In Situ zymography

Mice were sacrificed and tissues dissected as above for biomechanics and placed in 1X zinc buffered formalin (36.7 mM ZnCl₂, 27.3mM ZnAc₂ x 2H₂O, and 0.63 mM CaAc₂ in 0.1M Tris, pH 7.4) (Hadler-Olsen et al., 2010). Samples were embedded in paraffin without ethanol washing and sectioned at 5 microns. Sections were placed on slides and deparaffinized at 59°C for 1 hour. Samples were deparaffinized in 3x xylene baths and rehydrated in graded ethanol baths. 1mg DQ *elastin, *gelatin, or *type 1 collagen (Molecular Probes, Eugene, OR) was reconstituted with 1mL deionized water and subsequently re-diluted 1:50 in reaction buffer (50mM Tris-HCl, 150mM NaCl, 5mM CaCl₂,

and 0.2mM sodium azide (pH 7.6). 250uL solution as placed atop tissue sections in a humid box at 37°C. Sections were rinsed with deionized water and fixed with 10% formalin for 10 minutes in the dark. Sections were washed in PBS and coverslips mounted with DAPI (Invitrogen). Tissues were kept in the dark until confocal imaging at 20x using a Zeiss LSM880 microscope. An EDTA + substrate negative control was used, although its inhibition of fluorescence was not seen.

3.4.12 Collagenase and Elastase Activity Assays

Flash frozen cervical tissues were processed as previously described (Wieslander et al., 2008). Briefly, tissues were minced on ice and washed with cold PBS + 2mM N-methylamine (NMA) 3x. Tissues were frozen pulverized and 0.5M NaAc, pH 4 + NMA added to each sample before homogenization with a ground glass homogenizer. Samples were then placed on a rotator overnight 4°C. The next morning, samples were centrifuged for 30 mins at 4°C. Supernatant was kept at -20°C and pellet re-homogenized in sodium acetate buffer before being placed on the rotator at 4°C for 5 hours. Samples were centrifuged for 30 mins at 4°C and supernatant kept at -20°C. Pellet was re-homogenized in sodium acetate buffer before being placed on the rotator at 4°C for 30 minutes. Samples were centrifuged for 30 mins at 4°C and supernatant kept at -20°C. Pellet was discarded. Supernatants were pooled and dialyzed overnight in deionized water + NMA. The next morning, samples were lyophilized until liquid was completely removed. Pellet was resuspended in 60% NH₄SO₄ and rotated overnight at 4°C. The next day, sample was centrifuged at max speed for 20 minutes and supernatant discarded. Pellet was resuspended in 2/3 (uL/dry weight) in assay buffer provided in EnzChek Kits (Molecular Probes, Eugene,

OR). Assays were carried out according to kit protocol. Samples, blanks, positive (enzyme) and negative (enzyme + inhibitor) controls were added to DQ substrate and fluorescence measured using 495nm absorbance and 515nm emission spectra for gelatinase and collagenase, 505/515nm excitation/emission for elastase.

3.4.13 Neutrophil Elastase Assay

Flash frozen cervixes from day 15, day 15 LPS 1, 2, and 4 hours post IU treatment were washed with PBS + n-methyl amine. Tissues were homogenized in 300uL 50mM Tris, 1mM CaCl₂, and 0.5mM ZnCl₂ (Gibbs, Warner, Weiss, Johnson, & Varani, 1999). 2mM Methoxysuccinyl-Ala-Ala-Pro-Val-p-nitroanilide substrate (Calbiochem, EMD Millipore cat # 454454) was used in each reaction and positive control purified human neutrophil elastase (Enzo, Fisher Scientific, cat # BML-SE284-0100) used. N-methyloxysuccinyl-Ala-ala-Pro-Val-chloromethyl ketone (Molecular Probes) was used as an elastase inhibitor. Relative absorbance was measured over time at 405nm.

3.4.14 Intrauterine IL1B administration

5ug mouse IL1B (Cell signaling, cat #5204SF) was injected intrauterine on day 15 of gestation as above for LPS. Mice were sacrificed 4 and 8 hours after treatment and tissues collected.

3.4.15 Anakinra

In IP Anakinra experiments, 25mg/kg Anakinra was injected IP 1 hour prior to LPS treatment. 100ug LPS in 100uL sterile H₂O was injected intraperitoneally. In IU Anakinra experiments, 25mg/kg Anakinra was injected intrauterine 15 minutes before another dose of

Anakinra and 5mg/mL LPS were injected intrauterine. In mice that were sacrificed 4 hours post-LPS injection, a third dose of Anakinra was injected IP at hour 3 post-LPS injection.

A.

GO ID	All Inflammation Preterm Transcripts	Count	p-value
0006508 BP	proteolysis	107	0.0339
0008233 MF	peptidase activity	75	0.00131

C.

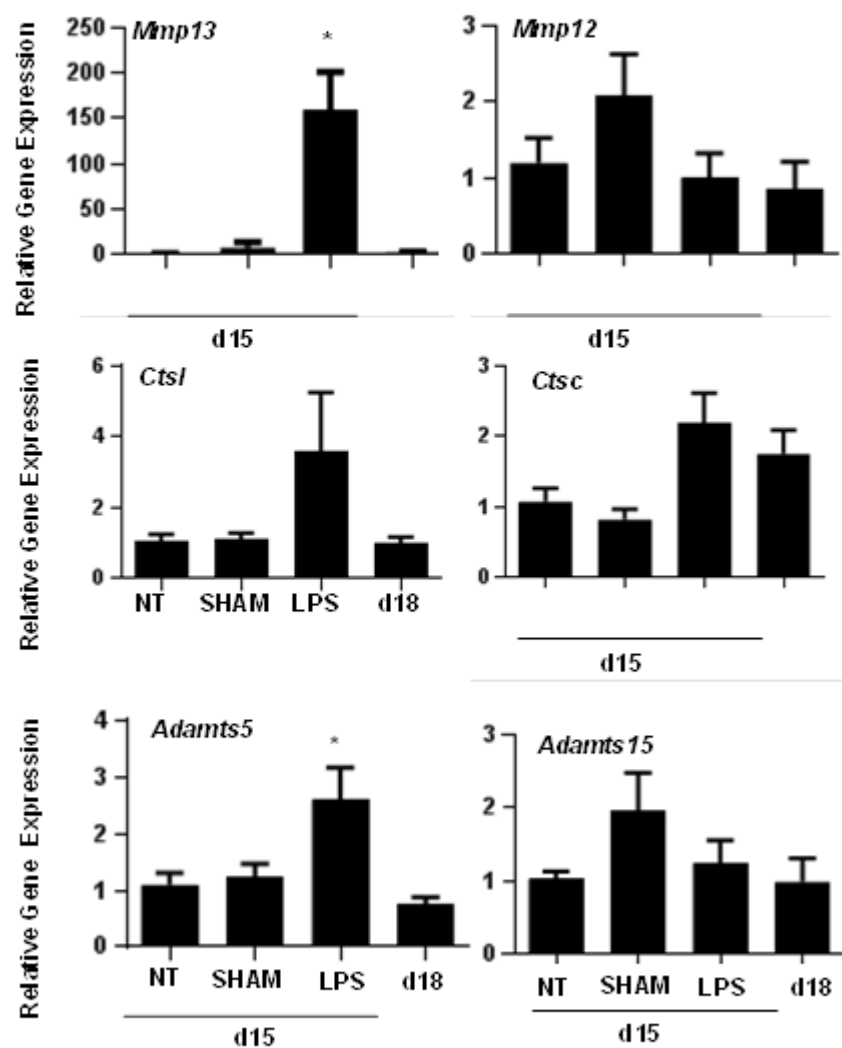
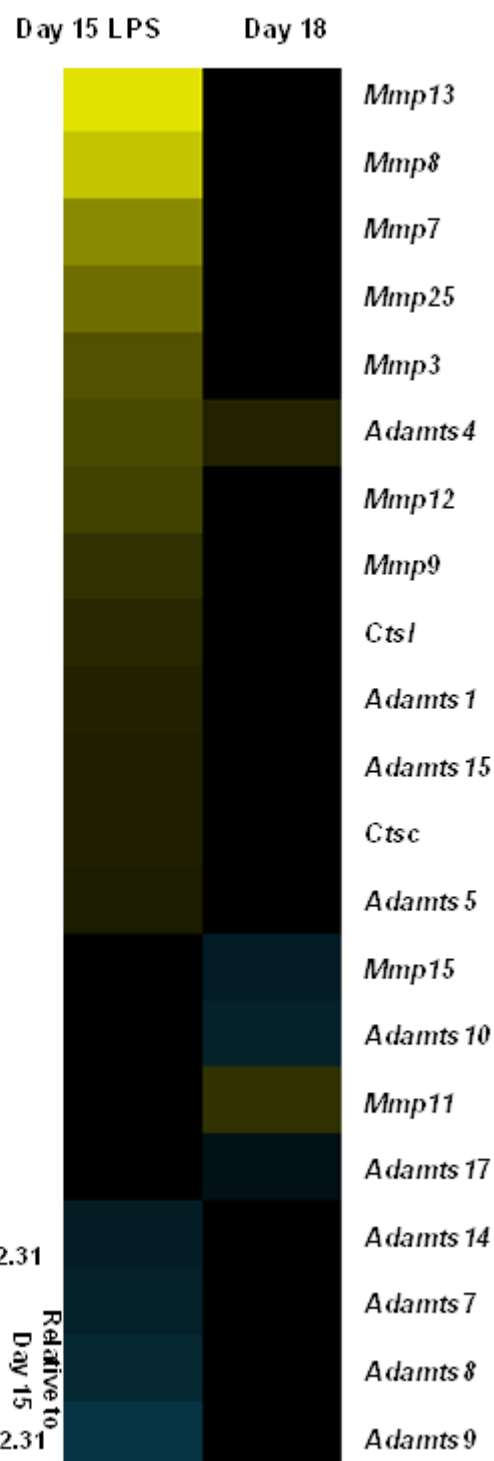
B. Proteases

Figure 3.1. Protease genes and pathways are upregulated in the cervix during LPS-mediated preterm birth exclusively.

(A) Gene ontology biological process Proteolysis and molecular function Peptidase Activity are enriched in the gene set exclusive to LPS-mediated preterm birth. Count refers to the number of genes from the data set that are a part of the GO pathways. (B) Heatmap of selected proteases and their expression pattern in day 15 LPS cervices vs day 15 cervices (LPS preterm) and in day 18 cervices vs day 15 cervices (term). (C) qPCR results of selected protease genes showing relative gene expression on day 15, day 15 sham, day 15 LPS, and day 18. The values expressed are mean \pm SEM. (n=4-6 cervices per group, One way ANOVA * $P < 0.05$ relative to day 15).

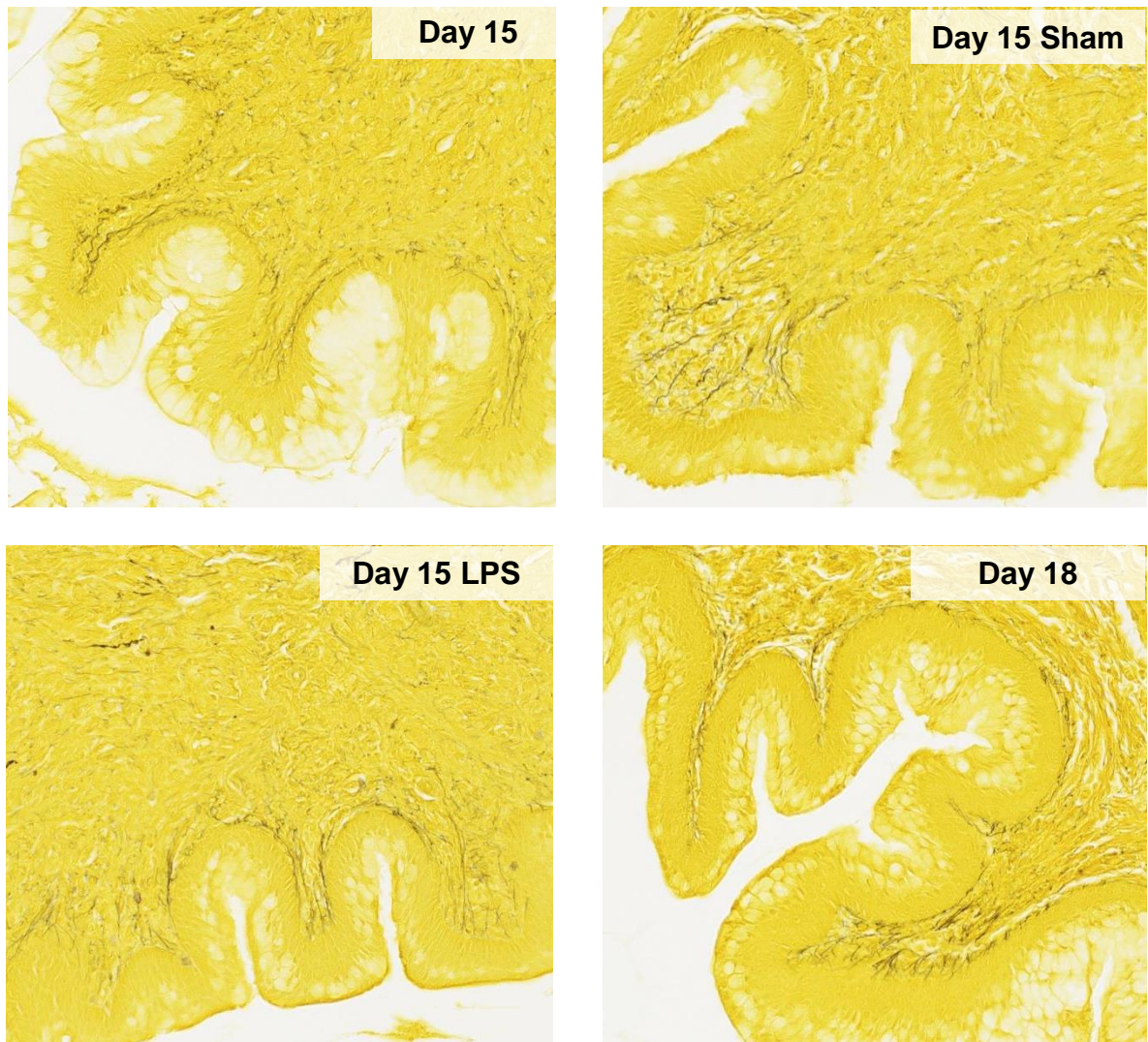


Figure 3.2. Elastin staining in the cervix demonstrates similar morphology in LPS-mediated preterm and term birth.

20x images of transverse sectioned mouse cervixes stained using Hart's variation of Verhoeff Van Gieson staining for elastin on day 15, day 15 sham, day 15 LPS, and day 18 of gestation. Elastin is most concentrated in the sub-epithelial stroma region of the cervix and less so throughout the stroma. (n=3-4 cervixes imaged per group and representative images selected).

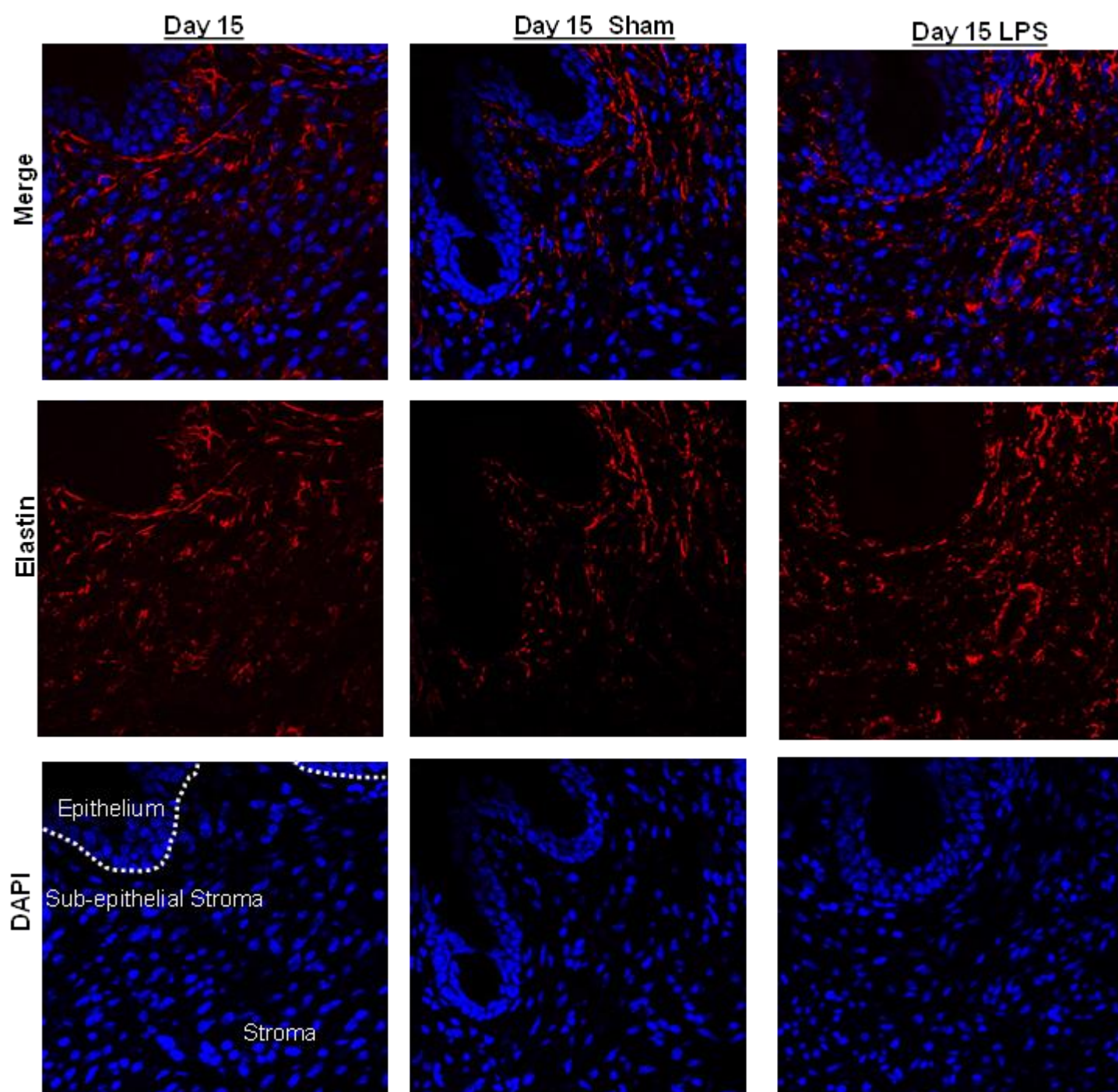


Figure 3.3. Immunofluorescence staining for tropoelastin suggests altered cervical elastin morphology upon LPS treatment on day 15.

Immunofluorescence imaging of tropoelastin (red), nuclei by DAPI (blue), and merged images in cervical sections from day 15, day 15 sham, and day 15 LPS mice. Elastin is most concentrated in the subepithelial stroma region, directly below the superimposed white dotted line between the epithelium and stroma, and can be visualized in long fiber structures, presumed to be elastin integrated into elastic fibers, on day 15 and day 15 sham. Most long fibers are lost upon LPS treatment on day 15, and shorter fibers are seen. N= 3 mice per group. Signal intensity was optimized for day 15, and the same settings were used for day 15 sham and day 15 LPS.

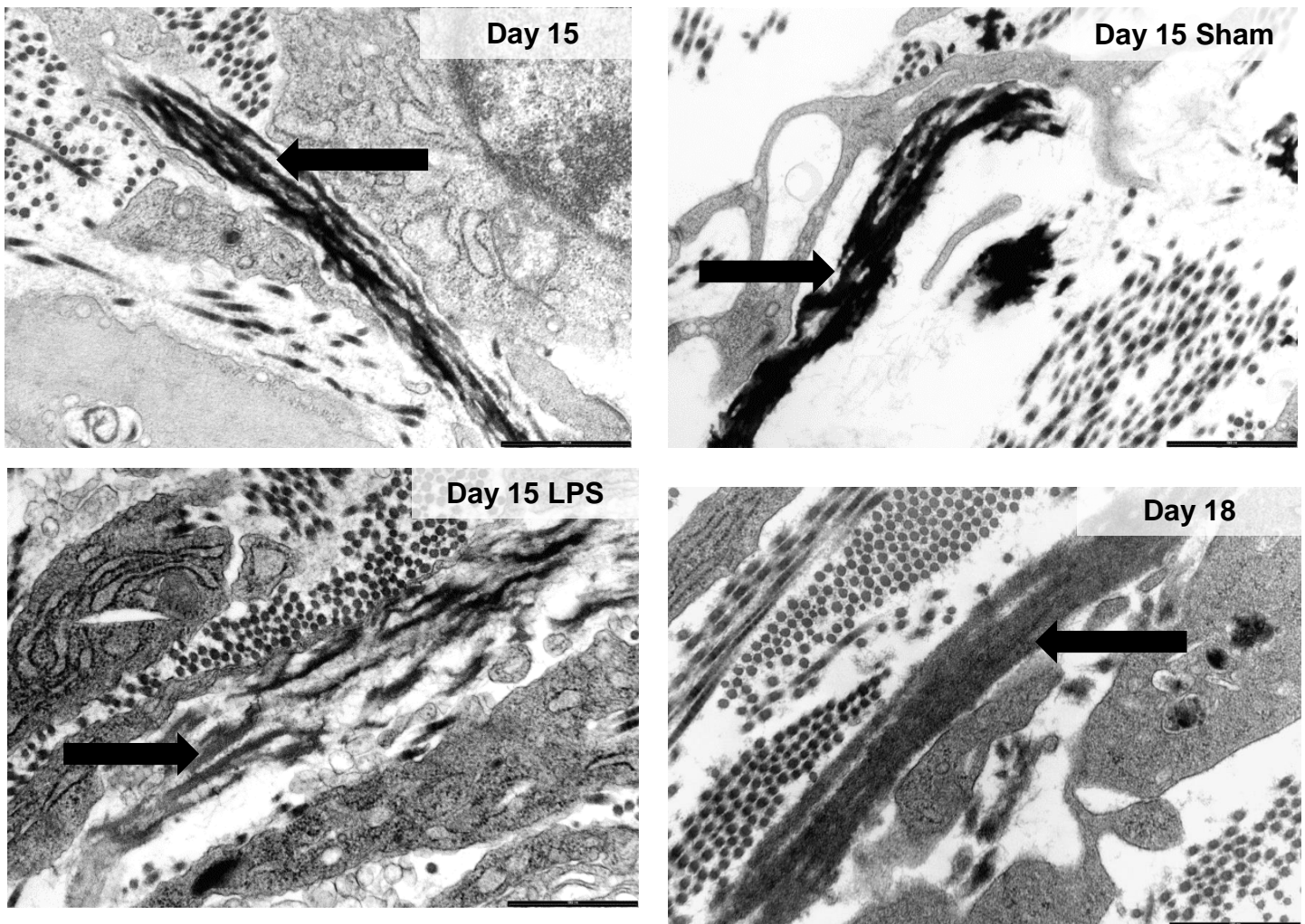
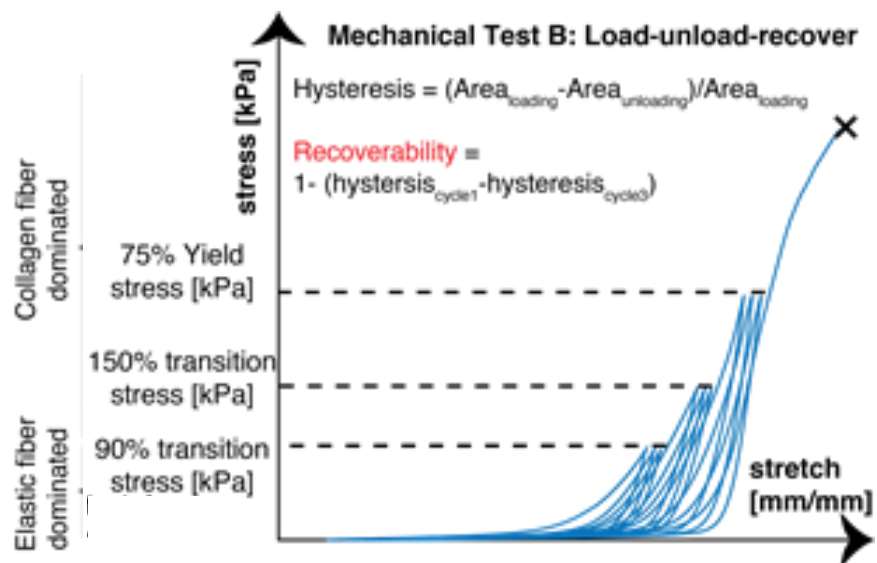


Figure 3.4 Elastic fiber ultrastructure is disrupted in the cervix of LPS-treated mice before onset of preterm birth.

Transmission electron microscopy (TEM) analysis of elastic fibers in cervixes from day 15, day 15 sham, day 15 LPS, and day 18 mice. Elastic fiber ultrastructure (black arrows) is abnormal in day 15 LPS compared to day 15 and sham. (n=3 mice per group). Scale bar: 1000nm

A.



B.

Recoverability at 75% Yield Force

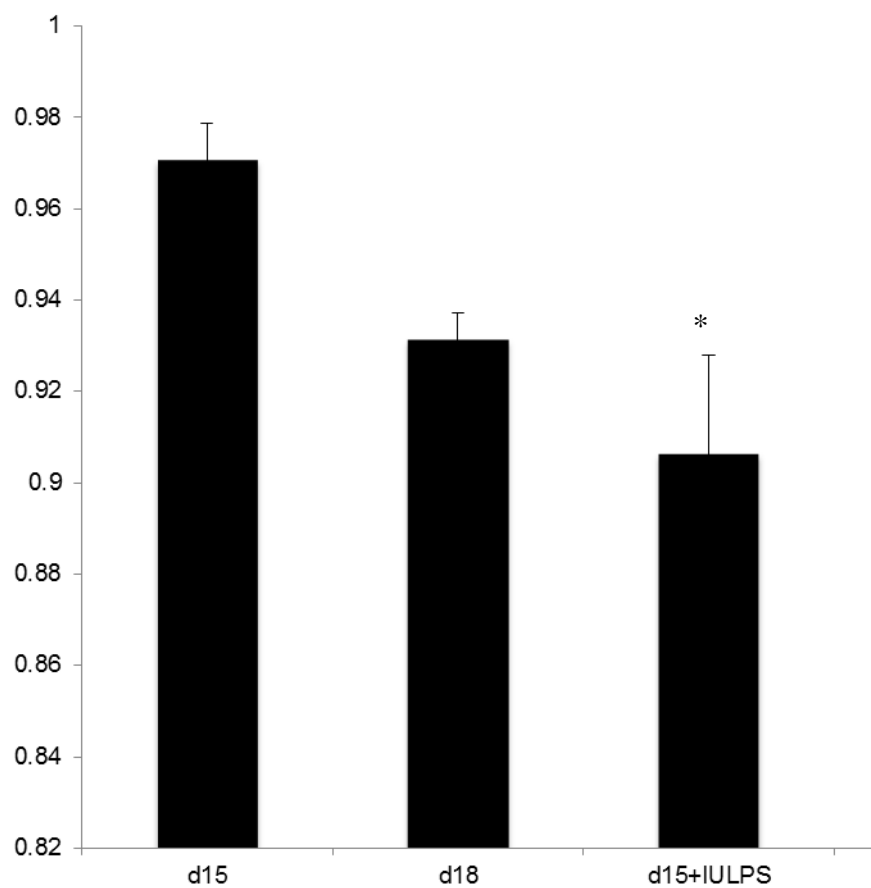
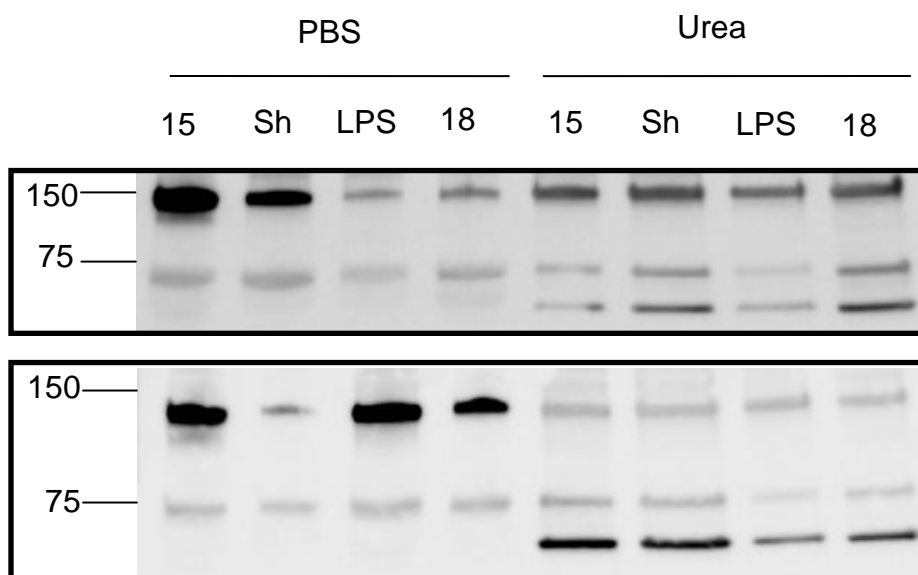


Figure 3.5. Cervical biomechanical studies indicates reduced resilience in LPS-mediated preterm birth but not at term.

(A) Schematic of load-unload-recovery biomechanical studies conducted at Columbia University demonstrating various stress increments at which tissue resilience of mouse cervixes was tested. (B) Graph demonstrating reduced tissue resilience in day 15 LPS compared to day 15 when tested at 75% yield force. N=3-4 cervixes per group.

A.



B.

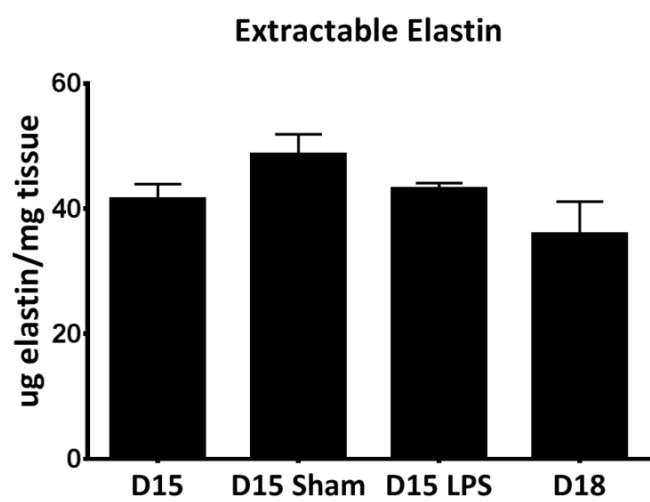


Figure 3.6. Cervical elastin solubility and extractability in LPS-mediated preterm and term birth. (A) Two, of 4, representative immunoblots of PBS and Urea extracts of mouse cervical samples from day 15 (15), day 15 sham (Sh), day 15 LPS (LPS), and day 18 (18). Dimerized tropoelastin measures 144kDa while monomeric tropoelastin around 72kDa. (B) Results from two separate Fastin Elastin extractability assays. Data are graphed as mean \pm SEM. (n=6 total samples per bar from two separate experiments)

A.

120

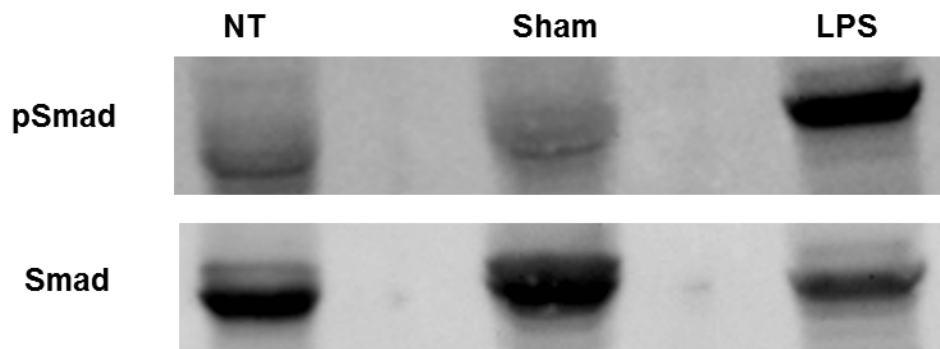
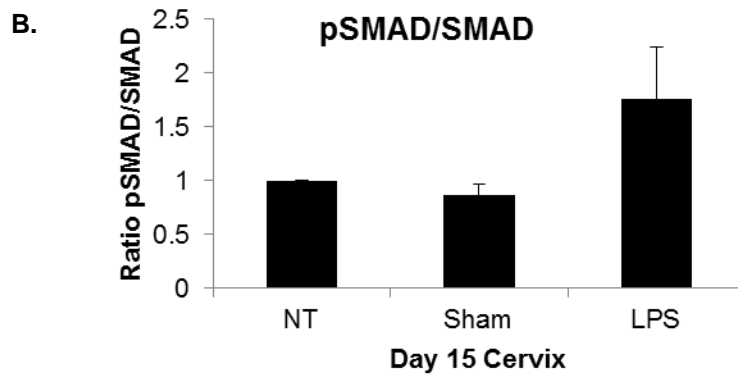
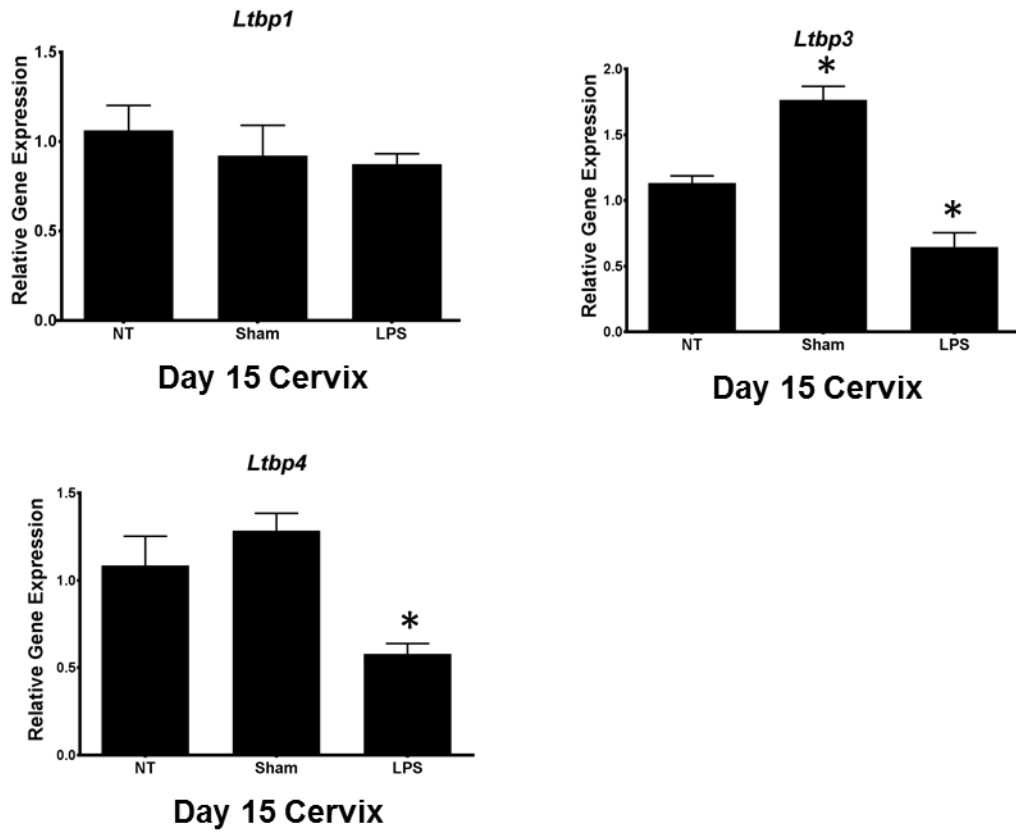


Figure 3.7. Latent TGF β Binding Proteins and phosphorylation of SMAD2/3 in LPS-mediated preterm birth. (A) qPCR results showing relative gene expression of latent TGF β binding proteins (*ltbp*) on day 15 (NT), day 15 sham (sham), and day 15 LPS (LPS). The values expressed are mean \pm SEM. (n=6-8 cervixes per group, One way ANOVA * P<0.05 relative to day 15). (B) Quantification and representative immunoblot (of three) of phosphoSmad 2/3 (pSmad) and Smad2/3 in day 15 (15), day 15 sham (Sh), and day 15 LPS samples. No statistical significance with Sham or LPS treatment compared to day 15 using One-way ANOVA & Tukey's Multiple comparison test.

A.

Substrate	DQ *Elastin, DQ*Gelatin, DQ*Collagen		Soluble Elastin	AAPV-pNA
Enzyme tested	elastases (MMP12, ELANE, CTSL) gelatinases (MMP2, MMP9) collagenases (MMP1, 8, 13)		Non-specific elastases	Leukocyte elastases
Experiment	<i>in situ</i> zymography	EnzChek assay kit	Measurement of liberated amino acids	Kinetic assay
Results	No difference in localization or fluorescence	Protein isolation method inhibits enzyme activity	Unable to optimize experiment	No change in activity day 15 LPS vs day 15

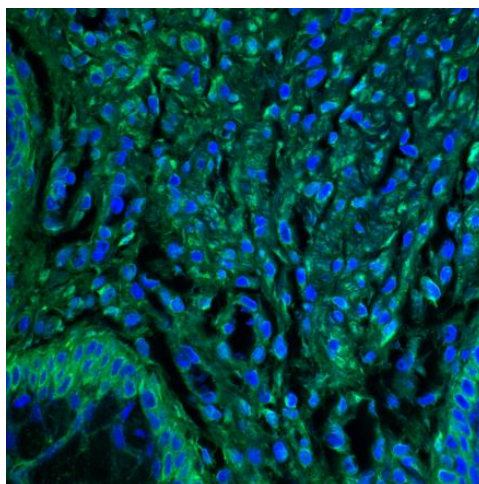
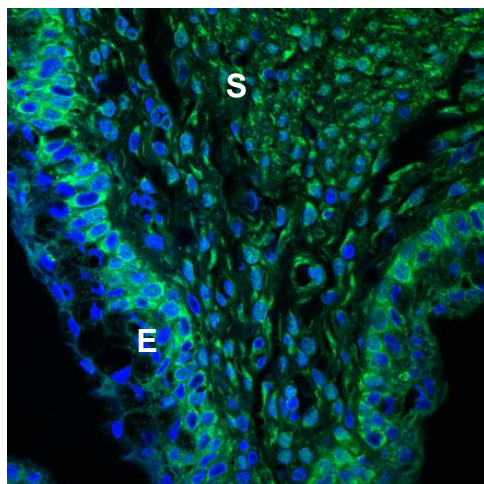
B. Day 15Day 15 LPS

Figure 3.8. Assays measuring protease activity in LPS-mediated preterm birth. (A)

Table depicting details of 4 protease activity assays used to compare endogenous protease activity in day 15 LPS and day 15 cervixes. **(B)** Images obtained via confocal microscopy demonstrating background fluorescence in day 15 and day 15 LPS cervixes in both the epithelium (E) and stroma (S) in *in situ* zymography experiments with type 1 collagen (shown here), elastin, and gelatin substrates.

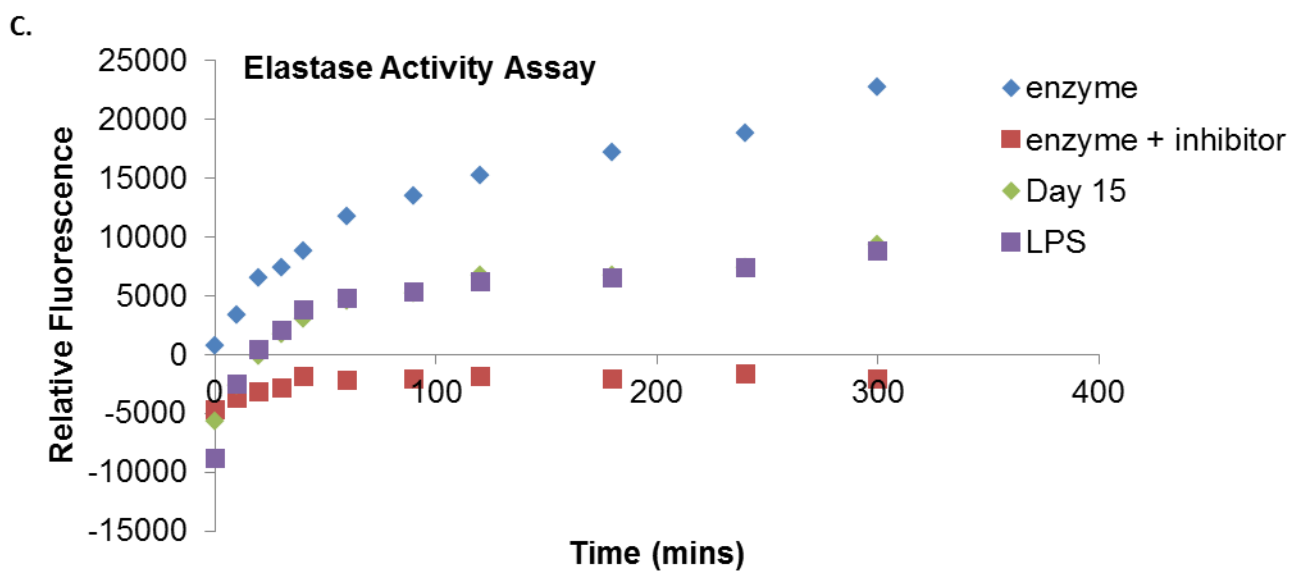
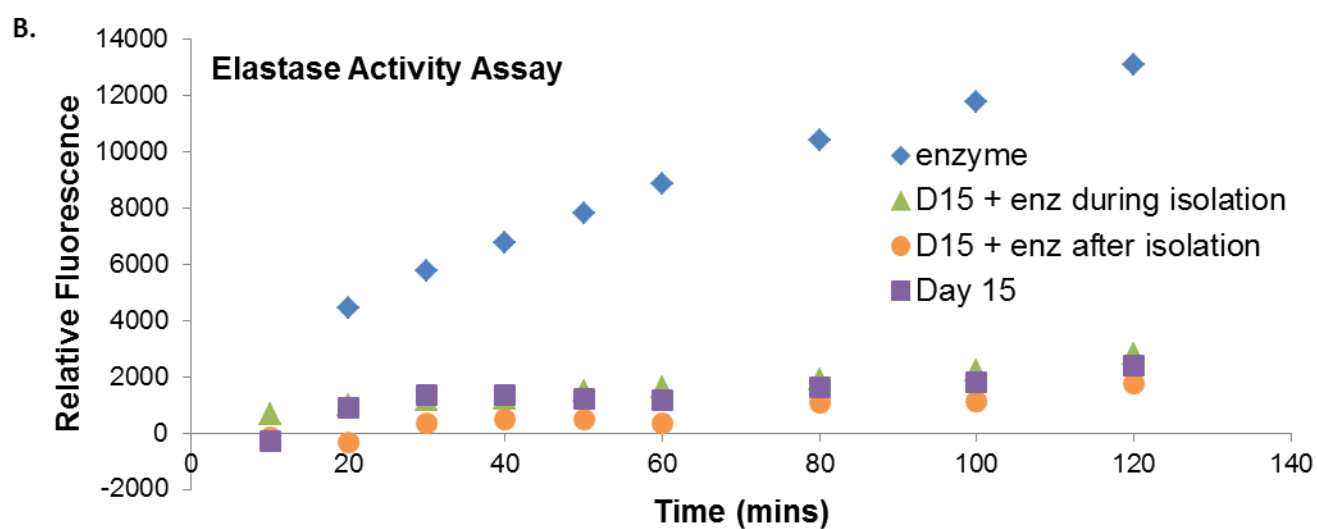
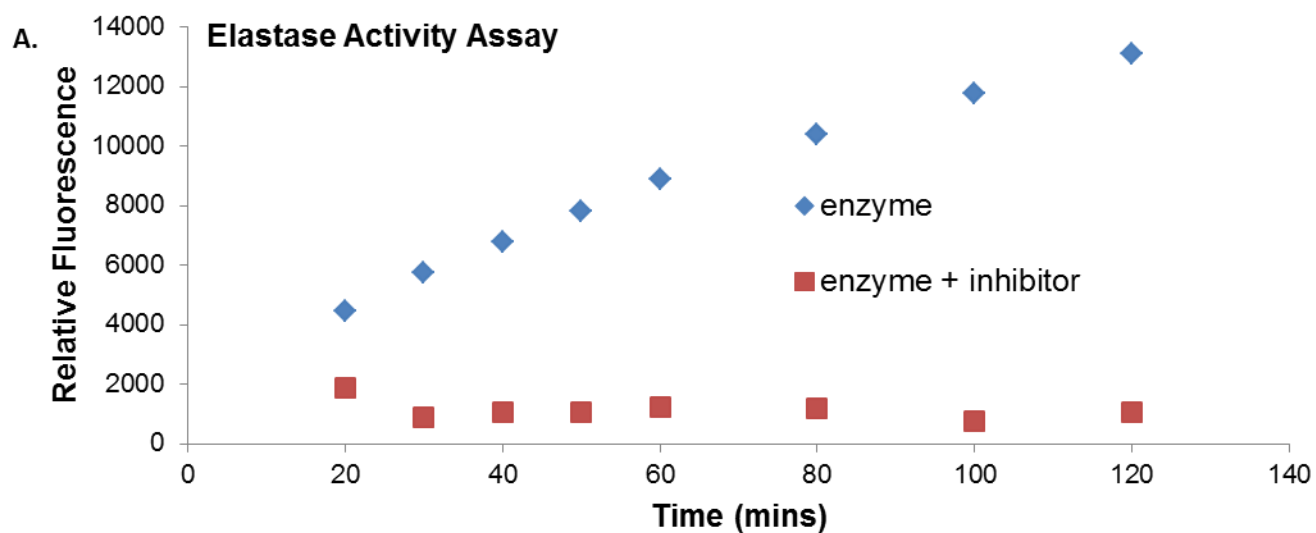


Figure 3.9. Elastase Activity Assays

(A) Graph demonstrating change in fluorescence over time with positive (purified elastase) and negative (purified elastase + elastase inhibitor) controls. (B) Graph demonstrating change in fluorescence over time with positive control (purified elastase enzyme), day 15 cervix extracts (day 15), and enzyme spiked into the isolation protocol during the process and after the process. (C) Graph demonstrating change in fluorescence over time with positive (purified elastase) and negative (purified elastase + elastase inhibitor) controls, day 15, and day 15 LPS cervix extracts.

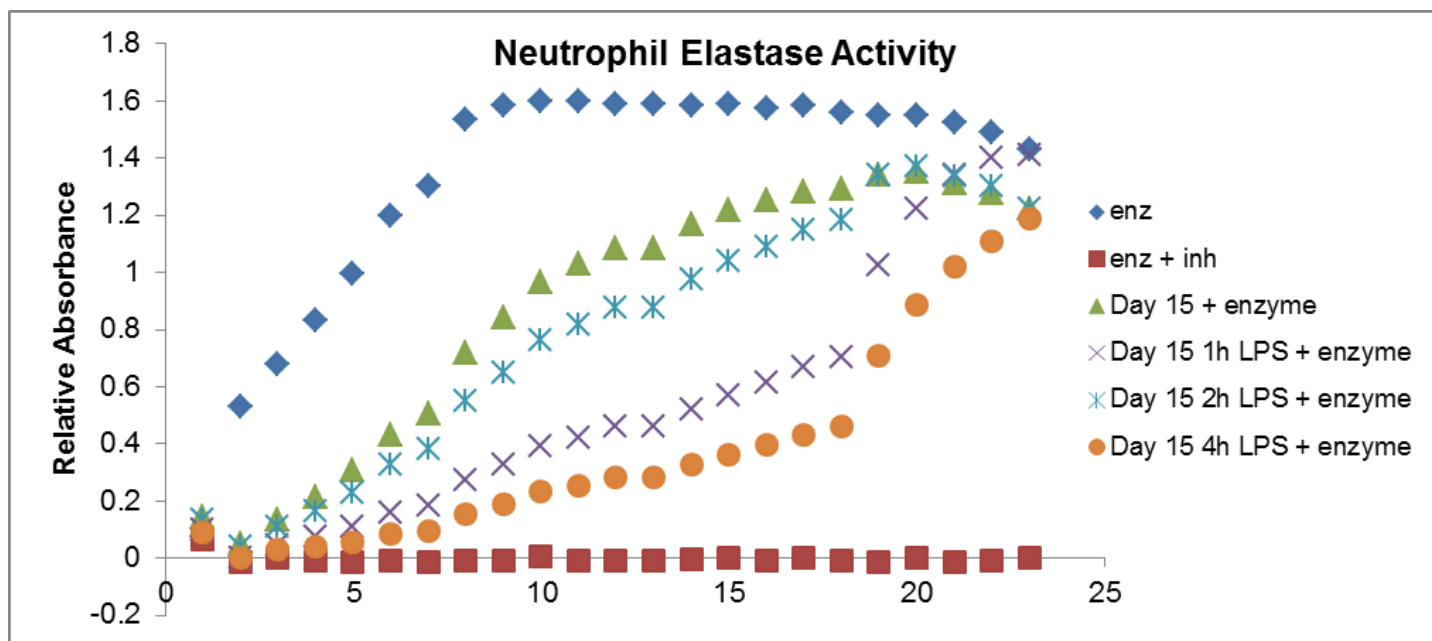


Figure 3.10. Neutrophil Elastase Activity Assay

Graph demonstrating change in absorbance over time with positive (purified neutrophil elastase) and negative (purified neutrophil elastase + elastase inhibitor) over time with 50uL whole tissue lysate from day 15, 1hour post LPS treatment, 2 hour post LPS treatment, and 4hour post LPS treatment cervicis.

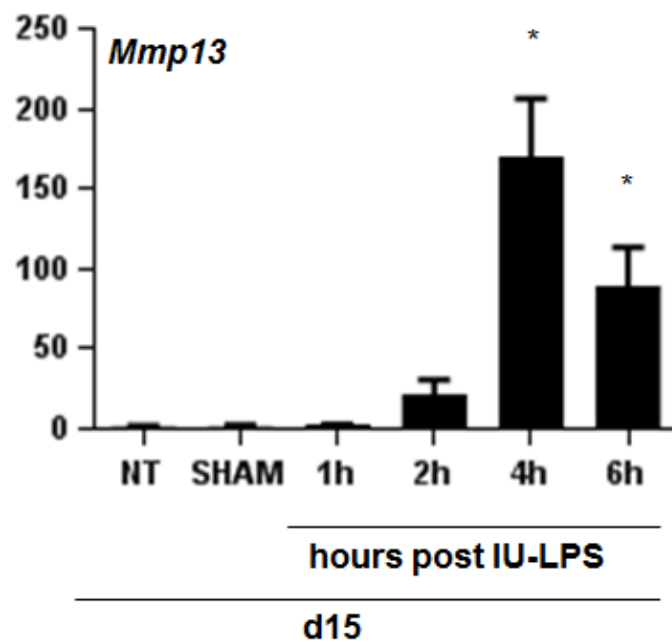
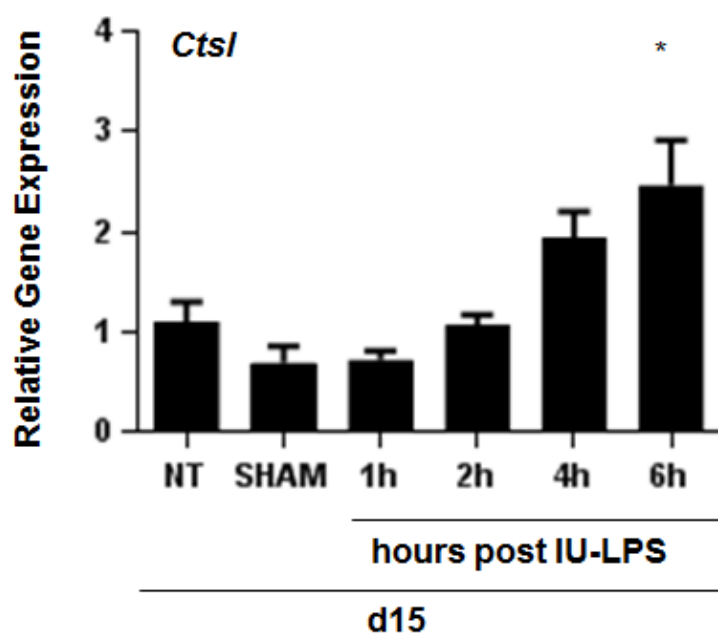
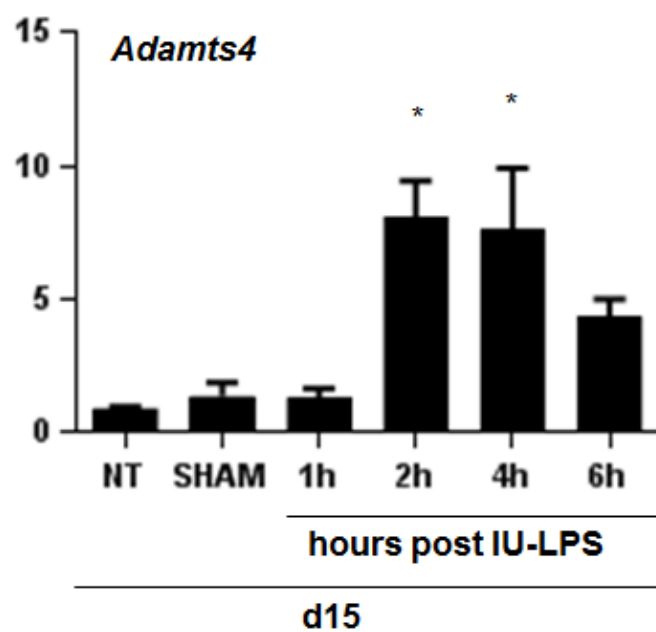
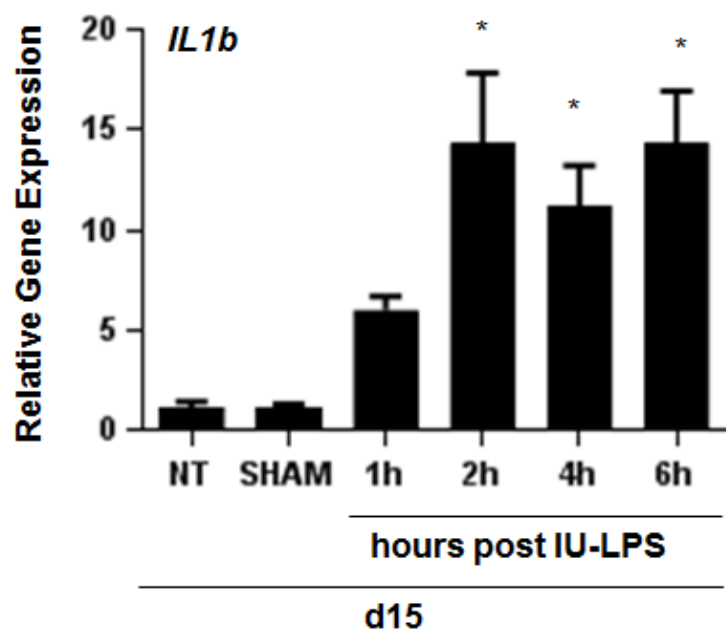


Figure 3.11. Time course of *IL1b*, *Adamts4*, *Ctsl*, and *Mmp13* gene upregulation in response to intrauterine LPS.

Gene expression analysis by qPCR demonstrates *IL1b* transcription is significantly induced in the mouse cervix by 2 hours post IU-LPS treatment and sustained at the 4 and 6 hour marks. Gene expression of proteases *Adamts4* is significantly upregulated at 2 and 4 hour time points, *Ctsl* by 6 hours, and *Mmp13* at 4 and 6 hours post IU-LPS compared to untreated day 15 (NT) samples. (n=4-6 samples per group, p<0.05 compared to day 15, Bars represent mean \pm S.E.M. One-way ANOVA)

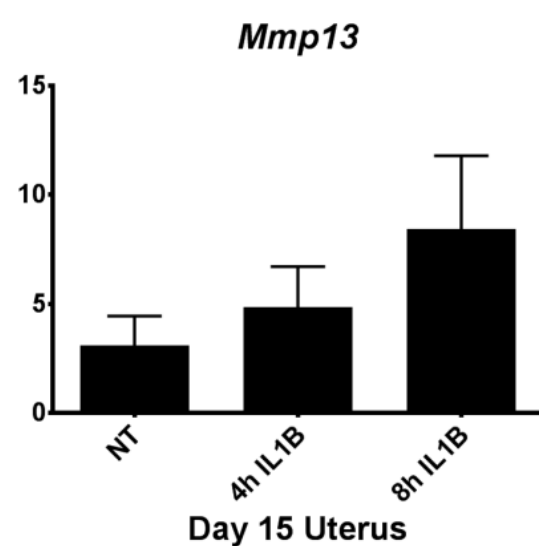
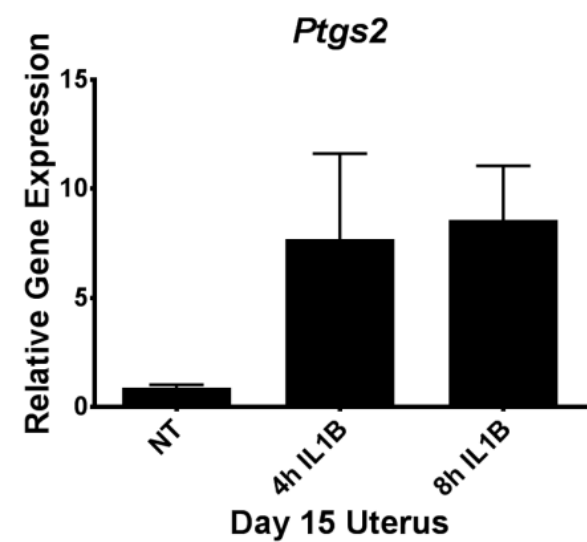
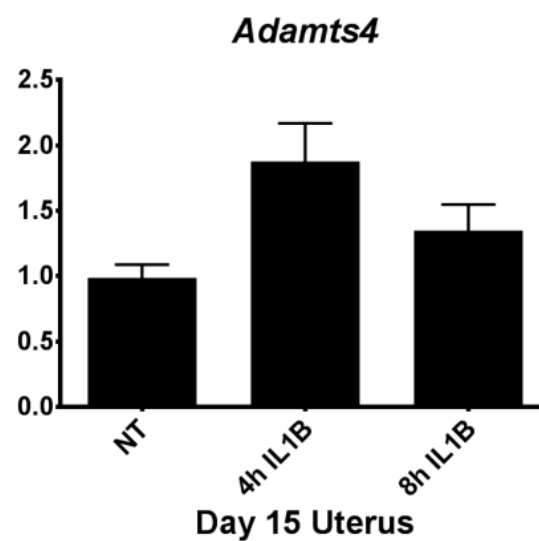
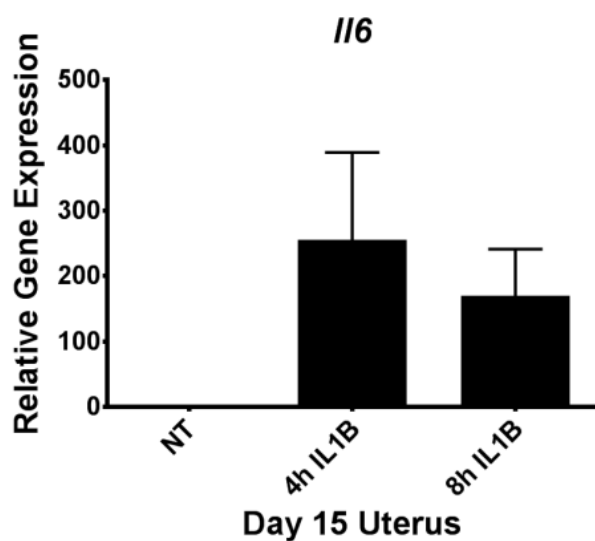
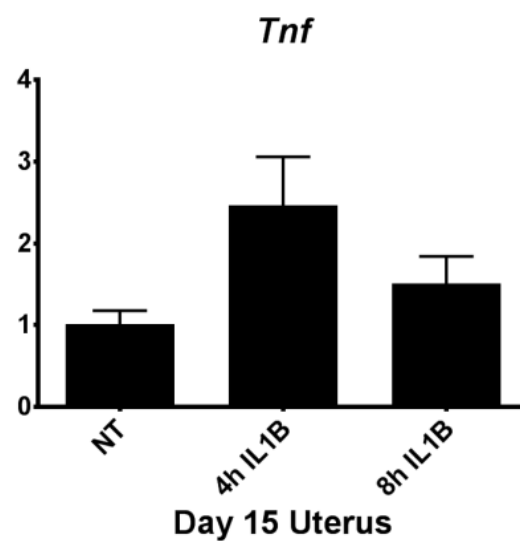
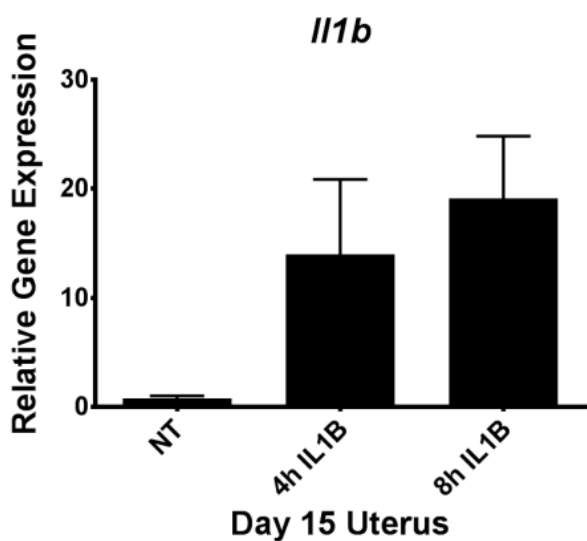


Figure 3.12. Intrauterine IL1B alone does not upregulate proinflammatory and protease genes in uterus. (A) Gene expression analysis by qPCR demonstrates trends of gene expression increases in the uterus in response to IL1B at 4 and 8 hour post-surgery time points. No statistical significance for any gene is reached. (n=4-8 samples per group, bars represent mean \pm S.E.M. One-way ANOVA).

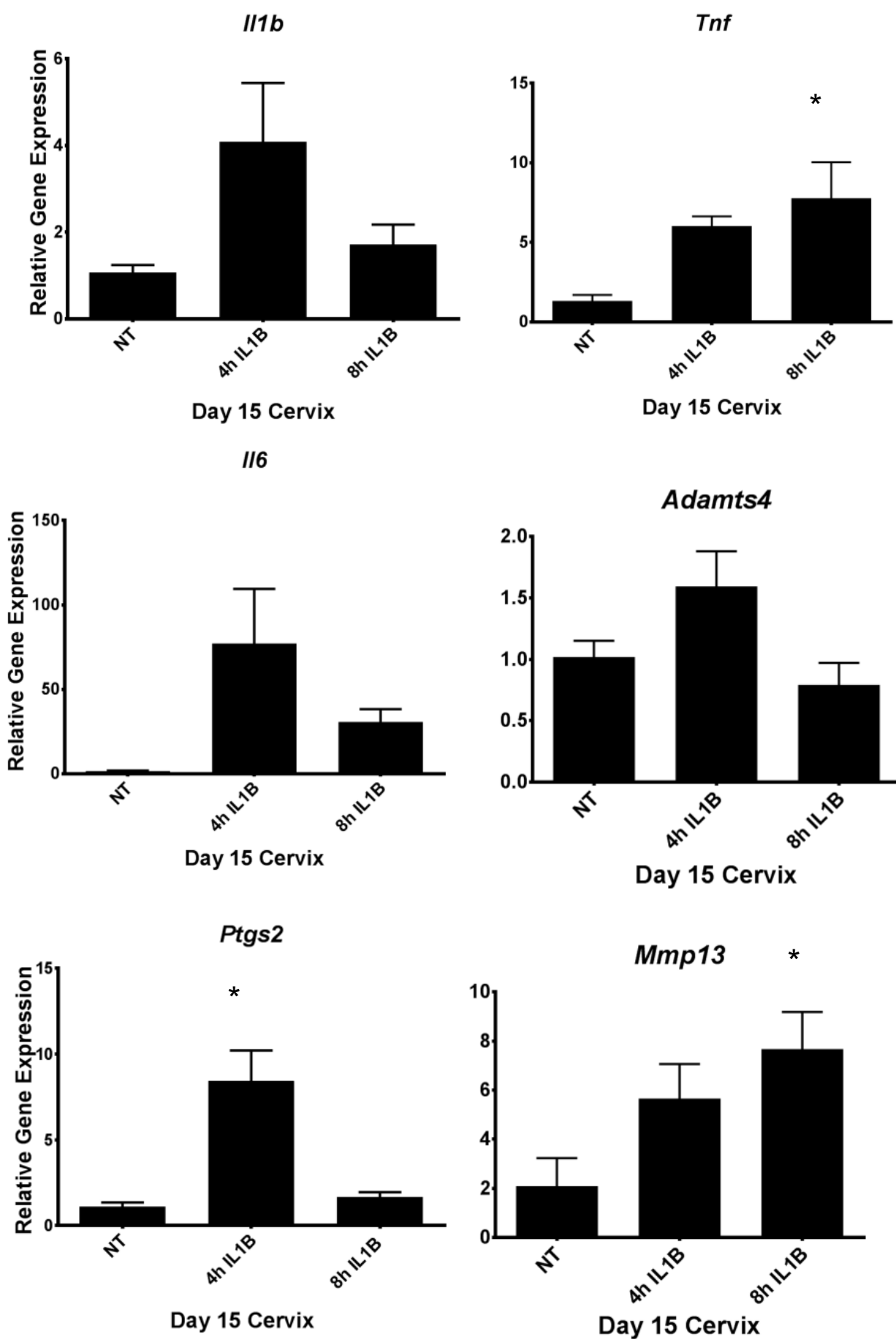
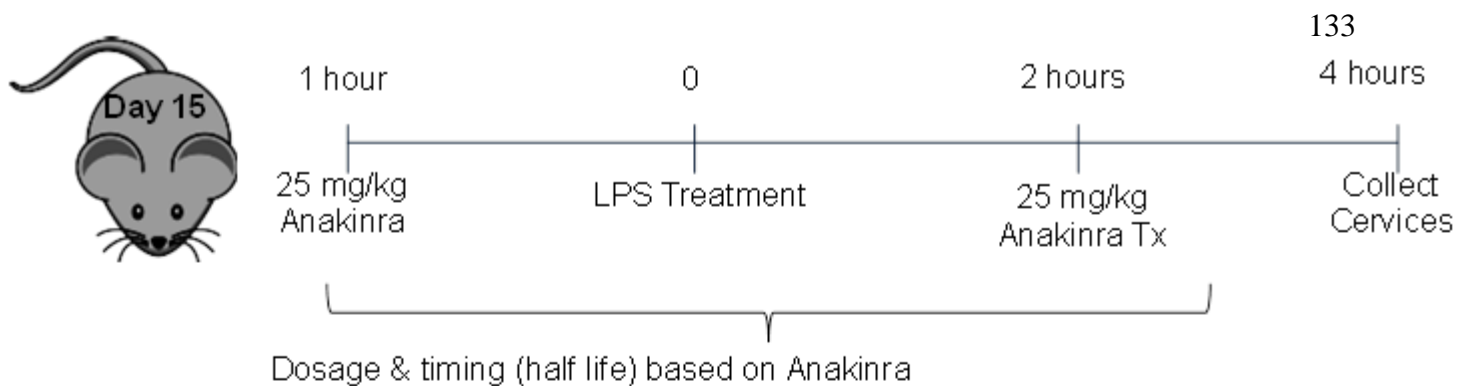


Figure 3.13. Intrauterine IL1B influences proinflammatory and protease gene expression in the cervix. (A) Gene expression analysis by qPCR demonstrates an increase in *Ptgs2* gene expression 4 hours after intrauterine application of IL1B compared to nontreated samples. Transcripts of proinflammatory *Tnf* and protease *Mmp13* are upregulated in the cervix 8 hours after intrauterine IL1B treatment. (n=6-8 samples per group, bars represent mean \pm S.E.M. One-way ANOVA).

A.



B.

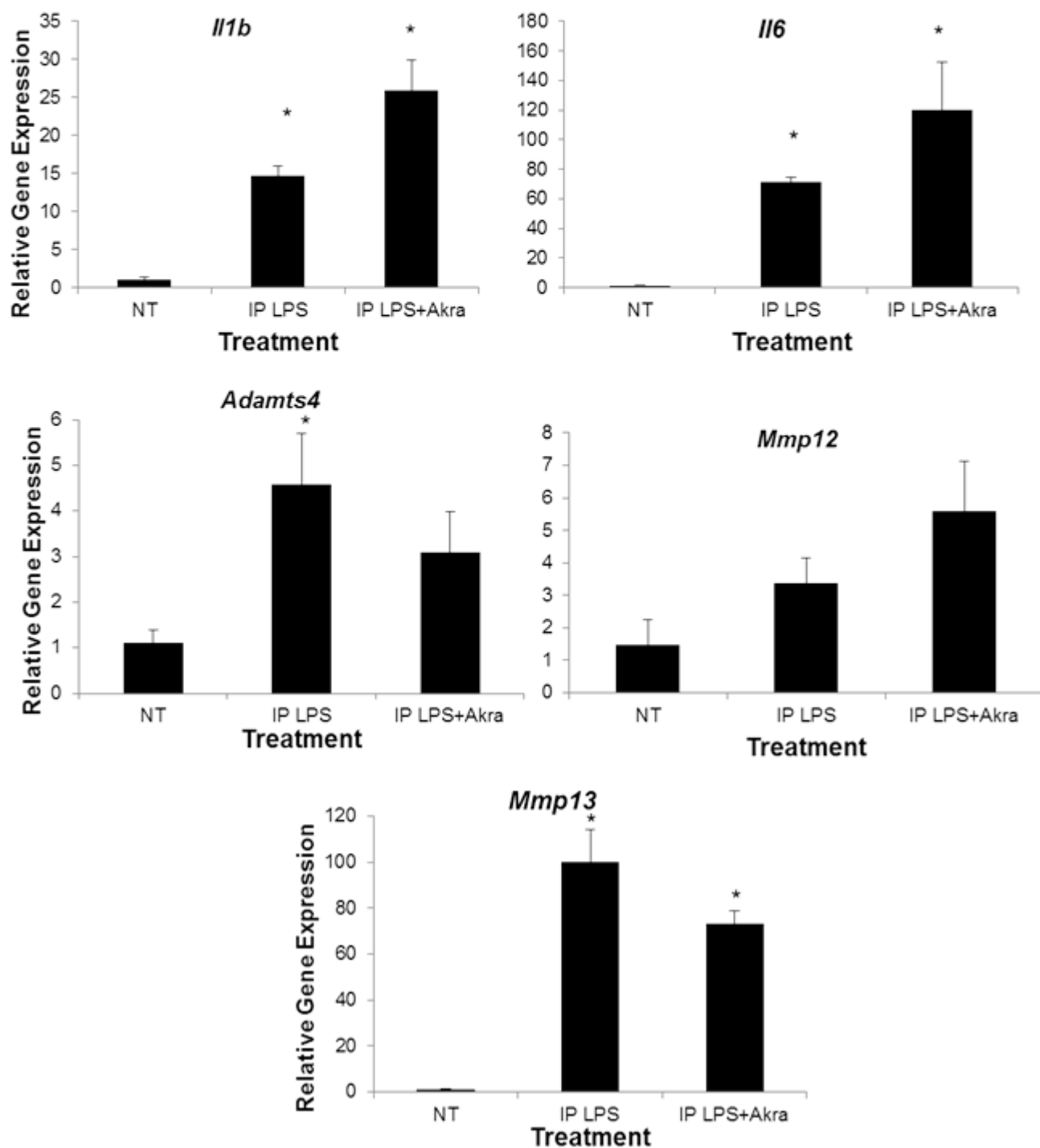


Figure 3.14. IP administration of Anakinra does not abrogate upregulation of proteases in response to IP LPS (A) Schematic demonstrating timeline and dosage regimen for Anakinra and LPS (B) Gene expression analysis by qPCR demonstrates induction of *Il1b*, *Il6*, and *Mmp13* genes in response to both IP LPS and IP LPS + Anakinra with no decline in expression with Anakinra treatment. (n=3-4 samples per group, p<0.05 compared to day 15, Bars represent mean \pm S.E.M. One-way ANOVA)

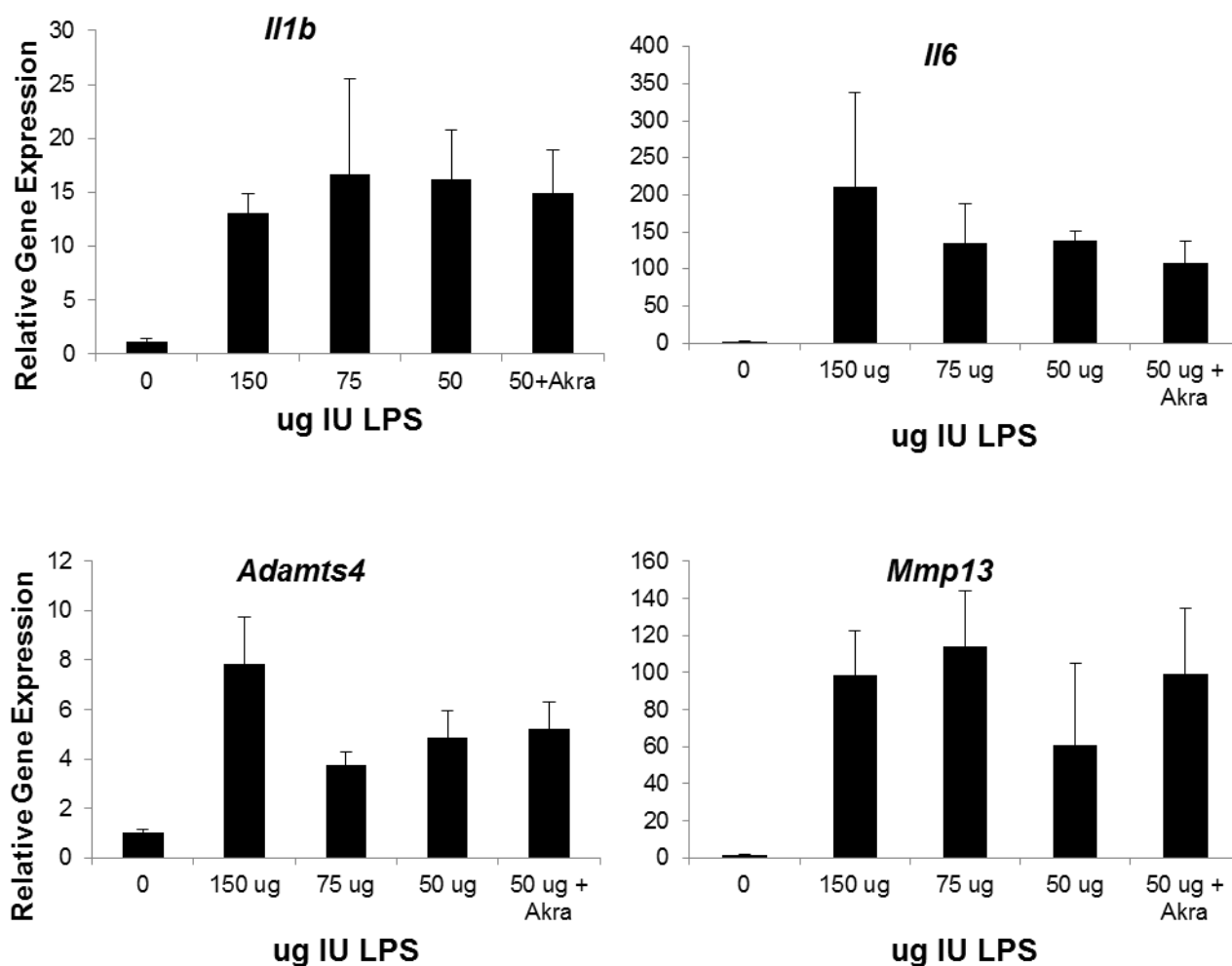


Figure 3.15. IP administration of Anakinra does not abrogate upregulation of proteases in response to IU LPS. Gene expression analysis by qPCR for proinflammatory and protease genes in response to a variety of LPS concentrations administered intrauterine. Similar induction of these genes is seen with Anakinra treatment with 50ug LPS concentration. (n=3-6 samples per group, $p < 0.05$ compared to day 15, Bars represent mean \pm S.E.M. One-way ANOVA)

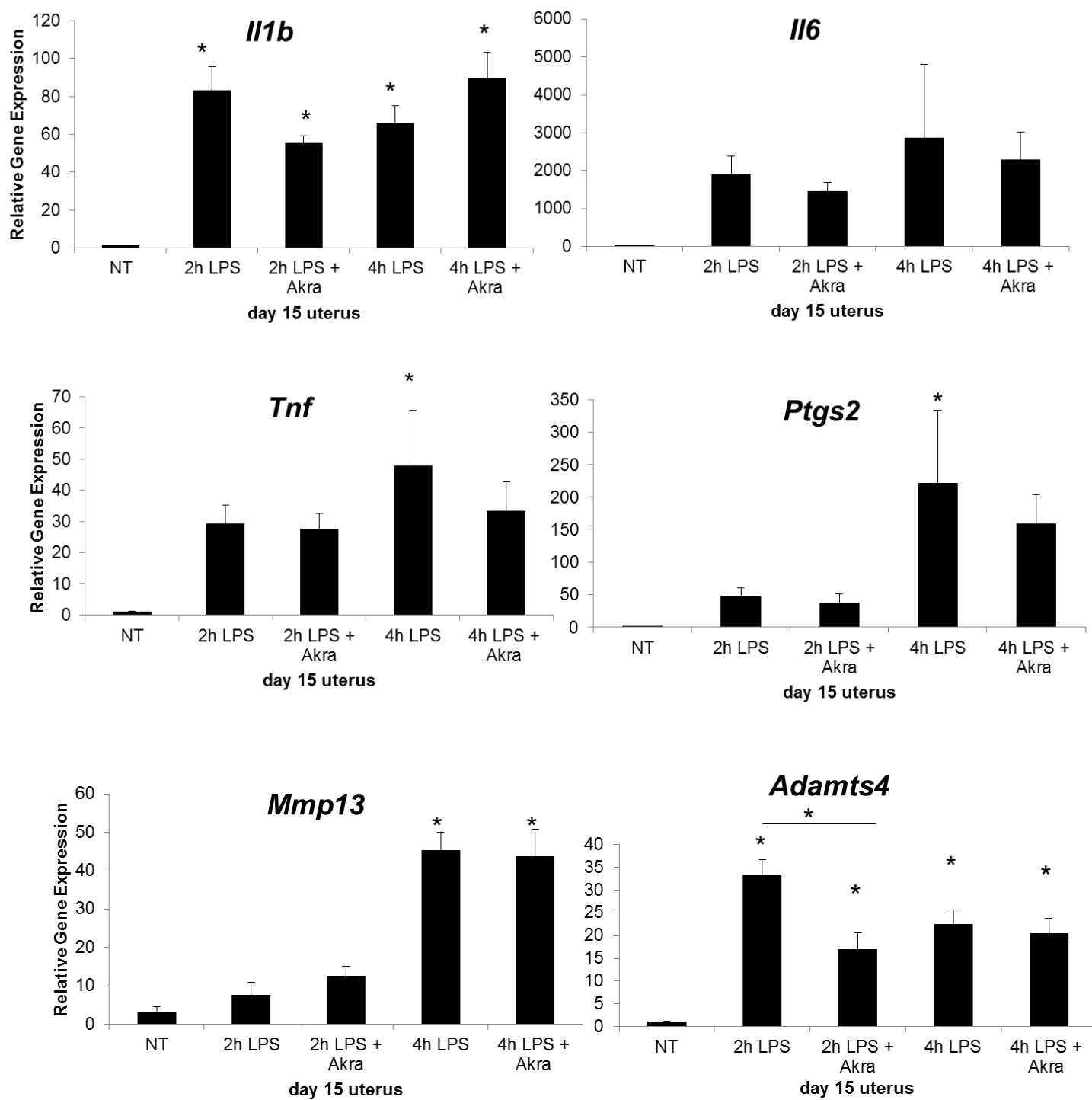


Figure 3.16. IU administration of Anakinra fails to prevent uterine upregulation of proinflammatory and protease expression in response to LPS. Gene expression analysis by qPCR for proinflammatory and protease genes in the day 15 mouse uterus in response to intrauterine LPS \pm intrauterine Anakinra. (n=4-5 samples per group, $p < 0.05$ compared to day 15, Bars represent mean \pm S.E.M. One-way ANOVA)

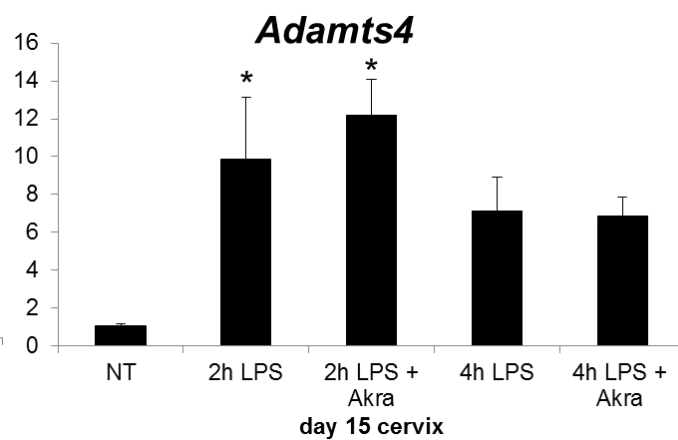
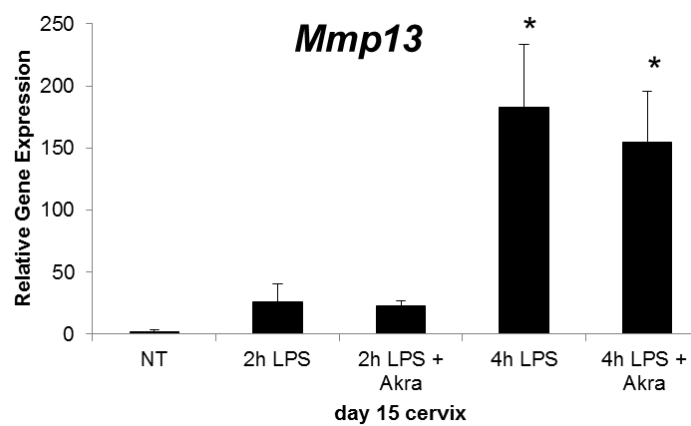
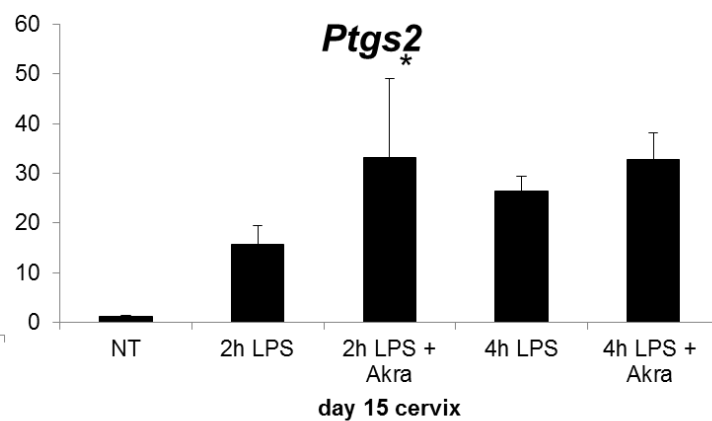
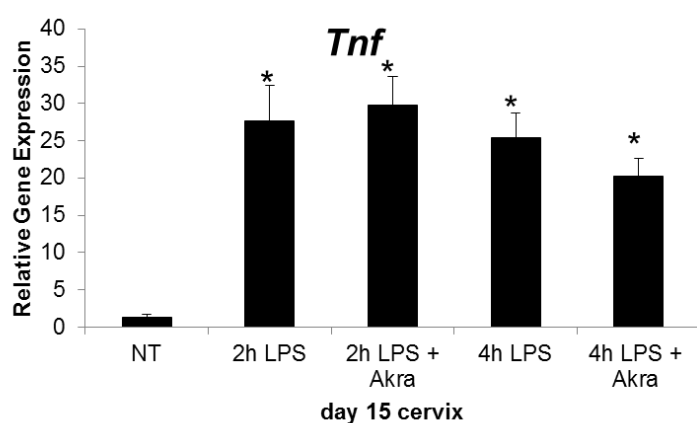
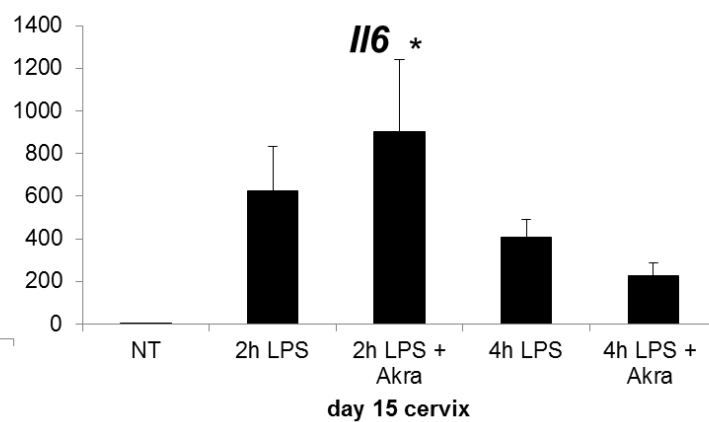
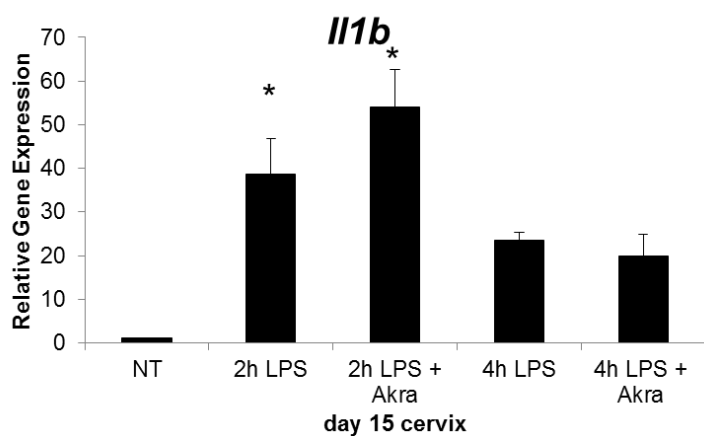


Figure 3.17. IU administration of Anakinra fails to prevent cervical upregulation of proinflammatory and protease expression in response to LPS. Gene expression analysis by qPCR for proinflammatory and protease genes in the day 15 mouse cervix in response to intrauterine LPS \pm intrauterine Anakinra. (n=4-5 samples per group, $p < 0.05$ compared to day 15, Bars represent mean \pm S.E.M. One-way ANOVA)

CHAPTER FOUR

Postpartum Studies & A Look Ahead

4.1 Introduction

Multiple avenues of investigation, including previously published studies on unique immune cell populations and dependence on prostaglandins, provided the first evidence of the unique nature of cervical changes during LPS-mediated preterm birth compared to cervical ripening at the end of pregnancy. The findings described in this dissertation expand this understanding to include potential mechanisms driving LPS-mediated preterm birth—specifically investigations into protease regulated disruption of elastic fibers that may be driving the loss of cervical compliance and leading to premature delivery. In light of the discovery that cervical elastic fiber ultrastructure is disrupted in LPS-mediated preterm birth, additional questions are raised. How are the disrupted elastic fibers repaired postpartum to ensure the cervix regains its structural integrity need for subsequent pregnancies?

As mentioned in chapter 3, elastic fiber synthesis is thought to be confined to times of organismal development due to the need to coordinate a number of different genes involved with processing, assembly, and crosslinking of tropoelastin molecules in and around the microfibrillar scaffold (Wagenseil & Mecham, 2007). In response to injury in the adult, elastic fibers have been shown to repair in a manner that compromises the functionality of the structure (Chrzanowski, Keller, Cerreta, Mandl, & Turino, 1980;

Shifren & Mecham, 2006). An exception to this finding occurs in the female reproductive tract where elastic fibers undergo significant remodeling in pregnancy and postpartum. Specifically, proper turnover of elastic fiber in the vagina have been found to be crucial for prevention of pelvic organ prolapse following birth (Budatha et al., 2013; Drewes et al., 2007; Wieslander et al., 2008). Understanding how elastic fibers, and more broadly the entire ECM, repair following a term delivery or an LPS-mediated preterm birth may provide insights into the mechanisms underlying established preterm birth risk factors.

According to a Pew Research analysis of U.S. Census Bureau's June 2015 Supplement of the Current Population Survey, the average family in the United States has 2.4 children (Livingston G, 2015). The steps of cervical ripening, labor and delivery are, more often than not, repeated and usually accelerated processes. Some sort of tissue change and/or "muscle memory" is postulated to occur during the postpartum repair process that lends itself to the quicker labor and delivery processes often seen in subsequent pregnancies. Knowing the extensive remodeling that both collagen fibers and elastic fibers undergo throughout pregnancy, it would follow that a return to a nonpregnant state would involve a number of both cellular and extracellular repair processes that require an appropriate amount of time (Akins et al., 2010; Nallasamy et al., 2017a). As an example, in the mammary gland stroma of the rat, it is known that the postpartum tissue repair process does not return the ECM to a nonpregnant virgin state (Maller et al., 2013). In fact, the differences in collagen structure in the nonpregnant,

postpartum state protect against full-fledged tumor growth and invasive phenotypes of cancer cells when compared to nulliparous nonpregnant ECM.

An understanding of the mechanisms governing postpartum tissue repair of the cervix is incomplete yet warranted, given the clinical observation that a short interval between delivery of one pregnancy and conception of a second increases a mother's risk of a preterm delivery (DeFranco, Ehrlich, & Muglia, 2014; Khoshnood et al., 1998; Klerman et al., 1998). In addition to these observations demonstrating the necessity of sufficient time for the physiological processes to take place, it is also well established that a preterm birth is the most significant risk factor for future preterm births (Ferrero et al., 2016). In fact, the risk of preterm birth in a current pregnancy increases with the number of previous preterm births (Bloom et al., 2001). **The clinical observations of the repetitive nature of preterm birth led to the development of the hypothesis that inappropriate ECM remodeling during tissue repair contributes to the compromised mechanical function of the cervix and consequently preterm birth in future pregnancies.** This chapter will highlight the initial studies undertaken to investigate postpartum changes with respect to both elastin and collagen following a birth at term and an infection-mediated preterm birth.

4.2 Results

4.2.1 Experimental setup

Studies in postpartum tissues were undertaken to define phases of repair (2-4 hours, 24 hours, 48 hours, and 96 hours) following a birth at term and a birth preterm due to inflammation in mice in their first pregnancy (figure 4.1A).

4.2.2 Changes in 24-hour postpartum collagen fiber parameters following an LPS-mediated preterm birth

To investigate collagen fiber morphological parameters in the postpartum mouse cervix, second harmonic generation (SHG) imaging was completed in samples collected 24 hours following a birth at term (lactating moms) and an LPS-mediated preterm birth (non-lactating moms) in the mid-stroma. Both anisotropy, or the difference in fiber directionality when measured along various degrees of orientation, and fiber diameter were decreased in postpartum LPS-mediated preterm birth samples compared to postpartum term samples (figure 4.1 B, C).

4.2.3 Lactation affects 21-day postpartum collagen fiber parameters

Given the differences in collagen fiber anisotropy and fiber diameter at the 24-hour mark following a birth at term and a preterm birth mediated by LPS, the next set of experiments focused on the 21-day mark postpartum. This time point was chosen due to the accepted 21-28 day post-delivery weaning schedule for mice. At this point, it was predicted that the postpartum tissue repair process would be complete, at least in the mice that delivered their first pregnancy at term. Similar to 24 hours postpartum experiments, collagen fiber anisotropy and fiber diameter were measured from SHG images of 21-day postpartum samples following a birth at term (lactating) or a preterm birth (not lactating) mediated by LPS. These groups were compared to virgin nonpregnant cervix samples.

As anticipated, parous cervix samples have measurable differences in collagen morphologies including anisotropy and fiber diameter compared to nonpregnant samples (figure 4.2 A, B). In cervix samples 21 days postpartum following delivery at term, anisotropy is decreased and fiber diameter increased compared to cervixes from nonpregnant virgin mice. In cervix samples 21 days postpartum following a preterm delivery mediated by LPS, both anisotropy and fiber diameter are decreased compared to both nonpregnant and 21-day postpartum term samples. Given that pups from mice that deliver preterm are unfit for life outside the womb and die shortly after delivery if not before delivery due to inflammation, mothers in this category are inherently not lactating. In contrast, mothers that delivered at term and were evaluated 21 days postpartum were allowed to nurse their pups for the full three weeks.

To test the influence of lactation on collagen fiber morphological parameters, a second 21-day experiment was performed in which half of mothers were allowed to nurse their pups, as before, and the other half were not (non-lactating group, NL). Interestingly when compared to term non-lactating mice, both groups of term lactating had significantly lower anisotropy of collagen fibers (figure 4.2 C). The significant differences in anisotropy seen between the first set of term (lactating) and preterm samples were not sustained when the term group was not lactating, and anisotropy measurements between term lactating groups 1 and 2 were significantly different.

4.2.4 Elastic fiber ultrastructure following term and infection preterm birth

Given that elastic fiber ultrastructure is disrupted in the cervix during inflammation-mediated preterm birth, investigations of ultrastructure during the postpartum repair

process were undertaken. 24 hour postpartum cervix samples from mice that delivered at term and mice that delivered preterm due to inflammation were imaged using transmission electron microscopy (TEM). Elastic fibers in the sub-epithelial stroma were the focus of the TEM experiments (figure 4.3). Overall, elastic fiber ultrastructure was highly variable both after a birth at term and after a preterm birth mediated by LPS. In both groups, there were long fibers with much elastin and little microfibrillar scaffold showing and also fragmented, disrupted elastic fibers with little stained elastin atop the scaffold. Making any sweeping comparisons between the two would be difficult, given the intra-group variability.

4.2.5 Biomechanical changes following LPS-mediated preterm birth

In an attempt to assess a functional output of tissue repair and to define the phases of cervical tissue repair following delivery, load-to-break biomechanical testing was carried out. Normalized maximum stiffness, measured prior to tissue break, was significantly decreased 24 and 48 hours following an LPS-mediated preterm birth compared to term (figure 4.4). Yield force 48 hours after an LPS-mediated preterm birth was significantly lower than in samples after a term delivery. Interestingly, four days postpartum following an LPS-mediated preterm birth, normalized yield force was increased compared to a birth at term. While future studies are required, the preliminary biomechanical findings suggest differences in the rate or process of ECM repair after LPS-mediated preterm vs term birth.

4.3 Discussion

Understanding how normal repair processes occur is central to physiological forays into the ever-changing tissue environment. In the pregnant cervix, there exists an utmost need to balance tissue competency with early and steady ECM changes to accommodate the need for ripening and dilation prior to successful delivery of offspring. The postpartum tissue repair process must strike a balance too—both a quick return to the physiological state of non-pregnancy, with the understanding in rodents that fertilization for subsequent pregnancies can happen on the same day as delivery of previous pregnancies and a well-orchestrated and thorough repair to ensure competency in future pregnancies must occur. Additionally, the reproductive biology field lacks an understanding of the pathology of an acutely inflammation-laden environment in LPS-mediated preterm birth that needs to overcome the push toward a fibrotic phenotype and to shift to repair the cervix to a fully functional tissue.

This portion of my thesis project, although in the descriptive and characterization stages, I would argue is the most patient oriented and clinically pressing. These experiments are a logical beginning to answering the natural question of “what next” in relation to inflammation-mediated preterm birth studies.

Is the overall physiologic postpartum tissue repair process after a birth at term as chaotic as it appears with respect to elastic fiber ultrastructure? It is known that during the early hours postpartum, an increased number of immune cells including neutrophils and macrophages invade the tissue and are assumed to carry out a number of proinflammatory mediated processes involved in tissue repair (Holt et al., 2011). Both

proinflammatory M1 and tissue repair M2 macrophages are induced at term. The relative polarization of cervical macrophages with LPS may differ. Given that during an LPS-mediated preterm birth, these activate immune cells increase in number some 7-9 hours prior to delivery, how might their proinflammatory actions be harnessed and utilized, yet not allowed to become out of control and lead to chronic inflammation? Basic histological staining to assess cell proliferation (Ki67), apoptosis (TUNEL), and general tissue structure (H&E and Trichrome) of term and LPS-preterm samples 24 hours and 21 days postpartum were used to attempt to answer these general questions. No differences between the two groups at either time point were evident (data not shown).

Second harmonic generation imaging of collagen fiber morphologies following a term and inflammation-mediated preterm birth was derailed after samples from two sets of mice that delivered at term and allowed to nurse their pups for 21 days had significantly different anisotropy values. These images were taken in the midstroma before it was determined that the only measurable, and admittedly modest, changes in collagen fiber spacing parameters in response to LPS occurred in the sub-epithelial stroma exclusively (Nallasamy et al, manuscript in preparation). A third set of tissues from animals that delivered at term, half allowed to nurse their pups and half not, and preterm due to inflammation will need to be imaged in both the mid and sub-epithelial stroma for a more complete picture of collagen morphology postpartum.

Future studies in second pregnancies following a preterm birth will investigate the potential of premature compromised cervical competency. Biomechanical studies completed on samples at mid and late gestational time points of second mouse

pregnancies following a preterm birth may yield interesting changes in tissue stiffness, or even tissue resilience as touched upon in chapter 3, indicating reduced cervical competency below the threshold of an overt phenotype (i.e. preterm delivery) when compared to mice in their second pregnancies following a birth at term. Observational studies of second pregnancies following an inflammation-mediated preterm birth are not expected to yield spontaneous preterm deliveries, as occurs at increased frequency in humans. Due to the differences in gravitational forces felt by the uterus of mice (quadrupedal) and humans (bipedal), mice that delivered their first pregnancies preterm birth due to inflammation would likely be protected from increased risk of spontaneous preterm delivery in their second pregnancies.

Given the recent data indicating the once promising treatment for recurrent preterm birth, namely 17-alpha hydroxyprogesterone caproate, failed to prolong gestation in women with a history of preterm delivery, basic science must continue to push forward for a mechanistic understanding of how the physiologic becomes pathologic, both during cervical ripening and during postpartum tissue repair (Nelson et al., 2017).

The overall goal of my thesis project was to uncover the cervical molecular mechanisms involved in inflammation-mediated preterm birth. With previously published data demonstrating the unique features present during inflammation-mediated preterm birth compared to cervical ripening at term, I undertook a transcriptomics study to add to our understanding of both modes of delivery (Gonzalez, Dong, Romero, & Girardi, 2011; Holt et al., 2011). I aimed to identify novel and exclusive pathways in the cervix during

inflammation-mediated preterm birth for further molecular investigation to understand how the cervix is becoming compliant in response to infection, leading to preterm birth. I sought to investigate regulation of gene expression by small and long noncoding RNAs as well.

RNA-seq studies provided a cornucopia of polyA and small RNA data. In agreement with previous studies, this method identified unique cervical transcriptome profiles in term and inflammation-mediated preterm birth. A number of genes previously identified via qPCR to be differentially regulated on day 18 and/or in day 15 LPS were similarly identified in the RNA-seq data set (Holt et al., 2011; B. C. Timmons et al., 2014). As anticipated, many proinflammatory pathways were upregulated in the cervix in response to LPS.

Through literature searches and gene ontology pathway analyses, inflammasome activation was discovered to be a novel and exclusive cervical pathway occurring during inflammation-mediated preterm birth. The series of molecular events involved in inflammasome activation link upstream pathogen sensing to downstream proinflammatory responses in a number of physiologic and pathologic disease states throughout the body. Recent literature indicates a number of reproductive tissues including cell types at the fetomaternal interface are able to mount an inflammasome activation response during physiological parturition (Romero et al., 2016). Especially of interest is the finding that these tissues utilize inflammasome activation in response to pathologic stimuli that may specifically lead to poor fetal and maternal outcomes (Gomez-Lopez et al., 2017). In the cervix, however, during normal parturition, genes

involved in inflammasome activation are not upregulated as they are in inflammation-mediated preterm birth.

Inflammasome activation represented an exciting avenue for further investigation given its role in prostaglandin influx, a process previously shown to be essential for LPS-mediated preterm birth and not at term (Rathinam & Fitzgerald, 2016; B. C. Timmons et al., 2014; von Moltke et al., 2012). Pathways involved in cell death, which is another potential outcome of inflammasome activation, were also upregulated in the cervix during inflammation-mediated preterm birth and not at term.

Another interesting group of genes identified in the RNA-seq dataset are proteases. A group of commonly upregulated proteases in day 15 LPS and day 18 target proteoglycans and are likely involved in physiologic changes in the cervix at the end of pregnancy. A subset of proteases known to target major ECM structural components collagen and elastin are upregulated in the cervix during inflammation-mediated preterm birth and not at term.

Immunofluorescence experiments comparing day 15 LPS to day 15 controls demonstrate subtle changes to the morphology of elastic fibers, located in the sub-epithelial stroma of the cervix. Ultrastructure studies using transmission electron microscopy demonstrate striking disruption of cervical elastic fibers during inflammation-mediated preterm birth and not at term. Work done by others in the lab demonstrates collagen fiber morphological changes in similar regions of the cervix during LPS-mediated preterm birth (Nallasamy et al, manuscript in preparation). The

disrupted elastic fibers and more porous collagen fiber morphology both occur in the sub-epithelial stroma region of the cervix upon LPS treatment on day 15 of pregnancy.

Measurable IL1B protein in the mouse cervix, another potential consequence of inflammasome activation, was hypothesized to be a direct link between the inflammasome pathway and upregulated proteases, given its role in upregulating protease in another model of inflammation—osteoarthritis (N. Li et al., 2010; Mengshol et al., 2000). To test this hypothesis, IL1B was injected intrauterine and cervical protease gene expression was analyzed. To test the necessity of IL1B signaling in cervical protease upregulation during inflammation, mice treated with intrauterine LPS were also treated with intrauterine Anakinra, an IL1B receptor antagonist and cervical protease gene expression was analyzed. Overall, the findings from these experiments were not supportive of the hypothesis that IL1B is necessary and/or sufficient for protease induction in the pregnant mouse cervix, which highlights the probability that multiple pathways are involved in the gene regulation during inflammation.

And as highlighted above, preliminary postpartum studies indicate the dynamic nature of the ECM persists well into the tissue repair phase of cervical remodeling. First determining how the ECM repairs following a birth at term will allow for later comparisons to and contrasts with tissue repair following an inflammation-mediated preterm birth. Understanding how the physiologic turns pathologic may shed light onto the problem of recurrent preterm birth.

It would be tempting, however, to focus clinical and translational research on just the women at greatest identifiable risk of preterm birth—those with previous preterm

deliveries. Preventing preterm births before they happen the first time is an ambitious yet truly important goal, although scientific understanding of *why* and *how* preterm deliveries happen is lacking. Even if clinicians could identify populations for whom a therapeutic intervention could prolong gestation, with which therapy would they treat these women? A two-pronged problem in preterm birth exists—which criteria can physicians use to identify those at risk and what therapeutic modalities can be used to treat? Likely only with a greater understanding of the basic biology underlying pregnancy will progress be made across the globe to decrease the number of babies born too soon.

4.4 Materials & Methods

4.4.1 Mice

All animal studies were conducted in accordance with the standards of humane animal care as described in the NIH Guide for the Care and Use of Laboratory Animals. The research protocols were approved by the IACUC office at the University of Texas Southwestern Medical Center. Day 13 pregnant ICR mice from Charles River were housed under a 12 h-light/12 h- dark cycle at 22°C. For postpartum studies following an LPS-mediated preterm birth, on day 15 of pregnancy, 75ug LPS (E. coli O55:B5 Sigma, St. Louis, MO) was injected intraperitoneally. Mice were observed for delivery of first pup and sacrificed at various time points thereafter. For postpartum studies following a

birth at term, day 19 mice were observed for delivery of first pup and sacrificed at various time points thereafter.

4.4.2 Second harmonic generation imaging and analyses

Mice were sacrificed and cervical tissue frozen in OCT. 8um frozen sections were topped with PBS and imaged using a Zeiss LSM880 microscope at 900nm wavelength. Images were taken in the mid-stroma region and analyzed using ImageJ and the Bio-Formats Macro plugin. Fiber diameter and anisotropy for 4 images per sample, n=3-4 cervixes, were measured and means graphed with SEM deviation.

4.4.3 Transmission electron microscopy

TEM was carried out as previously described (Nallasamy et al., 2017a). Briefly, mice were perfused with heparinized saline then glutaraldehyde and paraformaldehyde fixatives in sodium cacodylate buffer. Cervical tissue was removed and fixed in glutaraldehyde in sodium cacodylate buffer overnight at 4°C. The cervix was then sliced in transverse sections and processed as previously described (Nallasamy et al., 2017a). A Tecnai G2 spirit transmission electron microscope at 120 kV and a side mounted SIS Morada 11 megapixel CCD camera were used for image acquisition.

4.4.5 Biomechanical testing

Mice were sacrificed and cervical tissue collected without removal of uterine and vaginal tissue. Samples were flash frozen and sent on dry ice overnight to collaborators at Columbia University, NY. Biomechanics testing was carried out as previously described (Nallasamy et al., 2017a; Yoshida et al., 2014; Yoshida, Mahendroo, Vink, Wapner, & Myers, 2016). Briefly, two sutures were laced through the central os and attached to an

Instron load cell in PBS bath. Samples were pulled at 0.1mm/s tension rate until they broke. Stiffness was calculated at maximum local slope along the loading curve while yield stress the maximum stress sustained by these at break point.

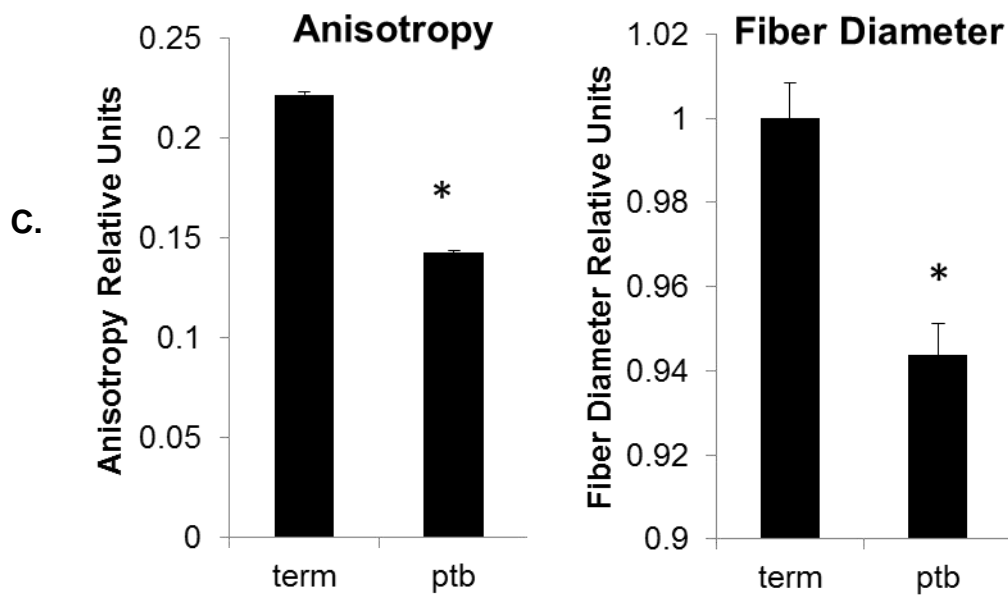
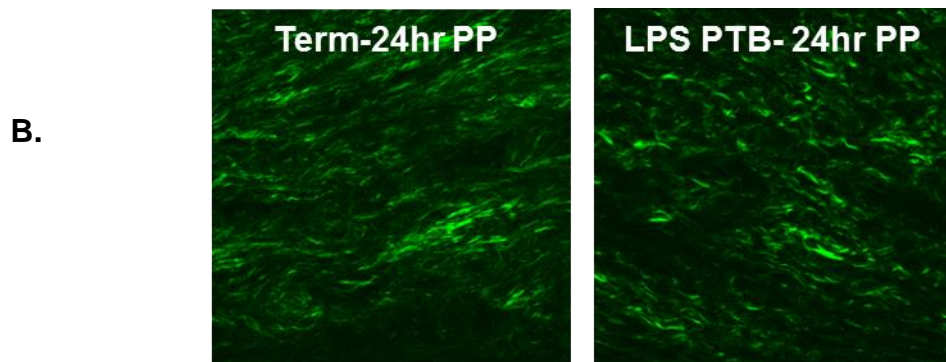
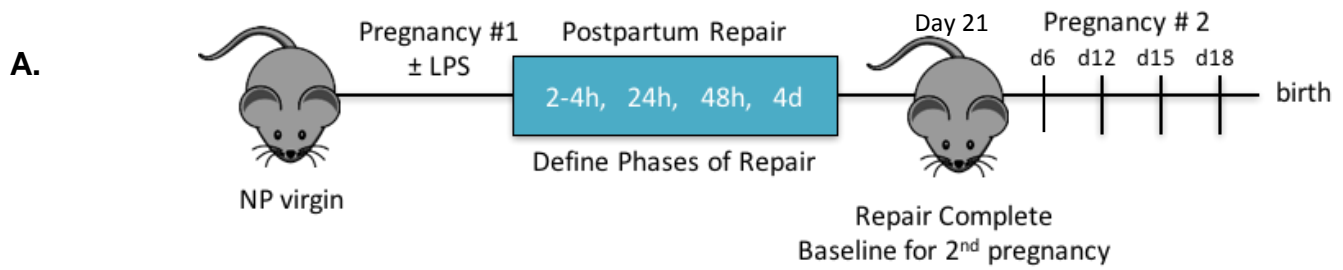
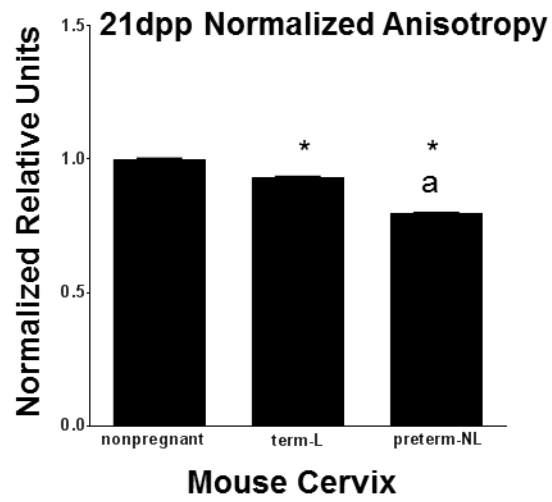


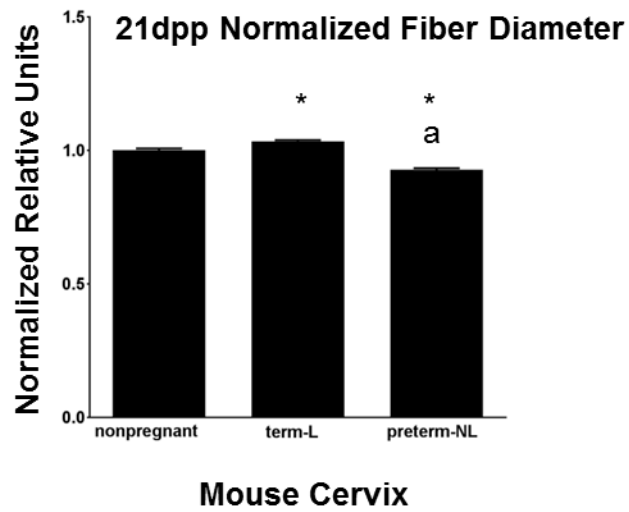
Figure 4.1. Postpartum tissue repair experimental scheme and cervical collagen fiber differences 24hours after a term or LPS-mediate preterm birth.

(A) Experimental plan for postpartum tissue repair project following a birth at term and a preterm birth mediated by inflammation. (B) Second harmonic generation images 24 hours postpartum demonstrate morphological changes in collagen fibers in the mid-stroma of mice that delivered on day 18 (term, lactating) or on day 15 after an LPS-mediated preterm birth (LPS PTB, not lactating). (C) Quantitation of fiber diameter and anisotropy measurements in 24 hour postpartum samples following a term birth (term) or an inflammation-mediated preterm birth (ptb). Analyses completed using ImageJ. The values expressed are mean \pm SEM. (n=3 cervixes in term and 4 cervixes in preterm, t-test *p<0.05)

A.



B.



C.

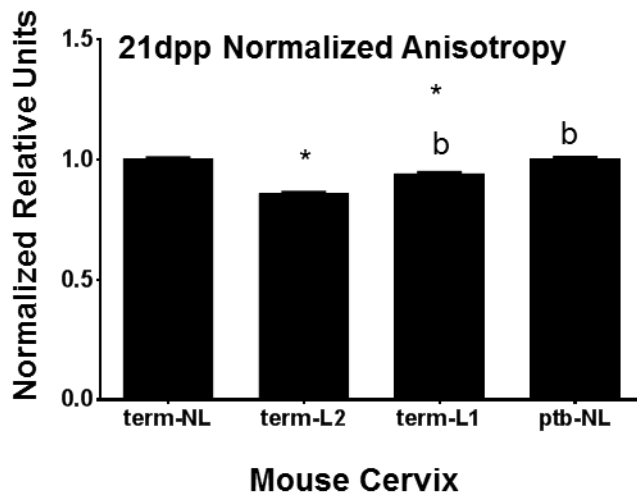
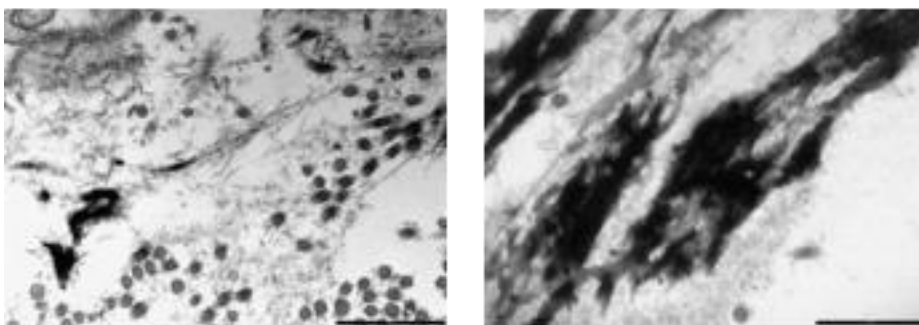


Figure 4.2. Cervical collagen fiber diameter and anisotropy differences 21 days after a term or LPS-mediated preterm birth.

(A) Quantitation of anisotropy measurements in nonpregnant, 21 days postpartum after a term birth with lactation (term-L), and 21 days postpartum after an inflammation-mediated preterm birth without lactation (ptb-NL) mice completed on SHG images using ImageJ. The values expressed are mean \pm SEM. (n=3 cervixes per group, One way ANOVA, Tukey's multiple comparisons test, *P<0.05) (B) Quantitation of fiber diameter measurements in nonpregnant, 21 days postpartum after a term birth with lactation (term-L), and 21 days postpartum after an inflammation-mediated preterm birth without lactation (ptb-NL) mice completed on SHG images using ImageJ. The values expressed are mean \pm SEM. (n=3 cervixes per group, One way ANOVA, Tukey's multiple comparisons test, *P<0.05). (C) Quantitation of anisotropy measurements using ImageJ on SHG images of mouse cervixes 21 days after a term birth without lactation (term-NL), 21 days after a term birth with lactation, group 2 (term-L2), 21 days after a term birth with lactation group 1 (term-L1), and 21 days after a preterm birth without lactation (ptb-NL). The values expressed are mean \pm SEM. (n=3 cervixes per group, One way ANOVA, Tukey's multiple comparisons test, *P<0.05 vs nonpregnant; a P<0.05 vs term-L, b P<0.05 vs term-L2)

24hr postpartum Term



24hr postpartum Preterm

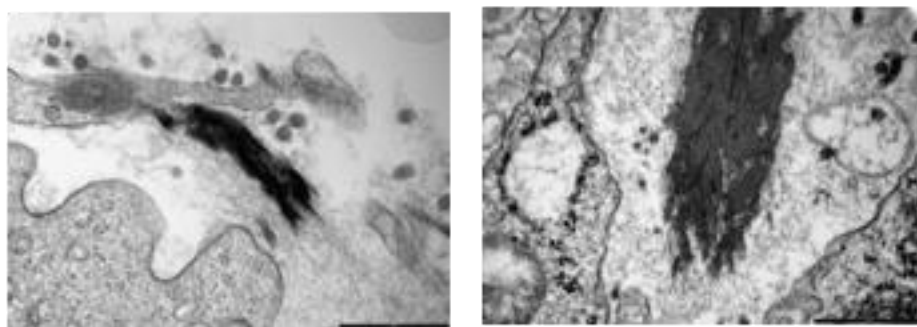
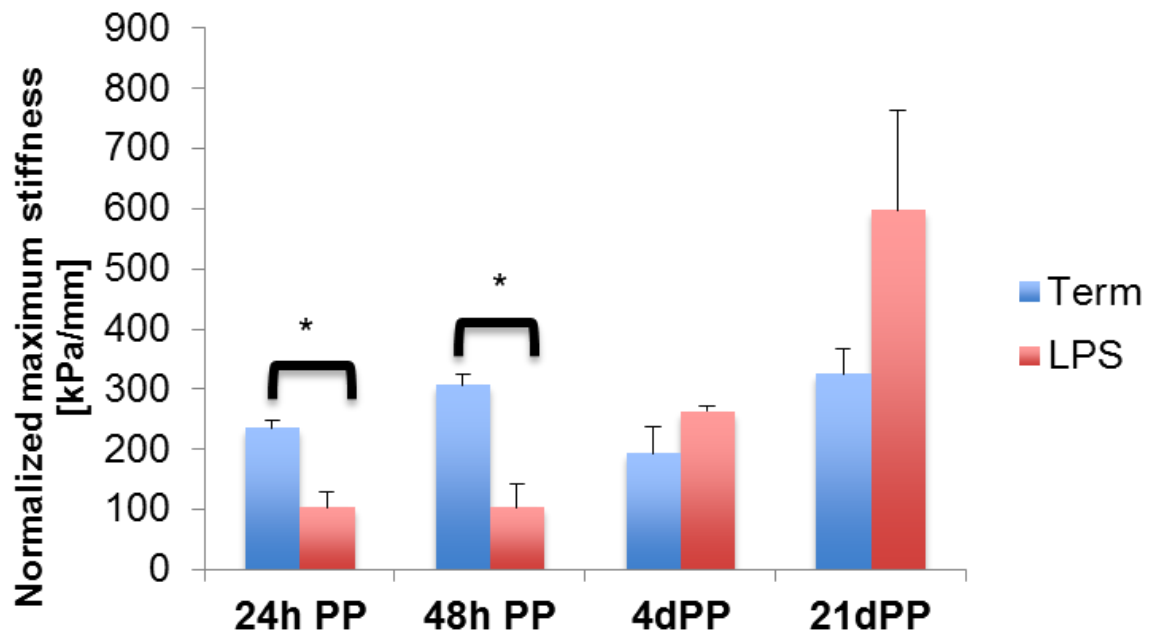


Figure 4.3. Transmission Electron Microscopy Images in 24-hour postpartum term and LPS-mediated preterm mouse cervixes.

(A) 26,500x images of elastic fibers in mouse cervixes 24 hours after a term or LPS-mediated preterm birth. Images are representative from two different mice although 3 mice total per group were imaged.

Normalized Maximum Stiffness



Normalized Yield Force

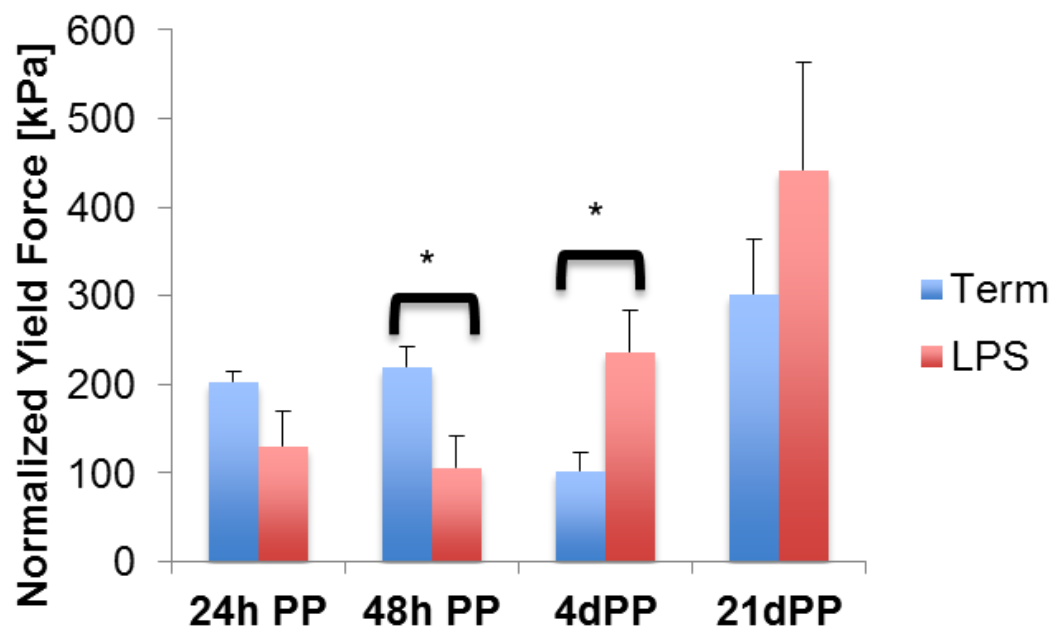


Figure 4.4. Load-to-break tissue biomechanical parameters measured in postpartum samples following a birth at term or a preterm birth mediated by LPS.

(A) Normalized maximum stiffness measurements at 24 hours (24h PP), 48 hours (48h PP), 4 days (4dpp), and 21 days (21dpp) postpartum mouse cervix samples. (n=3-4 cervixes per group, t-test *P<0.05) (B) Normalized yield force measured at 24 hours (24h PP), 48 hours (48h PP), 4 days (4dpp), and 21 days (21dpp) postpartum mouse cervix samples. The values expressed are mean \pm SEM. (n=3-4 cervixes per group, t-test *P<0.05)

BIBLIOGRAPHY

- . (2007). In R. E. Behrman & A. S. Butler (Eds.), *Preterm Birth: Causes, Consequences, and Prevention*. Washington (DC).
- Aagaard, K., Riehle, K., Ma, J., Segata, N., Mistretta, T. A., Coarfa, C., . . . Versalovic, J. (2012). A metagenomic approach to characterization of the vaginal microbiome signature in pregnancy. *PLoS One*, *7*(6), e36466. doi:10.1371/journal.pone.0036466
- Abdollah, S., Macias-Silva, M., Tsukazaki, T., Hayashi, H., Attisano, L., & Wrana, J. L. (1997). TbetaRI phosphorylation of Smad2 on Ser465 and Ser467 is required for Smad2-Smad4 complex formation and signaling. *J Biol Chem*, *272*(44), 27678-27685.
- Akgul, Y. M., M. (2014). *Cervical Changes Accompanying Birth* (A. T. Y. Anne Croy, Francesco J. DeMayo and S. Lee Adamson Ed.): Elsevir.
- Akins, M. L., Luby-Phelps, K., Bank, R. A., & Mahendroo, M. (2011). Cervical softening during pregnancy: regulated changes in collagen cross-linking and composition of matricellular proteins in the mouse. *Biol Reprod*, *84*(5), 1053-1062. doi:10.1095/biolreprod.110.089599
- Akins, M. L., Luby-Phelps, K., & Mahendroo, M. (2010). Second harmonic generation imaging as a potential tool for staging pregnancy and predicting preterm birth. *J Biomed Opt*, *15*(2), 026020. doi:10.1117/1.3381184
- Alfirevic, Z., Stampalija, T., Roberts, D., & Jorgensen, A. L. (2012). Cervical stitch (cerclage) for preventing preterm birth in singleton pregnancy. *Cochrane Database Syst Rev*(4), CD008991. doi:10.1002/14651858.CD008991.pub2
- American College of, O., & Gynecologists. (2014). ACOG Practice Bulletin No.142: Cerclage for the management of cervical insufficiency. *Obstet Gynecol*, *123*(2 Pt 1), 372-379. doi:10.1097/01.AOG.0000443276.68274.cc
- American College of, O., Gynecologists, & Committee on Practice, B.-O. (2012). ACOG practice bulletin no. 127: Management of preterm labor. *Obstet Gynecol*, *119*(6), 1308-1317. doi:10.1097/AOG.0b013e31825af2f0
- Anders, H. J., & Schaefer, L. (2014). Beyond tissue injury-damage-associated molecular patterns, toll-like receptors, and inflammasomes also drive regeneration and fibrosis. *J Am Soc Nephrol*, *25*(7), 1387-1400. doi:10.1681/ASN.2014010117
- Anum, E. A., Springel, E. H., Shriver, M. D., & Strauss, J. F., 3rd. (2009). Genetic contributions to disparities in preterm birth. *Pediatr Res*, *65*(1), 1-9. doi:10.1203/PDR.0b013e31818912e7
- Asquith, D. L., Miller, A. M., Reilly, J., Kerr, S., Welsh, P., Sattar, N., & McInnes, I. B. (2011). Simultaneous activation of the liver X receptors (LXRalpha and LXRbeta) drives murine collagen-induced arthritis disease pathology. *Ann Rheum Dis*, *70*(12), 2225-2228. doi:10.1136/ard.2011.152652
- Barone, W. R., Feola, A. J., Moalli, P. A., & Abramowitch, S. D. (2012). The Effect of Pregnancy and Postpartum Recovery on the Viscoelastic Behavior of the Rat Cervix. *J Mech Med Biol*, *12*(1), 12500091-125000917. doi:10.1142/S0219519412004399

- Bartlett, S. R., Sawdy, R., & Mann, G. E. (1999). Induction of cyclooxygenase-2 expression in human myometrial smooth muscle cells by interleukin-1beta: involvement of p38 mitogen-activated protein kinase. *J Physiol*, *520 Pt 2*, 399-406.
- Bereza, T., Tomaszewski, K. A., Balajewicz-Nowak, M., Mizia, E., Pasternak, A., & Walocha, J. (2012). The vascular architecture of the supravaginal and vaginal parts of the human uterine cervix: a study using corrosion casting and scanning electron microscopy. *J Anat*, *221(4)*, 352-357. doi:10.1111/j.1469-7580.2012.01550.x
- Berghella, V., Odibo, A. O., To, M. S., Rust, O. A., & Althuisius, S. M. (2005). Cerclage for short cervix on ultrasonography: meta-analysis of trials using individual patient-level data. *Obstet Gynecol*, *106(1)*, 181-189. doi:10.1097/01.AOG.0000168435.17200.53
- Bevis, D. C. (1951). Treatment of habitual abortion. *Lancet*, *2(6675)*, 207.
- Bloom, S. L., Yost, N. P., McIntire, D. D., & Leveno, K. J. (2001). Recurrence of preterm birth in singleton and twin pregnancies. *Obstet Gynecol*, *98(3)*, 379-385.
- Brough, D., Le Feuvre, R. A., Wheeler, R. D., Solovyova, N., Hilfiker, S., Rothwell, N. J., & Verkhatsky, A. (2003). Ca²⁺ stores and Ca²⁺ entry differentially contribute to the release of IL-1 beta and IL-1 alpha from murine macrophages. *J Immunol*, *170(6)*, 3029-3036.
- Brough, D., & Rothwell, N. J. (2007). Caspase-1-dependent processing of pro-interleukin-1beta is cytosolic and precedes cell death. *J Cell Sci*, *120(Pt 5)*, 772-781. doi:10.1242/jcs.03377
- Budatha, M., Silva, S., Montoya, T. I., Suzuki, A., Shah-Simpson, S., Wieslander, C. K., . . . Yanagisawa, H. (2013). Dysregulation of protease and protease inhibitors in a mouse model of human pelvic organ prolapse. *PLoS One*, *8(2)*, e56376. doi:10.1371/journal.pone.0056376
- Buhimschi, C. S., Sora, N., Zhao, G., & Buhimschi, I. A. (2009). Genetic background affects the biomechanical behavior of the postpartum mouse cervix. *Am J Obstet Gynecol*, *200(4)*, 434 e431-437. doi:10.1016/j.ajog.2008.11.005
- Burris, H. H., Collins, J. W., Jr., & Wright, R. O. (2011). Racial/ethnic disparities in preterm birth: clues from environmental exposures. *Curr Opin Pediatr*, *23(2)*, 227-232. doi:10.1097/MOP.0b013e328344568f
- Cerretti, D. P., Kozlosky, C. J., Mosley, B., Nelson, N., Van Ness, K., Greenstreet, T. A., . . . et al. (1992). Molecular cloning of the interleukin-1 beta converting enzyme. *Science*, *256(5053)*, 97-100.
- Chang, G., Mouillet, J. F., Mishima, T., Chu, T., Sadovsky, E., Coyne, C. B., . . . Sadovsky, Y. (2017). Expression and trafficking of placental microRNAs at the fetomaternal interface. *FASEB J*, *31(7)*, 2760-2770. doi:10.1096/fj.201601146R
- Chi, S. W., Zang, J. B., Mele, A., & Darnell, R. B. (2009). Argonaute HITS-CLIP decodes microRNA-mRNA interaction maps. *Nature*, *460(7254)*, 479-486. doi:10.1038/nature08170

- Chow, L., & Lye, S. J. (1994). Expression of the gap junction protein connexin-43 is increased in the human myometrium toward term and with the onset of labor. *Am J Obstet Gynecol*, 170(3), 788-795.
- Chrzanowski, P., Keller, S., Cerreta, J., Mandl, I., & Turino, G. M. (1980). Elastin content of normal and emphysematous lung parenchyma. *Am J Med*, 69(3), 351-359.
- Chwalisz, K. (1994). The use of progesterone antagonists for cervical ripening and as an adjunct to labour and delivery. *Hum Reprod*, 9 Suppl 1, 131-161.
- Cicchillitti, L., Di Stefano, V., Isaia, E., Crimaldi, L., Fasanaro, P., Ambrosino, V., . . . Martelli, F. (2012). Hypoxia-inducible factor 1-alpha induces miR-210 in normoxic differentiating myoblasts. *J Biol Chem*, 287(53), 44761-44771. doi:10.1074/jbc.M112.421255
- Coeshott, C., Ohnemus, C., Pilyavskaya, A., Ross, S., Wieczorek, M., Kroona, H., . . . Cheronis, J. (1999). Converting enzyme-independent release of tumor necrosis factor alpha and IL-1beta from a stimulated human monocytic cell line in the presence of activated neutrophils or purified proteinase 3. *Proc Natl Acad Sci U S A*, 96(11), 6261-6266.
- Colige, A., Vandenberghe, I., Thiry, M., Lambert, C. A., Van Beeumen, J., Li, S. W., . . . Nusgens, B. V. (2002). Cloning and characterization of ADAMTS-14, a novel ADAMTS displaying high homology with ADAMTS-2 and ADAMTS-3. *J Biol Chem*, 277(8), 5756-5766. doi:10.1074/jbc.M105601200
- Conde-Agudelo, A., Rosas-Bermudez, A., Castano, F., & Norton, M. H. (2012). Effects of birth spacing on maternal, perinatal, infant, and child health: a systematic review of causal mechanisms. *Stud Fam Plann*, 43(2), 93-114.
- Conde-Agudelo, A., Rosas-Bermudez, A., & Kafury-Goeta, A. C. (2006). Birth spacing and risk of adverse perinatal outcomes: a meta-analysis. *JAMA*, 295(15), 1809-1823. doi:10.1001/jama.295.15.1809
- Csapo, A. I., & Pinto-Dantas, C. A. (1965). The effect of progesterone on the human uterus. *Proc Natl Acad Sci U S A*, 54(4), 1069-1076.
- da Fonseca, E. B., Bittar, R. E., Carvalho, M. H., & Zugaib, M. (2003). Prophylactic administration of progesterone by vaginal suppository to reduce the incidence of spontaneous preterm birth in women at increased risk: a randomized placebo-controlled double-blind study. *Am J Obstet Gynecol*, 188(2), 419-424.
- da Silva, A. A., Simoes, V. M., Barbieri, M. A., Bettiol, H., Lamy-Filho, F., Coimbra, L. C., & Alves, M. T. (2003). Young maternal age and preterm birth. *Paediatr Perinat Epidemiol*, 17(4), 332-339.
- Dallas, S. L., Keene, D. R., Bruder, S. P., Saharinen, J., Sakai, L. Y., Mundy, G. R., & Bonewald, L. F. (2000). Role of the latent transforming growth factor beta binding protein 1 in fibrillin-containing microfibrils in bone cells in vitro and in vivo. *J Bone Miner Res*, 15(1), 68-81. doi:10.1359/jbmr.2000.15.1.68
- Davis, M. E., & Wied, G. L. (1957). 17-alpha-HYDROXYPROGESTERONE acetate; an effective progestational substance on oral administration. *J Clin Endocrinol Metab*, 17(10), 1237-1244. doi:10.1210/jcem-17-10-1237

- DeFranco, E. A., Ehrlich, S., & Muglia, L. J. (2014). Influence of interpregnancy interval on birth timing. *Bjog-an International Journal of Obstetrics and Gynaecology*, *121*(13), 1633-1640. doi:10.1111/1471-0528.12891
- Dennis, G., Jr., Sherman, B. T., Hosack, D. A., Yang, J., Gao, W., Lane, H. C., & Lempicki, R. A. (2003). DAVID: Database for Annotation, Visualization, and Integrated Discovery. *Genome Biol*, *4*(5), P3.
- Dinarello, C. A., Simon, A., & van der Meer, J. W. (2012). Treating inflammation by blocking interleukin-1 in a broad spectrum of diseases. *Nat Rev Drug Discov*, *11*(8), 633-652. doi:10.1038/nrd3800
- Donders, G. G., Van Calsteren, K., Bellen, G., Reybrouck, R., Van den Bosch, T., Riphagen, I., & Van Lierde, S. (2009). Predictive value for preterm birth of abnormal vaginal flora, bacterial vaginosis and aerobic vaginitis during the first trimester of pregnancy. *BJOG*, *116*(10), 1315-1324. doi:10.1111/j.1471-0528.2009.02237.x
- Donker, R. B., Mouillet, J. F., Nelson, D. M., & Sadovsky, Y. (2007). The expression of Argonaute2 and related microRNA biogenesis proteins in normal and hypoxic trophoblasts. *Mol Hum Reprod*, *13*(4), 273-279. doi:10.1093/molehr/gam006
- Drewes, P. G., Yanagisawa, H., Starcher, B., Hornstra, I., Csiszar, K., Marinis, S. I., . . . Word, R. A. (2007). Pelvic organ prolapse in fibulin-5 knockout mice: pregnancy-induced changes in elastic fiber homeostasis in mouse vagina. *Am J Pathol*, *170*(2), 578-589. doi:10.2353/ajpath.2007.060662
- Elovitz, M. A., Brown, A. G., Anton, L., Gilstrap, M., Heiser, L., & Bastek, J. (2014). Distinct cervical microRNA profiles are present in women destined to have a preterm birth. *Am J Obstet Gynecol*, *210*(3), 221 e221-211. doi:10.1016/j.ajog.2013.12.043
- Elovitz, M. A., Wang, Z., Chien, E. K., Rychlik, D. F., & Phillippe, M. (2003). A new model for inflammation-induced preterm birth: the role of platelet-activating factor and Toll-like receptor-4. *Am J Pathol*, *163*(5), 2103-2111. doi:10.1016/S0002-9440(10)63567-5
- Fantuzzi, G. (2001). Lessons from interleukin-deficient mice: the interleukin-1 system. *Acta Physiol Scand*, *173*(1), 5-9. doi:10.1046/j.1365-201X.2001.00879.x
- Ferrero, D. M., Larson, J., Jacobsson, B., Di Renzo, G. C., Norman, J. E., Martin, J. N., Jr., . . . Simpson, J. L. (2016). Cross-Country Individual Participant Analysis of 4.1 Million Singleton Births in 5 Countries with Very High Human Development Index Confirms Known Associations but Provides No Biologic Explanation for 2/3 of All Preterm Births. *PLoS One*, *11*(9), e0162506. doi:10.1371/journal.pone.0162506
- Ferruzzi, J., Bersi, M. R., Uman, S., Yanagisawa, H., & Humphrey, J. D. (2015). Decreased elastic energy storage, not increased material stiffness, characterizes central artery dysfunction in fibulin-5 deficiency independent of sex. *J Biomech Eng*, *137*(3). doi:10.1115/1.4029431
- Fink, S. L., & Cookson, B. T. (2006). Caspase-1-dependent pore formation during pyroptosis leads to osmotic lysis of infected host macrophages. *Cell Microbiol*, *8*(11), 1812-1825. doi:10.1111/j.1462-5822.2006.00751.x

- Fonseca, E. B., Celik, E., Parra, M., Singh, M., Nicolaides, K. H., & Fetal Medicine Foundation Second Trimester Screening, G. (2007). Progesterone and the risk of preterm birth among women with a short cervix. *N Engl J Med*, *357*(5), 462-469. doi:10.1056/NEJMoa067815
- Fuchs, A. R., Fuchs, F., Husslein, P., & Soloff, M. S. (1984). Oxytocin receptors in the human uterus during pregnancy and parturition. *Am J Obstet Gynecol*, *150*(6), 734-741.
- Gao, L., Rabbitt, E. H., Condon, J. C., Renthal, N. E., Johnston, J. M., Mitsche, M. A., . . . Mendelson, C. R. (2015). Steroid receptor coactivators 1 and 2 mediate fetal-to-maternal signaling that initiates parturition. *J Clin Invest*, *125*(7), 2808-2824. doi:10.1172/JCI78544
- Gibbs, D. F., Warner, R. L., Weiss, S. J., Johnson, K. J., & Varani, J. (1999). Characterization of matrix metalloproteinases produced by rat alveolar macrophages. *Am J Respir Cell Mol Biol*, *20*(6), 1136-1144. doi:10.1165/ajrcmb.20.6.3483
- Girard, S., Tremblay, L., Lepage, M., & Sebire, G. (2010). IL-1 receptor antagonist protects against placental and neurodevelopmental defects induced by maternal inflammation. *J Immunol*, *184*(7), 3997-4005. doi:10.4049/jimmunol.0903349
- Goldenberg, R. L., Culhane, J. F., Iams, J. D., & Romero, R. (2008). Epidemiology and causes of preterm birth. *Lancet*, *371*(9606), 75-84. doi:10.1016/S0140-6736(08)60074-4
- Goldstein, P., Berrier, J., Rosen, S., Sacks, H. S., & Chalmers, T. C. (1989). A Meta-Analysis of Randomized Control Trials of Progestational Agents in Pregnancy. *British Journal of Obstetrics and Gynaecology*, *96*(3), 265-274. doi:DOI 10.1111/j.1471-0528.1989.tb02385.x
- Gomez-Lopez, N., Romero, R., Xu, Y., Plazyo, O., Unkel, R., Leng, Y., . . . Hassan, S. S. (2017). A Role for the Inflammasome in Spontaneous Preterm Labor With Acute Histologic Chorioamnionitis. *Reprod Sci*, 1933719116687656. doi:10.1177/1933719116687656
- Gonzalez, J. M., Dong, Z., Romero, R., & Girardi, G. (2011). Cervical remodeling/ripening at term and preterm delivery: the same mechanism initiated by different mediators and different effector cells. *PLoS One*, *6*(11), e26877. doi:10.1371/journal.pone.0026877
- Gonzalez, J. M., Xu, H., Chai, J., Ofori, E., & Elovitz, M. A. (2009). Preterm and term cervical ripening in CD1 Mice (*Mus musculus*): similar or divergent molecular mechanisms? *Biol Reprod*, *81*(6), 1226-1232. doi:10.1095/biolreprod.108.075309
- Gracie, J. A., Robertson, S. E., & McInnes, I. B. (2003). Interleukin-18. *J Leukoc Biol*, *73*(2), 213-224.
- Gray, C., McCowan, L. M., Patel, R., Taylor, R. S., & Vickers, M. H. (2017). Maternal plasma miRNAs as biomarkers during mid-pregnancy to predict later spontaneous preterm birth: a pilot study. *Sci Rep*, *7*(1), 815. doi:10.1038/s41598-017-00713-8
- Gross, G., Imamura, T., Vogt, S. K., Wozniak, D. F., Nelson, D. M., Sadovsky, Y., & Muglia, L. J. (2000). Inhibition of cyclooxygenase-2 prevents inflammation-

- mediated preterm labor in the mouse. *Am J Physiol Regul Integr Comp Physiol*, 278(6), R1415-1423.
- Guo, H., Callaway, J. B., & Ting, J. P. (2015). Inflammasomes: mechanism of action, role in disease, and therapeutics. *Nat Med*, 21(7), 677-687. doi:10.1038/nm.3893
- Haas, D. M., Benjamin, T., Sawyer, R., & Quinney, S. K. (2014). Short-term tocolytics for preterm delivery - current perspectives. *Int J Womens Health*, 6, 343-349. doi:10.2147/IJWH.S44048
- Haas, D. M., Imperiale, T. F., Kirkpatrick, P. R., Klein, R. W., Zollinger, T. W., & Golichowski, A. M. (2009). Tocolytic therapy: a meta-analysis and decision analysis. *Obstet Gynecol*, 113(3), 585-594. doi:10.1097/AOG.0b013e318199924a
- Haddad, R., Tromp, G., Kuivaniemi, H., Chaiworapongsa, T., Kim, Y. M., Mazor, M., & Romero, R. (2006). Human spontaneous labor without histologic chorioamnionitis is characterized by an acute inflammation gene expression signature. *Am J Obstet Gynecol*, 195(2), 394 e391-324. doi:10.1016/j.ajog.2005.08.057
- Hadler-Olsen, E., Kanapathipillai, P., Berg, E., Svineng, G., Winberg, J. O., & Uhlin-Hansen, L. (2010). Gelatin in situ zymography on fixed, paraffin-embedded tissue: zinc and ethanol fixation preserve enzyme activity. *J Histochem Cytochem*, 58(1), 29-39. doi:10.1369/jhc.2009.954354
- Hardy, D. B., Janowski, B. A., Corey, D. R., & Mendelson, C. R. (2006). Progesterone receptor plays a major antiinflammatory role in human myometrial cells by antagonism of nuclear factor-kappaB activation of cyclooxygenase 2 expression. *Mol Endocrinol*, 20(11), 2724-2733. doi:10.1210/me.2006-0112
- Hashimoto, Y., Kondo, C., & Katunuma, N. (2015). An Active 32-kDa Cathepsin L Is Secreted Directly from HT 1080 Fibrosarcoma Cells and Not via Lysosomal Exocytosis. *PLoS One*, 10(12), e0145067. doi:10.1371/journal.pone.0145067
- Hassan, S. S., Romero, R., Haddad, R., Hendler, I., Khalek, N., Tromp, G., . . . Malone, J., Jr. (2006). The transcriptome of the uterine cervix before and after spontaneous term parturition. *Am J Obstet Gynecol*, 195(3), 778-786. doi:10.1016/j.ajog.2006.06.021
- Hassan, S. S., Romero, R., Pineles, B., Tarca, A. L., Montenegro, D., Erez, O., . . . Kim, C. J. (2010). MicroRNA expression profiling of the human uterine cervix after term labor and delivery. *Am J Obstet Gynecol*, 202(1), 80 e81-88. doi:10.1016/j.ajog.2009.08.016
- Hediger, M. L., Scholl, T. O., Schall, J. I., & Krueger, P. M. (1997). Young maternal age and preterm labor. *Ann Epidemiol*, 7(6), 400-406.
- Herzog, C., Haun, R. S., Kaushal, V., Mayeux, P. R., Shah, S. V., & Kaushal, G. P. (2009). Meprin A and meprin alpha generate biologically functional IL-1beta from pro-IL-1beta. *Biochem Biophys Res Commun*, 379(4), 904-908. doi:10.1016/j.bbrc.2008.12.161
- Hillier, S. L., Martius, J., Krohn, M., Kiviat, N., Holmes, K. K., & Eschenbach, D. A. (1988). A case-control study of chorioamnionic infection and histologic chorioamnionitis in prematurity. *N Engl J Med*, 319(15), 972-978. doi:10.1056/NEJM198810133191503

- Hoang, M., Potter, J. A., Gysler, S. M., Han, C. S., Guller, S., Norwitz, E. R., & Abrahams, V. M. (2014). Human fetal membranes generate distinct cytokine profiles in response to bacterial Toll-like receptor and nod-like receptor agonists. *Biol Reprod*, *90*(2), 39. doi:10.1095/biolreprod.113.115428
- Holt, R., Timmons, B. C., Akgul, Y., Akins, M. L., & Mahendroo, M. (2011). The molecular mechanisms of cervical ripening differ between term and preterm birth. *Endocrinology*, *152*(3), 1036-1046. doi:10.1210/en.2010-1105
- House, M., & Socrate, S. (2006). The cervix as a biomechanical structure. *Ultrasound Obstet Gynecol*, *28*(6), 745-749. doi:10.1002/uog.3850
- . Implantation, Embryogenesis, and Placental Development. (2010). In K. J. L. F. Gary Cunningham, Steven L. Bloom, John C. Hauth, Dwight J. Rouse, and Catherine Y. Spong (Ed.), *Williams Obstetrics* (23 ed., pp. 36-77). USA: McGraw-Hill Education.
- Jeffcoat, M. K., Geurs, N. C., Reddy, M. S., Cliver, S. P., Goldenberg, R. L., & Hauth, J. C. (2001). Periodontal infection and preterm birth: results of a prospective study. *J Am Dent Assoc*, *132*(7), 875-880.
- Jo, E. K., Kim, J. K., Shin, D. M., & Sasakawa, C. (2016). Molecular mechanisms regulating NLRP3 inflammasome activation. *Cell Mol Immunol*, *13*(2), 148-159. doi:10.1038/cmi.2015.95
- Joergensen, J. S., Kjaer Weile, L. K., & Lamont, R. F. (2014). The early use of appropriate prophylactic antibiotics in susceptible women for the prevention of preterm birth of infectious etiology. *Expert Opin Pharmacother*, *15*(15), 2173-2191. doi:10.1517/14656566.2014.950225
- Johnson, J. W. C., Austin, K. L., Jones, G. S., Davis, G. H., & King, T. M. (1975). Efficacy of 17alpha-Hydroxyprogesterone Caproate in Prevention of Premature Labor. *New England Journal of Medicine*, *293*(14), 675-680. doi:Doi 10.1056/Nejm197510022931401
- Keirse, M. J. (1990). Progestogen administration in pregnancy may prevent preterm delivery. *Br J Obstet Gynaecol*, *97*(2), 149-154.
- Kelleher, C. M., McLean, S. E., & Mecham, R. P. (2004). Vascular extracellular matrix and aortic development. *Curr Top Dev Biol*, *62*, 153-188. doi:10.1016/S0070-2153(04)62006-0
- Kelwick, R., Desanlis, I., Wheeler, G. N., & Edwards, D. R. (2015). The ADAMTS (A Disintegrin and Metalloproteinase with Thrombospondin motifs) family. *Genome Biol*, *16*, 113. doi:10.1186/s13059-015-0676-3
- Kenyon, S. L., Taylor, D. J., Tarnow-Mordi, W., & Group, O. C. (2001). Broad-spectrum antibiotics for spontaneous preterm labour: the ORACLE II randomised trial. ORACLE Collaborative Group. *Lancet*, *357*(9261), 989-994.
- Khoshnood, B., Lee, K. S., Wall, S., Hsieh, H. L., & Mittendorf, R. (1998). Short interpregnancy intervals and the risk of adverse birth outcomes among five racial/ethnic groups in the United States. *Am J Epidemiol*, *148*(8), 798-805.
- Kim, D., Perte, G., Trapnell, C., Pimentel, H., Kelley, R., & Salzberg, S. L. (2013). TopHat2: accurate alignment of transcriptomes in the presence of insertions,

- deletions and gene fusions. *Genome Biol*, 14(4), R36. doi:10.1186/gb-2013-14-4-r36
- Kindinger, L. M., MacIntyre, D. A., Lee, Y. S., Marchesi, J. R., Smith, A., McDonald, J. A., . . . Bennett, P. R. (2016). Relationship between vaginal microbial dysbiosis, inflammation, and pregnancy outcomes in cervical cerclage. *Sci Transl Med*, 8(350), 350ra102. doi:10.1126/scitranslmed.aag1026
- Kirschke, H., Kembhavi, A. A., Bohley, P., & Barrett, A. J. (1982). Action of rat liver cathepsin L on collagen and other substrates. *Biochem J*, 201(2), 367-372.
- Klerman, L. V., Cliver, S. P., & Goldenberg, R. L. (1998). The impact of short interpregnancy intervals on pregnancy outcomes in a low-income population. *Am J Public Health*, 88(8), 1182-1185.
- Kosa, J. L., Guendelman, S., Pearl, M., Graham, S., Abrams, B., & Kharrazi, M. (2011). The association between pre-pregnancy BMI and preterm delivery in a diverse southern California population of working women. *Matern Child Health J*, 15(6), 772-781. doi:10.1007/s10995-010-0633-4
- Kumarswamy, R., & Thum, T. (2013). Non-coding RNAs in cardiac remodeling and heart failure. *Circ Res*, 113(6), 676-689. doi:10.1161/CIRCRESAHA.113.300226
- Lee, G. S., Subramanian, N., Kim, A. I., Aksentjevich, I., Goldbach-Mansky, R., Sacks, D. B., . . . Chae, J. J. (2012). The calcium-sensing receptor regulates the NLRP3 inflammasome through Ca²⁺ and cAMP. *Nature*, 492(7427), 123-127. doi:10.1038/nature11588
- Leitner, K., Al Shammery, M., McLane, M., Johnston, M. V., Elovitz, M. A., & Burd, I. (2014). IL-1 receptor blockade prevents fetal cortical brain injury but not preterm birth in a mouse model of inflammation-induced preterm birth and perinatal brain injury. *Am J Reprod Immunol*, 71(5), 418-426. doi:10.1111/aji.12216
- Leon, L. R., Conn, C. A., Glaccum, M., & Kluger, M. J. (1996). IL-1 type I receptor mediates acute phase response to turpentine, but not lipopolysaccharide, in mice. *Am J Physiol*, 271(6 Pt 2), R1668-1675.
- Leppert, P. C. (1995). Anatomy and physiology of cervical ripening. *Clin Obstet Gynecol*, 38(2), 267-279.
- Leppert, P. C. (1998). Proliferation and apoptosis of fibroblasts and smooth muscle cells in rat uterine cervix throughout gestation and the effect of the antiprogestone onapristone. *Am J Obstet Gynecol*, 178(4), 713-725.
- Leppert, P. C., Keller, S., Cerreta, J., Hosannah, Y., & Mandl, I. (1983). The content of elastin in the uterine cervix. *Arch Biochem Biophys*, 222(1), 53-58.
- Leppert, P. C., & Yu, S. Y. (1991). Three-dimensional structures of uterine elastic fibers: scanning electron microscopic studies. *Connect Tissue Res*, 27(1), 15-31.
- Leppert, P. C., Yu, S. Y., Keller, S., Cerreta, J., & Mandl, I. (1987). Decreased elastic fibers and desmosine content in incompetent cervix. *Am J Obstet Gynecol*, 157(5), 1134-1139.
- Leveno, K. J., McIntire, D. D., Bloom, S. L., Sibley, M. R., & Anderson, R. J. (2009). Decreased preterm births in an inner-city public hospital. *Obstet Gynecol*, 113(3), 578-584. doi:10.1097/AOG.0b013e318195e257

- Li, H., Ge, Q., Guo, L., & Lu, Z. (2013). Maternal plasma miRNAs expression in preeclamptic pregnancies. *Biomed Res Int*, 2013, 970265. doi:10.1155/2013/970265
- Li, N., Rivera-Bermudez, M. A., Zhang, M., Tejada, J., Glasson, S. S., Collins-Racie, L. A., . . . Yang, Z. (2010). LXR modulation blocks prostaglandin E2 production and matrix degradation in cartilage and alleviates pain in a rat osteoarthritis model. *Proc Natl Acad Sci U S A*, 107(8), 3734-3739. doi:10.1073/pnas.0911377107
- Li, P., Allen, H., Banerjee, S., Franklin, S., Herzog, L., Johnston, C., . . . et al. (1995). Mice deficient in IL-1 beta-converting enzyme are defective in production of mature IL-1 beta and resistant to endotoxic shock. *Cell*, 80(3), 401-411.
- Livingston G, P. K., Rohal M. (2015). Childlessness Falls, Family Size Grows among Highly Educated Women *Pew Research Center*. Washington, D.C.
- Lopez-Castejon, G., & Brough, D. (2011). Understanding the mechanism of IL-1beta secretion. *Cytokine Growth Factor Rev*, 22(4), 189-195. doi:10.1016/j.cytogfr.2011.10.001
- Mahendroo, M. S., Porter, A., Russell, D. W., & Word, R. A. (1999). The parturition defect in steroid 5alpha-reductase type 1 knockout mice is due to impaired cervical ripening. *Mol Endocrinol*, 13(6), 981-992. doi:10.1210/mend.13.6.0307
- Maller, O., Hansen, K. C., Lyons, T. R., Acerbi, I., Weaver, V. M., Prekeris, R., . . . Schedin, P. (2013). Collagen architecture in pregnancy-induced protection from breast cancer. *J Cell Sci*, 126(Pt 18), 4108-4110. doi:10.1242/jcs.121590
- Martin, J. A., Hamilton, B. E., Osterman, M. J., Curtin, S. C., & Matthews, T. J. (2015). Births: final data for 2013. *Natl Vital Stat Rep*, 64(1), 1-65.
- Martin, J. A., Hamilton, B. E., Osterman, M. J., Driscoll, A. K., & Mathews, T. J. (2017). Births: Final Data for 2015. *Natl Vital Stat Rep*, 66(1), 1.
- Martin, J. A., Hamilton, B. E., Sutton, P. D., Ventura, S. J., Menacker, F., & Munson, M. L. (2005). Births: final data for 2003. *Natl Vital Stat Rep*, 54(2), 1-116.
- Mason, R. W., Johnson, D. A., Barrett, A. J., & Chapman, H. A. (1986). Elastinolytic activity of human cathepsin L. *Biochem J*, 233(3), 925-927.
- Massam-Wu, T., Chiu, M., Choudhury, R., Chaudhry, S. S., Baldwin, A. K., McGovern, A., . . . Kielty, C. M. (2010). Assembly of fibrillin microfibrils governs extracellular deposition of latent TGF beta. *J Cell Sci*, 123(Pt 17), 3006-3018. doi:10.1242/jcs.073437
- Mathur, R. S., Landgrebe, S., & Williamson, H. O. (1980). Progesterone, 17-hydroxyprogesterone, estradiol, and estriol in late pregnancy and labor. *Am J Obstet Gynecol*, 136(1), 25-27.
- Maynard, M. A., Evans, A. J., Hosomi, T., Hara, S., Jewett, M. A., & Ohh, M. (2005). Human HIF-3alpha4 is a dominant-negative regulator of HIF-1 and is down-regulated in renal cell carcinoma. *FASEB J*, 19(11), 1396-1406. doi:10.1096/fj.05-3788com
- Mechem, R. P. (2008). Methods in elastic tissue biology: elastin isolation and purification. *Methods*, 45(1), 32-41. doi:10.1016/j.ymeth.2008.01.007
- Meis, P. J., Klebanoff, M., Thom, E., Dombrowski, M. P., Sibai, B., Moawad, A. H., . . . Human Development Maternal-Fetal Medicine Units, N. (2003). Prevention of

- recurrent preterm delivery by 17 alpha-hydroxyprogesterone caproate. *N Engl J Med*, 348(24), 2379-2385. doi:10.1056/NEJMoa035140
- Mengshol, J. A., Vincenti, M. P., Coon, C. I., Barchowsky, A., & Brinckerhoff, C. E. (2000). Interleukin-1 induction of collagenase 3 (matrix metalloproteinase 13) gene expression in chondrocytes requires p38, c-Jun N-terminal kinase, and nuclear factor kappaB: differential regulation of collagenase 1 and collagenase 3. *Arthritis Rheum*, 43(4), 801-811. doi:10.1002/1529-0131(200004)43:4<801::AID-ANR10>3.0.CO;2-4
- Merline, R., Schaefer, R. M., & Schaefer, L. (2009). The matricellular functions of small leucine-rich proteoglycans (SLRPs). *J Cell Commun Signal*, 3(3-4), 323-335. doi:10.1007/s12079-009-0066-2
- Mesiano, S. (2013). *The Endocrinology of Human Pregnancy and Fetal-Placental Neuroendocrine Development* (Seventh ed.): Elsevier Inc.
- Miao, E. A., Alpuche-Aranda, C. M., Dors, M., Clark, A. E., Bader, M. W., Miller, S. I., & Aderem, A. (2006). Cytoplasmic flagellin activates caspase-1 and secretion of interleukin 1beta via Ipaf. *Nat Immunol*, 7(6), 569-575. doi:10.1038/ni1344
- Mohamed, J. S., Hajira, A., Lopez, M. A., & Boriek, A. M. (2015). Genome-wide Mechanosensitive MicroRNA (MechanomiR) Screen Uncovers Dysregulation of Their Regulatory Networks in the mdm Mouse Model of Muscular Dystrophy. *J Biol Chem*, 290(41), 24986-25011. doi:10.1074/jbc.M115.659375
- Mouillet, J. F., Chu, T., Nelson, D. M., Mishima, T., & Sadovsky, Y. (2010). MiR-205 silences MED1 in hypoxic primary human trophoblasts. *FASEB J*, 24(6), 2030-2039. doi:10.1096/fj.09-149724
- Mulla, M. J., Salmon, J. E., Chamley, L. W., Brosens, J. J., Boeras, C. M., Kavathas, P. B., & Abrahams, V. M. (2013). A role for uric acid and the Nalp3 inflammasome in antiphospholipid antibody-induced IL-1beta production by human first trimester trophoblast. *PLoS One*, 8(6), e65237. doi:10.1371/journal.pone.0065237
- Nadeau-Vallee, M., Obari, D., Quiniou, C., Lubell, W. D., Olson, D. M., Girard, S., & Chemtob, S. (2016). A critical role of interleukin-1 in preterm labor. *Cytokine Growth Factor Rev*, 28, 37-51. doi:10.1016/j.cytogfr.2015.11.001
- Nadeem, L., Shynlova, O., Matysiak-Zablocki, E., Mesiano, S., Dong, X., & Lye, S. (2016). Molecular evidence of functional progesterone withdrawal in human myometrium. *Nat Commun*, 7, 11565. doi:10.1038/ncomms11565
- Nallasamy, S., Yoshida, K., Akins, M., Myers, K., Iozzo, R., & Mahendroo, M. (2017a). Steroid Hormones Are Key Modulators of Tissue Mechanical Function via Regulation of Collagen and Elastic Fibers. *Endocrinology*, 158(4), 950-962. doi:10.1210/en.2016-1930
- Nallasamy, S., Yoshida, K., Akins, M., Myers, K., Iozzo, R., & Mahendroo, M. (2017b). Steroid hormones are key modulators of tissue mechanical function via regulation of collagen and elastic fibers. *Endocrinology*. doi:10.1210/en.2016-1930
- Nelson, D. B., McIntire, D. D., McDonald, J., Gard, J., Turrichi, P., & Leveno, K. J. (2017). 17-alpha Hydroxyprogesterone caproate did not reduce the rate of recurrent preterm birth in a prospective cohort study. *Am J Obstet Gynecol*. doi:10.1016/j.ajog.2017.02.025

- Newburn-Cook, C. V., & Onyskiw, J. E. (2005). Is older maternal age a risk factor for preterm birth and fetal growth restriction? A systematic review. *Health Care Women Int*, 26(9), 852-875. doi:10.1080/07399330500230912
- Nordlander, S., Pott, J., & Maloy, K. J. (2014). NLRC4 expression in intestinal epithelial cells mediates protection against an enteric pathogen. *Mucosal Immunol*, 7(4), 775-785. doi:10.1038/mi.2013.95
- Norman, J. E., Marlow, N., Messow, C. M., Shennan, A., Bennett, P. R., Thornton, S., . . . group, O. s. (2016). Vaginal progesterone prophylaxis for preterm birth (the OPPTIMUM study): a multicentre, randomised, double-blind trial. *Lancet*, 387(10033), 2106-2116. doi:10.1016/S0140-6736(16)00350-0
- Obstetricians, A. C. o. P. B. A. C. o., & Gynecologist. (2003). ACOG Practice Bulletin. Clinical management guidelines for obstetrician-gynecologist. Number 43, May 2003. Management of preterm labor. *Obstet Gynecol*, 101(5 Pt 1), 1039-1047.
- Offenbacher, S., Katz, V., Fertik, G., Collins, J., Boyd, D., Maynor, G., . . . Beck, J. (1996). Periodontal infection as a possible risk factor for preterm low birth weight. *J Periodontol*, 67(10 Suppl), 1103-1113. doi:10.1902/jop.1996.67.10s.1103
- Osman, I., Young, A., Ledingham, M. A., Thomson, A. J., Jordan, F., Greer, I. A., & Norman, J. E. (2003). Leukocyte density and pro-inflammatory cytokine expression in human fetal membranes, decidua, cervix and myometrium before and during labour at term. *Mol Hum Reprod*, 9(1), 41-45.
- Ozasa, H., Tominaga, T., Nishimura, T., & Takeda, T. (1981). Lysyl oxidase activity in the mouse uterine cervix is physiologically regulated by estrogen. *Endocrinology*, 109(2), 618-621. doi:10.1210/endo-109-2-618
- Pilarczyk, K., Kozik, W., & Czerwinski, F. (2002). [Arteries of the uterine cervix in reproductive age in microangiographic studies]. *Ginekol Pol*, 73(12), 1179-1183.
- Rajabi, M. R., Solomon, S., & Poole, A. R. (1991). Biochemical evidence of collagenase-mediated collagenolysis as a mechanism of cervical dilatation at parturition in the guinea pig. *Biol Reprod*, 45(5), 764-772.
- Rathinam, V. A., & Fitzgerald, K. A. (2016). Inflammasome Complexes: Emerging Mechanisms and Effector Functions. *Cell*, 165(4), 792-800. doi:10.1016/j.cell.2016.03.046
- Read, C. P., Word, R. A., Ruscheinsky, M. A., Timmons, B. C., & Mahendroo, M. S. (2007). Cervical remodeling during pregnancy and parturition: molecular characterization of the softening phase in mice. *Reproduction*, 134(2), 327-340. doi:10.1530/REP-07-0032
- Reddick, K. L., Jhaveri, R., Gandhi, M., James, A. H., & Swamy, G. K. (2011). Pregnancy outcomes associated with viral hepatitis. *J Viral Hepat*, 18(7), e394-398. doi:10.1111/j.1365-2893.2011.01436.x
- Reifenstein, E. C., Jr. (1958). Clinical use of 17 alpha-hydroxyprogesterone 17-n-caproate in habitual abortion. *Ann N Y Acad Sci*, 71(5), 762-786.
- Renthal, N. E., Chen, C. C., Williams, K. C., Gerard, R. D., Prange-Kiel, J., & Mendelson, C. R. (2010). miR-200 family and targets, ZEB1 and ZEB2, modulate

- uterine quiescence and contractility during pregnancy and labor. *Proc Natl Acad Sci U S A*, 107(48), 20828-20833. doi:10.1073/pnas.1008301107
- Romero, R., Brody, D. T., Oyarzun, E., Mazor, M., Wu, Y. K., Hobbins, J. C., & Durum, S. K. (1989). Infection and labor. III. Interleukin-1: a signal for the onset of parturition. *Am J Obstet Gynecol*, 160(5 Pt 1), 1117-1123.
- Romero, R., Durum, S., Dinarello, C. A., Oyarzun, E., Hobbins, J. C., & Mitchell, M. D. (1989). Interleukin-1 stimulates prostaglandin biosynthesis by human amnion. *Prostaglandins*, 37(1), 13-22.
- Romero, R., Espinoza, J., Kusanovic, J. P., Gotsch, F., Hassan, S., Erez, O., . . . Mazor, M. (2006). The preterm parturition syndrome. *BJOG*, 113 Suppl 3, 17-42. doi:10.1111/j.1471-0528.2006.01120.x
- Romero, R., Mazor, M., & Tartakovsky, B. (1991). Systemic administration of interleukin-1 induces preterm parturition in mice. *Am J Obstet Gynecol*, 165(4 Pt 1), 969-971.
- Romero, R., & Stanczyk, F. Z. (2013). Progesterone is not the same as 17alpha-hydroxyprogesterone caproate: implications for obstetrical practice. *Am J Obstet Gynecol*, 208(6), 421-426. doi:10.1016/j.ajog.2013.04.027
- Romero, R., & Tartakovsky, B. (1992). The natural interleukin-1 receptor antagonist prevents interleukin-1-induced preterm delivery in mice. *Am J Obstet Gynecol*, 167(4 Pt 1), 1041-1045.
- Romero, R., Xu, Y., Plazyo, O., Chaemsaitong, P., Chaiworapongsa, T., Unkel, R., . . . Gomez-Lopez, N. (2016). A Role for the Inflammasome in Spontaneous Labor at Term. *Am J Reprod Immunol*. doi:10.1111/aji.12440
- Ruscheinsky, M., De la Motte, C., & Mahendroo, M. (2008). Hyaluronan and its binding proteins during cervical ripening and parturition: dynamic changes in size, distribution and temporal sequence. *Matrix Biol*, 27(5), 487-497. doi:10.1016/j.matbio.2008.01.010
- Sadowsky, D. W., Adams, K. M., Gravett, M. G., Witkin, S. S., & Novy, M. J. (2006). Preterm labor is induced by intraamniotic infusions of interleukin-1beta and tumor necrosis factor-alpha but not by interleukin-6 or interleukin-8 in a nonhuman primate model. *Am J Obstet Gynecol*, 195(6), 1578-1589. doi:10.1016/j.ajog.2006.06.072
- Saharinen, J., Hyytiainen, M., Taipale, J., & Keski-Oja, J. (1999). Latent transforming growth factor-beta binding proteins (LTBPs)--structural extracellular matrix proteins for targeting TGF-beta action. *Cytokine Growth Factor Rev*, 10(2), 99-117.
- Sanders, A. P., Burris, H. H., Just, A. C., Motta, V., Svensson, K., Mercado-Garcia, A., . . . Baccarelli, A. A. (2015). microRNA expression in the cervix during pregnancy is associated with length of gestation. *Epigenetics*, 10(3), 221-228. doi:10.1080/15592294.2015.1006498
- Sandy, J. D., Westling, J., Kenagy, R. D., Iruela-Arispe, M. L., Verscharen, C., Rodriguez-Mazaneque, J. C., . . . Clowes, A. W. (2001). Versican V1 proteolysis in human aorta in vivo occurs at the Glu441-Ala442 bond, a site that is cleaved by

- recombinant ADAMTS-1 and ADAMTS-4. *J Biol Chem*, 276(16), 13372-13378. doi:10.1074/jbc.M009737200
- Schroder, K., & Tschopp, J. (2010). The inflammasomes. *Cell*, 140(6), 821-832. doi:10.1016/j.cell.2010.01.040
- Scott, J. E. (1988). Proteoglycan-fibrillar collagen interactions. *Biochem J*, 252(2), 313-323.
- Sellin, M. E., Maslowski, K. M., Maloy, K. J., & Hardt, W. D. (2015). Inflammasomes of the intestinal epithelium. *Trends Immunol*, 36(8), 442-450. doi:10.1016/j.it.2015.06.002
- Shearman, R. P., & Garrett, W. J. (1963). Double-blind study of effect of 17-hydroxyprogesterone caproate on abortion rate. *Br Med J*, 1(5326), 292-295.
- Sheehan DC, H. B. (1980). *Theory and practice of histotechnology*: Columbia: Battelle Press.
- Shifren, A., & Mecham, R. P. (2006). The stumbling block in lung repair of emphysema: elastic fiber assembly. *Proc Am Thorac Soc*, 3(5), 428-433. doi:10.1513/pats.200601-009AW
- Simcox, R., Sin, W. T., Seed, P. T., Briley, A., & Shennan, A. H. (2007). Prophylactic antibiotics for the prevention of preterm birth in women at risk: a meta-analysis. *Aust N Z J Obstet Gynaecol*, 47(5), 368-377. doi:10.1111/j.1479-828X.2007.00759.x
- Sugawara, S., Uehara, A., Nochi, T., Yamaguchi, T., Ueda, H., Sugiyama, A., . . . Takada, H. (2001). Neutrophil proteinase 3-mediated induction of bioactive IL-18 secretion by human oral epithelial cells. *J Immunol*, 167(11), 6568-6575.
- Tang, D., Kang, R., Coyne, C. B., Zeh, H. J., & Lotze, M. T. (2012). PAMPs and DAMPs: signal 0s that spur autophagy and immunity. *Immunol Rev*, 249(1), 158-175. doi:10.1111/j.1600-065X.2012.01146.x
- Thornberry, N. A., Bull, H. G., Calaycay, J. R., Chapman, K. T., Howard, A. D., Kostura, M. J., . . . et al. (1992). A novel heterodimeric cysteine protease is required for interleukin-1 beta processing in monocytes. *Nature*, 356(6372), 768-774. doi:10.1038/356768a0
- Tibbetts, T. A., Conneely, O. M., & O'Malley, B. W. (1999). Progesterone via its receptor antagonizes the pro-inflammatory activity of estrogen in the mouse uterus. *Biol Reprod*, 60(5), 1158-1165.
- Timmons, B., Akins, M., & Mahendroo, M. (2010). Cervical remodeling during pregnancy and parturition. *Trends Endocrinol Metab*, 21(6), 353-361. doi:10.1016/j.tem.2010.01.011
- Timmons, B. C., Mitchell, S. M., Gilpin, C., & Mahendroo, M. S. (2007). Dynamic changes in the cervical epithelial tight junction complex and differentiation occur during cervical ripening and parturition. *Endocrinology*, 148(3), 1278-1287. doi:10.1210/en.2006-0851
- Timmons, B. C., Reese, J., Socrate, S., Ehinger, N., Paria, B. C., Milne, G. L., . . . Mahendroo, M. (2014). Prostaglandins are essential for cervical ripening in LPS-mediated preterm birth but not term or antiprogesterin-driven preterm ripening. *Endocrinology*, 155(1), 287-298. doi:10.1210/en.2013-1304

- Trapnell, C., Williams, B. A., Pertea, G., Mortazavi, A., Kwan, G., van Baren, M. J., . . . Pachter, L. (2010). Transcript assembly and quantification by RNA-Seq reveals unannotated transcripts and isoform switching during cell differentiation. *Nat Biotechnol*, *28*(5), 511-515. doi:10.1038/nbt.1621
- van Rooij, E., Sutherland, L. B., Thatcher, J. E., DiMaio, J. M., Naseem, R. H., Marshall, W. S., . . . Olson, E. N. (2008). Dysregulation of microRNAs after myocardial infarction reveals a role of miR-29 in cardiac fibrosis. *Proc Natl Acad Sci U S A*, *105*(35), 13027-13032. doi:10.1073/pnas.0805038105
- Vink, J. Y., Qin, S., Brock, C. O., Zork, N. M., Feltovich, H. M., Chen, X., . . . Gallos, G. (2016). A new paradigm for the role of smooth muscle cells in the human cervix. *Am J Obstet Gynecol*, *215*(4), 478 e471-478 e411. doi:10.1016/j.ajog.2016.04.053
- von Moltke, J., Trinidad, N. J., Moayeri, M., Kintzer, A. F., Wang, S. B., van Rooijen, N., . . . Vance, R. E. (2012). Rapid induction of inflammatory lipid mediators by the inflammasome in vivo. *Nature*, *490*(7418), 107-111. doi:10.1038/nature11351
- Wadhwa, P. D., Entringer, S., Buss, C., & Lu, M. C. (2011). The contribution of maternal stress to preterm birth: issues and considerations. *Clin Perinatol*, *38*(3), 351-384. doi:10.1016/j.clp.2011.06.007
- Wagenseil, J. E., & Mecham, R. P. (2007). New insights into elastic fiber assembly. *Birth Defects Res C Embryo Today*, *81*(4), 229-240. doi:10.1002/bdrc.20111
- Wang, H., Flach, H., Onizawa, M., Wei, L., McManus, M. T., & Weiss, A. (2014). Negative regulation of Hif1 α expression and TH17 differentiation by the hypoxia-regulated microRNA miR-210. *Nat Immunol*, *15*(4), 393-401. doi:10.1038/ni.2846
- White, B. A., Creedon, D. J., Nelson, K. E., & Wilson, B. A. (2011). The vaginal microbiome in health and disease. *Trends Endocrinol Metab*, *22*(10), 389-393. doi:10.1016/j.tem.2011.06.001
- Wieslander, C. K., Marinis, S. I., Drewes, P. G., Keller, P. W., Acevedo, J. F., & Word, R. A. (2008). Regulation of elastolytic proteases in the mouse vagina during pregnancy, parturition, and puerperium. *Biol Reprod*, *78*(3), 521-528. doi:10.1095/biolreprod.107.063024
- Williams, K. C., Renthall, N. E., Condon, J. C., Gerard, R. D., & Mendelson, C. R. (2012). MicroRNA-200a serves a key role in the decline of progesterone receptor function leading to term and preterm labor. *Proc Natl Acad Sci U S A*, *109*(19), 7529-7534. doi:10.1073/pnas.1200650109
- Yoshida, K., Jiang, H., Kim, M., Vink, J., Cremers, S., Paik, D., . . . Myers, K. (2014). Quantitative evaluation of collagen crosslinks and corresponding tensile mechanical properties in mouse cervical tissue during normal pregnancy. *PLoS One*, *9*(11), e112391. doi:10.1371/journal.pone.0112391
- Yoshida, K., Mahendroo, M., Vink, J., Wapner, R., & Myers, K. (2016). Material properties of mouse cervical tissue in normal gestation. *Acta Biomater*, *36*, 195-209. doi:10.1016/j.actbio.2016.03.005
- Yoshimura, K., & Hirsch, E. (2005). Effect of stimulation and antagonism of interleukin-1 signaling on preterm delivery in mice. *J Soc Gynecol Investig*, *12*(7), 533-538. doi:10.1016/j.jsigi.2005.06.006

- Zampetaki, A., Attia, R., Mayr, U., Gomes, R. S., Phinikaridou, A., Yin, X., . . . Mayr, M. (2014). Role of miR-195 in aortic aneurysmal disease. *Circ Res*, *115*(10), 857-866. doi:10.1161/CIRCRESAHA.115.304361
- Zhang, Y., Akins, M. L., Murari, K., Xi, J., Li, M. J., Luby-Phelps, K., . . . Li, X. (2012). A compact fiber-optic SHG scanning endomicroscope and its application to visualize cervical remodeling during pregnancy. *Proc Natl Acad Sci U S A*, *109*(32), 12878-12883. doi:10.1073/pnas.1121495109
- Zhao, Y., Yang, J., Shi, J., Gong, Y. N., Lu, Q., Xu, H., . . . Shao, F. (2011). The NLRC4 inflammasome receptors for bacterial flagellin and type III secretion apparatus. *Nature*, *477*(7366), 596-600. doi:10.1038/nature10510
- Zheng, H., Fletcher, D., Kozak, W., Jiang, M., Hofmann, K. J., Conn, C. A., . . . et al. (1995). Resistance to fever induction and impaired acute-phase response in interleukin-1 beta-deficient mice. *Immunity*, *3*(1), 9-19.
- Zhong, S., Joung, J. G., Zheng, Y., Chen, Y. R., Liu, B., Shao, Y., . . . Giovannoni, J. J. (2011). High-throughput illumina strand-specific RNA sequencing library preparation. *Cold Spring Harb Protoc*, *2011*(8), 940-949. doi:10.1101/pdb.prot5652